7. SITE 387: CRETACEOUS TO RECENT SEDIMENTARY EVOLUTION OF THE WESTERN BERMUDA RISE

The Shipboard Scientific Party[1]

SITE DATA

Position: 32°19.2′N, 67°40.0′W

Water Depth (PDR, sea level): 5117 meters

Water Depth (PDR, rig floor): 5127 meters

Bottom Felt at (rig floor): 5128 meters

Penetration: 794.5 meters

Number of Holes: 1

Number of Cores: 50

Total Length Cored: 467.9 meters

Total Core Recovered: 178.2 meters

Core Recovery: 38.1 per cent

Oldest Sediment Cored: Limestone
Bottoms at: 791.6 meters
Age: Late Berriasian/early Valanginian
Velocity: 2.77-3.88 km/sec

Nature of Basement: Basalt
Encountered at: ~ 791.6 meters
Velocity: 4.59-4.98 km/sec

Date Occupied: 1719Z hours, 1 August 1975

Date Departed: 1130Z hours, 7 August 1975

Time on Site: 5 days, 18 hours, 11 minutes

Principal Results: Site 387 penetrated 791.9 meters of sediment and 2.9 meters into basaltic crust on the western Bermuda Rise 220 km west of the Bermuda pedestal. The site was located between magnetic anomalies *M*-15 and *M*-16 of the Keathley lineations and in a position where Horizons A^T, A^C, A^*, and β were clearly developed. Seven lithologic units were recognized in the sedimentary sequence penetrated. They are (from bottom to top) limestone and chalk (upper Berriasian-Barremian), green-gray and black claystone Barremian to Cenomanian), multicolored claystones (?Turonian-Maestrichtian), marly chalk (upper Maestrichtian), siliceous turbidites, siliceous claystones and chert (lower Paleocene-middle Eocene), radiolarian mud (middle Eocene-upper Oligocene), and hemipelagic clay (?Miocene-Quaternary).

Sediment accumulation at Site 387 appears to have been nearly continuous, except for a possible hiatus or extremely low accumulation rates within the Upper Cretaceous multicolored claystones. Rapid sedimentation characterizes the Neocomian limestones (23 m/m.y.) and Eocene siliceous mudstones (48 m/m.y.). Both the black claystone and the multicolored claystone units at Site 387 are thinner than those observed at Site 386, and their rates of accumulation are lower. Black clay deposition persisted up to 5 m.y. longer at Site 387 than at Site 386, perhaps because of its location deeper in the basin, and minor black clays were deposited at Site 387 even into the Paleocene.

Acoustic Horizons A^T, A^C, A^*, and β correlate, respectively, with (a) the top of middle Eocene siliceous turbidites (approximate), (b) lower-middle Eocene chert, (c) Maestrichtian marly chalk above red claystones, and (d) the top of Barremian limestones beneath the black clays. Unlike Site 386, drilled 100 km south-southeast of the Bermuda pedestal, drilling at Site 387 recovered no volcaniclastic material obviously derived from Bermuda.

Calcareous clay directly overlying basalt dates the crust between anomalies *M*-15 and *M*-16 as upper Berriasian to lower Valanginian, and calcareous sediment inclusions in the basalt are of the same age. There is some evidence the basalt penetrated is a sill, but if the basalt was intrusive, it was probably emplaced very close to the contemporaneous Mid-Atlantic Ridge crest.

BACKGROUND AND OBJECTIVES

The general philosophy for drilling at Sites 386 and 387 was outlined in the Site 386 Report. The primary purpose of these sites was to examine in detail the late Mesozoic and Cenozoic sedimentary history of the western North Atlantic Basin, with special emphasis on the age and lithofacies of prominent reflecting horizons. Earlier drilling suggested that reflectors such as "Horizon *A*" and Horizon β may have specific lithostratigraphic and/or chronostratigraphic relationships that are valid throughout the western North Atlantic Basin. If similar relationships were found to exist at Sites 386 and 387, then hundreds of thousands of kilometers of continuous seismic profiles obtained in the region could be used as a more or less valid mapping tool in interpretation of sedimentation processes, sediment distribution, and oceanographic conditions.

Site 387 (Figure 1) was selected in an area where four specific reflectors are well developed and where the

---

[1] Brian E. Tucholke (Co-Chief Scientist), Lamont-Doherty Geological Observatory, Palisades, New York; Peter R. Vogt (Co-Chief Scientist), Naval Research Laboratory, Washington, D.C.; Kenneth R. Demars, University of Rhode Island, Kingston, Rhode Island (now at: University of Delaware, Newark, Delaware); Jon S. Galehouse, San Francisco State University, San Francisco, California; Robert L. Houghton, Woods Hole Oceanographic Institution, Woods Hole, Massachusetts (now at: University of Alberta, Edmonton, Alberta, Canada); Ansis Kaneps, Deep Sea Drilling Project, Scripps Institution of Oceanography, La Jolla, California; John W. Kendrick, Shell Development Company, Houston, Texas; I. N. McCave, University of East Anglia, Norwich, England; Charles L. McNulty, University of Texas, Arlington, Texas; Ivar O. Murdmaa, P. P. Shirshov Institute of Oceanology, Moscow, USSR; Hisatake Okada, Lamont-Doherty Geological Observatory, Palisades, New York (now at: Yamagata University, Yamagata, Japan); and Peter Rothe, Mineralogisch Petrografisches Institut der Universität Heidelberg, Heidelberg, Federal Republic of Germany (now at: Geographisches Institut der Universität Mannheim, Mannheim, Federal Republic of Germany).

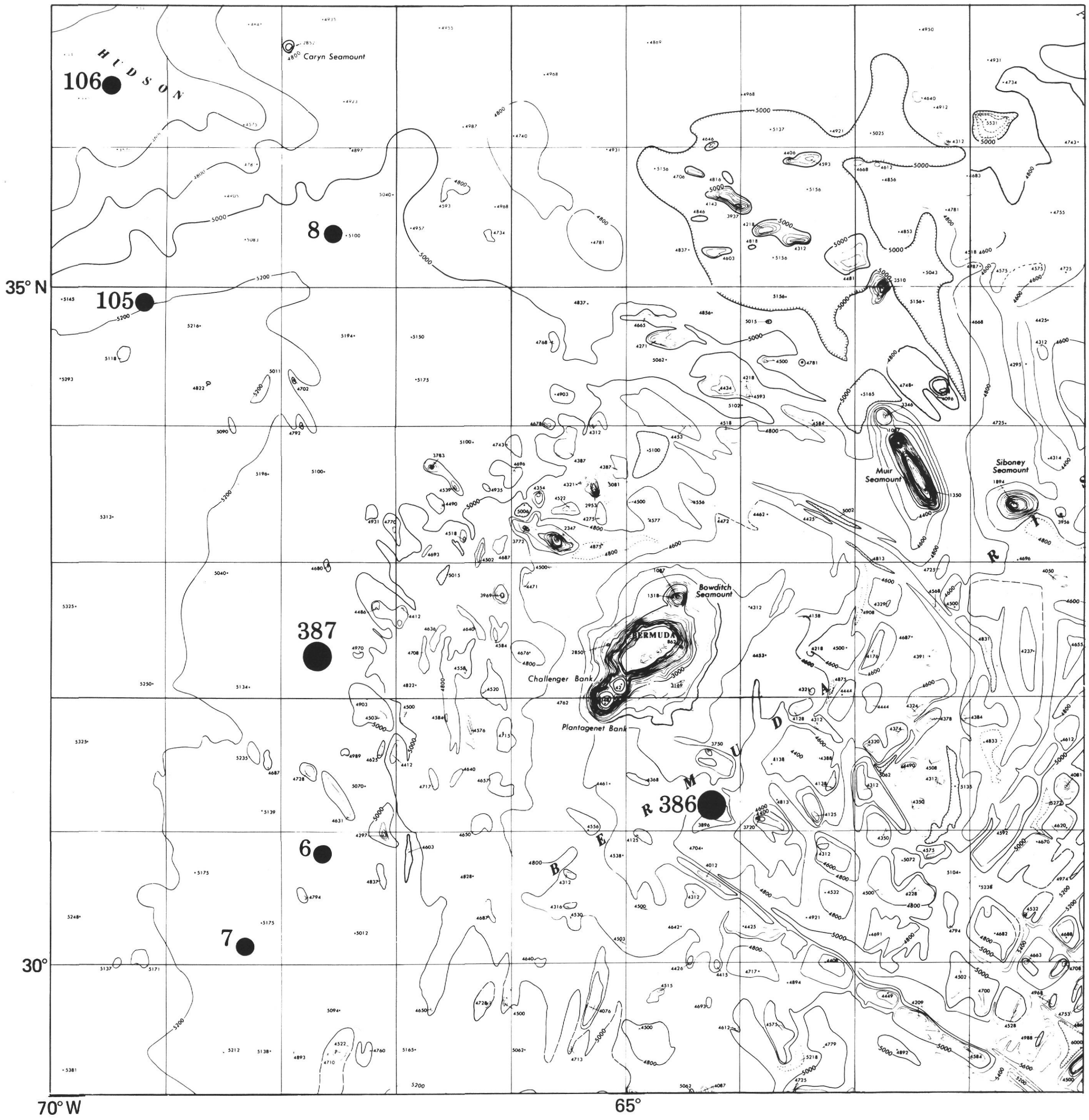

Figure 1. *Location of Site 387 on the western Bermuda Rise. Bathymetric contours in uncorrected meters.*

reflectors exhibit an acoustic character typical of that commonly observed elsewhere in the basin (Figure 2). The uppermost of these reflectors at Site 387 is Horizon A^T at 0.22 sec sub-bottom, underlain by Horizon A^C at 0.27 sec (see Site 386 Report, and Tucholke, this volume). Horizon A^* is well developed near 0.52 sec sub-bottom. A weak reflector between Horizons A^C and A^* is observed in the *Glomar Challenger* seismic profile, but its significance is uncertain. The deepest reflector at Site 386 is Horizon β near 0.68 sec. Horizon β tends to be thin and it irregularly drapes over the rough basement topography; at the time that sediments of Horizon β were deposited, Site 387 would have been located in the ridge-flank province.

Prior to Leg 43, a variety of closely spaced reflectors under the general heading "Horizon A" had been correlated with Eocene cherts at Sites 6 through 10 on the Bermuda Rise (Ewing et al., 1970), with a 60 to 90 m.y. hiatus at Sites 101 and 105 (Hollister, Ewing, et al., 1972), and with siliceous Eocene turbidites underlying

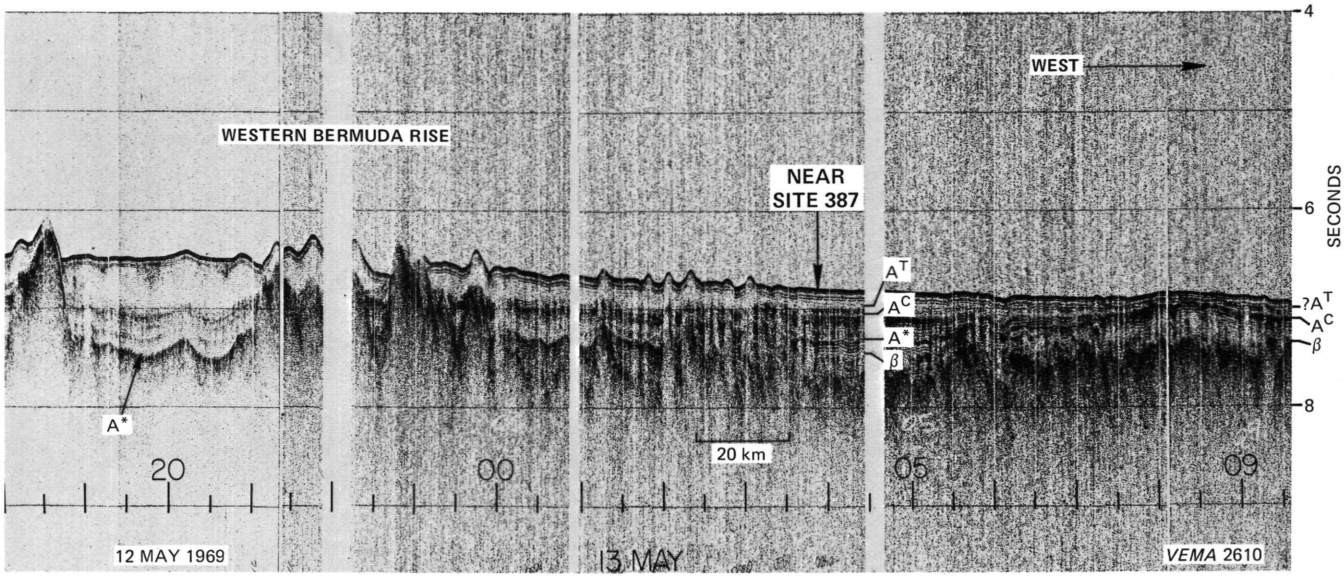

Figure 2. Vema *2610 reference profile near Site 387. Location of profile shown in Figure 3.*

upper Eocene to Holocene current-deposited clays at Site 28 (Tucholke and Ewing, 1974). The reflectors constituting "Horizon A" vary in a predictable manner between these sites, and the drill-site correlations suggested certain sedimentologic/acoustic relationships (erosion = thin single reflector; rapid deposition of siliceous detritus = complex reflector series; turbidites = reflector at the top of a highly reflective, closely laminated, reflective interval). Poor core recovery and discontinuous coring on earlier DSDP legs, however, left much doubt as to the universal validity of these preliminary correlations, and the Leg 43 program was designed to fill this gap in our knowledge. Previous Leg 43 drilling at Sites 384 and 385 had established that relatively thin interbeds of chert within small (<20 m) stratigraphic intervals could create a simple, single reflector in an otherwise rather homogeneous sedimentary section. At Site 386, south-southeast of Bermuda, the "Horizon A" reflectors are complex, and the cherts which normally provide the impedance contrast representing Horizon A^C are masked by an overlying middle Eocene calcareous sequence of similar impedance. Closely spaced coring at Site 387 would provide important control on the precise lithofacies more commonly associated with Horizon A^C.

Prior to Leg 43, Horizon A^* had been penetrated only at Site 105 (Ewing and Hollister, 1972). The tentative correlation made there with the seismic record suggested that A^* could represent an early Tertiary-Late Cretaceous transition from multicolored clays to underlying black clays. However, our drilling results at Site 386 indicated that Horizon A^* correlates with the top of a calcareous unit near the top of the multicolored clays; the transition from multicolored clay to black clay occurs deeper in the section and is not represented by a well-defined seismic horizon.

We were able to obtain a good seismic profile between Sites 386 and 387, with relatively few basement peaks interrupting the seismic horizons. This profile shows that the shallowest reflector at Site 386 (Horizon A^V, corresponding with the top of Oligocene volcaniclastic turbidites) becomes weaker and disappears westward, leaving a dual reflector pair (Horizons A^T and A^C) at Site 387. The deep Horizon A^* could be traced with only modest confidence between Sites 386 and 387, and drilling at Site 387 could help determine whether it shows the same age/lithofacies relationships as determined at Site 386.

Earlier drilling into Horizon β (Leg 11) indicated that β is a transition from black clay downward into Neocomian limestones. This transition marks the changing depositional conditions in the Hauterivian at Site 101, and in Hauterivian-Barremian at Site 105. These ages for β suggest that the horizon should not extend farther east than about the 115-m.y. crustal isochron on the western Bermuda Rise, provided β is roughly isochronous. Site 387 was located between anomalies *M*-15 and *M*-16 on crust inferred to be approximately 135 m.y. old (Larson and Hilde, 1975). Therefore, sediments at and below Horizon β in this area should record deposition during roughly the first 20-m.y. history of this parcel of oceanic crust, presumably in a province high on the flanks of the Early Cretaceous Mid-Atlantic Ridge. The irregular and "ponded" distribution of Horizon β on basement presently observed in the vicinity of Site 387 resembles the type of sediment distribution observed in many flank areas of the present mid-oceanic ridge, and Horizon β can be traced only a few tens of kilometers east of Site 387 in seismic profiles.

Until Leg 43, the *M*-series of magnetic anomalies (Keathley Sequence in the Atlantic; Vogt et al., 1971) had been dated by deep-sea drilling only near their young (*M*-4 to *M*-9) and old (*M*-24, *M*-25) limits. The ages of the intervening anomalies were interpolated between these end points with an assumption of constant spreading for the Hawaiian lineations in the Pacific

(Larson and Hilde, 1975). Determining a basement age at Site 387 was therefore of primary importance for calibrating the *M*-series and determining the spreading-rate history in the Cretaceous North Atlantic Basin.

OPERATIONS

Glomar Challenger steamed slightly north of due west between Sites 386 and 387, obtaining a good east-west profiler record across the southern Bermuda Rise. The satellite teletype failed while we were on Site 386 and could not be repaired; therefore, the track to Site 387 and the position of Site 387 were determined by celestial and Loran C fixes, the latter with generally poor reception. Site 387 was approached along course 297° PGC on 1 August 1975 (Figure 3). The *Glomar Challenger* profiler record closely matched the *Vema* 2610 reference profile (Figures 2 and 4), so that we were able to slow to 5 knots (1715Z) and drop the beacon (1719Z) above a well-defined seismic section without any need for a site survey by the *Challenger* (Figure 3). The seismic profiler record and its correlation to the drilling results are described later in this chapter.

Some difficulties were encountered in positioning over the beacon as it descended, but by 1900Z the ship was locked onto the beacon and the drill string was started down. At the request of the Cruise Operations Manager the heave compensator (HC) was rigged in order to test it for future IPOD use. Spud-in was at 0050 hours on 2 August, and the drill-pipe measurement of water depth (5118 m, compared to 5117 m PDR depth) was accepted as the official depth. The first core was obtained from a sub-bottom depth of 31.8 to 41.3 meters at 0255 hours (Table 1). At this time it was noticed that the slider on the HC was bending and allowing drill-string rotation of about 15°. The bending point in the slider was the same part that had bent in the aborted HC trial at Site 383. After Core 2 was retrieved at 0530 hours, the HC was removed for safety reasons.

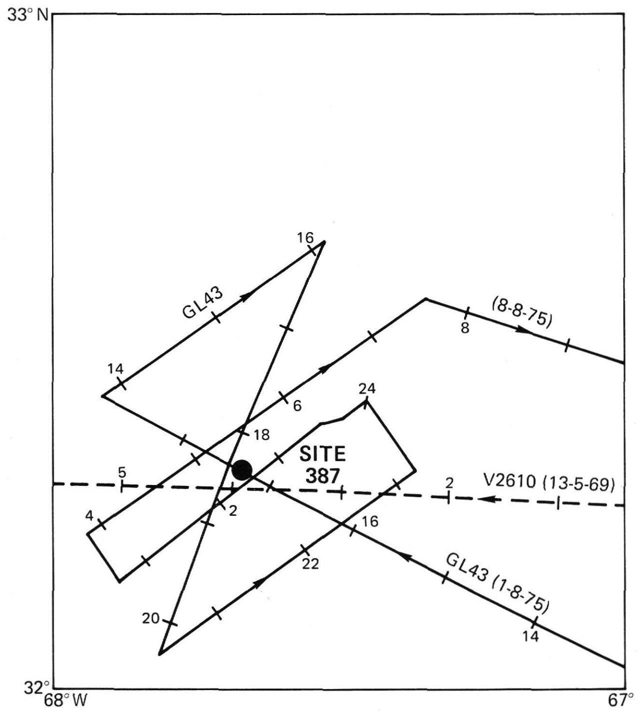

Figure 3. *Tracks of* Glomar Challenger *and* Vema *reference track in the vicinity of Site 387. Dates and times are annotated (*Challenger *times in GMT).*

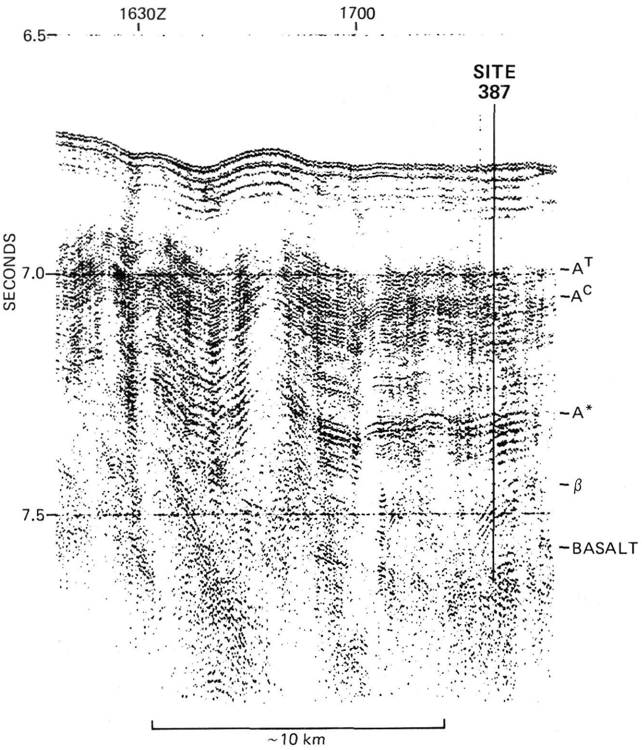

Figure 4. Glomar Challenger *profiler record approaching Site 387. Location of profile shown in Figure 3.*

The sedimentary section was cored mostly continuously or alternately below 137 meters (Figure 5). As at Site 386, very slow drilling was encountered in the Eocene section (see Figure 5 and also Site 386 Report, this volume) where numerous silicified claystones and porcelanitic chert beds were encountered. Core recovery in this interval was generally low because (1) the softer interbeds were easily washed away at the pump pressures required to drill the cherty layers and (2) the cherts frequently jammed in the core catcher, thus preventing further core recovery.

Drilling rates improved below the Eocene section and then began to drop again when we encountered the limestones of Horizon β (Core 28, 593.1 m). The transition between these limestones and the overlying gray and black claystones is gradational, consisting of interbedded layers of the two lithofacies. Core recovery was generally low at this level, apparently because the interbedded gray-black layers were softer and easily washed away. Judging from the core recovery, these softer beds probably dominate the limestone lithofacies between about 590 and 775 meters sub-bottom, even though our recovery was dominated by hard limestones.

Significantly better core recovery (6.6 m) and slower drilling were encountered in Core 49. Small, fine-

TABLE 1
Coring and Drilling Summary, Site 387

Core	Time (Day-Hour)	Total Depth[a] (m)	Sub-Bottom Depth (m)	Cored (m)	Recovered (m)	Recovered (%)	Lithology	Age[b]
1	2 – 0255	5159.8-5169.3	31.8-41.3	9.5	8.45	89	Clay and zeolitic clay	Pleist. (top)
2	2 – 0530	5226.5-5236.0	98.5-108.0	9.5	7.15	75	Zeolitic clay and rad mud	L.-M. Olig.
3	2 – 1000	5264.6-5274.1	136.6-146.1	9.5	2.79	29	Rad mud and clay	U. Eocene
4	2 – 1135	5274.1-5283.6	146.1-155.6	9.5	1.40	15	Rad mud	M. Eocene
5	2 – 1300	5283.6-5293.1	155.6-165.1	9.5	0.30	3	Rad mud	M. Eocene
6	2 – 1435	5293.1-5302.6	165.1-174.6	9.5	3.50	37	Rad mud	M. Eocene
7	2 – 1600	5302.6-5312.2	174.6-184.2	9.6	9.4	98	Rad mud and ooze	M. Eocene
8	2 – 1715	5312.2-5321.7	184.2-193.7	9.5	2.50	26	Rad mud and nanno rad mud	M. Eocene
9	2 – 1835	5321.7-5331.2	193.7-203.2	9.5	9.60	101	Rad mud and nanno rad mud	M. Eocene
10	2 – 2012	5331.2-5340.8	203.2-212.8	9.6	9.52	99	Muddy rad ooze and rad mud	M. Eocene
11	2 – 2145	5340.8-5350.3	212.8-222.3	9.5	1.27	13	Muddy rad ooze	M. Eocene
12	2 – 2335	5350.3-5359.8	222.3-231.8	9.5	0.60	6	Rad mud and chert	M. Eocene
13	3 – 0155	5359.8-5369.3	231.8-241.3	9.5	2.95	31	Claystone, nanno claystone, chert	M. Eocene
14	3 – 0605	5369.3-5378.7	241.3-250.7	9.4	1.64	17	Silicified claystone and chert	M. Eocene
15	3 – 0805	5378.7-5388.1	250.7-260.1	9.4	0.25	3	Silicified rad mudstone and chert	M. Eocene
16	3 – 1000	5388.1-5397.6	260.1-269.6	9.5	3.90	41	Silicified claystone and chert	L.-M. Eocene
17	3 – 1220	5397.6-5407.1	269.6-279.1	9.5	2.25	24	Silicified claystone, chert, and silicified calcareous claystone	L.-M. Eocene
18	3 – 1442	5416.7-5426.2	288.7-298.2	9.5	1.60	17	Silicified claystone, chert, and silicified calcareous claystone	L. Eocene
19	3 – 1710	5435.7-5445.2	307.7-317.2	9.5	4.40	46	Claystone and sponge spicule mudstone	L. Eocene
20	3 – 1940	5454.7-5464.2	326.7-336.2	9.5	4.20	44	Claystone, silty claystone, and nanno claystone	L. Eocene
21	3 – 2210	5473.7-5483.2	345.7-355.2	9.5	2.85	30	Rad mudstone, calcareous claystone, and chert	L. Eocene
22	4 – 0020	5483.2-5492.8	355.2-364.8	9.4	3.21	34	Rad mudstone	L. Eocene
23	4 – 0235	5502.3-5511.8	374.3-383.8	9.5	7.55	80	Silicified claystone	L. Eocene
24	4 – 0420	5521.3-5530.8	393.3-402.8	9.5	1.13	12	Silicified claystone	L. Paleo.
25	4 – 0640	5530.8-5540.2	402.8-412.2	9.4	3.95	42	Silicified claystone	L. Paleo
26	4 – 0815	5540.2-5549.8	412.2-421.7	9.5	4.40	46	Silicified claystone	L. Paleo.
27	4 – 1020	5568.8-5578.4	440.8-450.4	9.6	9.70	101	Claystone, calcareous claystone, and marly chalk	U. Maestr.
28	4 – 1207	5587.9-5597.4	459.9-469.4	9.5	0.60	6	Marly chalk	U. Maestr.
29	4 – 1405	5597.4-5606.9	469.4-478.9	9.5	4.95	53	Claystone	U. Camp.-L. Maestr.
30	4 – 1607	5616.5-5626.0	488.5-498.0	9.5	1.00	11	Claystone, rad mudstone, and muddy radiolarite	Cenomanian
31	4 – 1744	5635.5-5645.1	507.5-517.1	9.6	1.00	11	Claystone	U. Alb.-Cen.
32	4 – 1955	5645.1-5654.6	517.1-526.6	9.5	9.36	99	Claystone	U. Alb.-Cen.
33	4 – 2130	5654.6-5664.2	526.6-536.2	9.6	3.89	40	Claystone	U. Alb.-Cen.
34	4 – 2323	5664.2-5673.7	536.2-545.7	9.5	5.26	55	Claystone, rad mudstone, and muddy radiolarite	Albian
35	5 – 0110	5673.7-5683.3	545.7-555.3	9.6	6.68	69	Claystone, rad mudstone, and muddy radiolarite	Albian
36	5 – 0255	5683.3-5692.8	555.3-564.8	9.5	5.72	60	Claystone	Albian
37	5 – 0545	5702.3-5711.8	574.3-583.8	9.5	5.42	57	Claystone and rad mudstone	Haut./Barr.-Alb.
38	5 – 0745	5721.1-5730.6	593.1-602.6	9.5	1.65	17	Chalk and marly chalk	Haut./Barr.-Alb.
39	5 – 1053	5749.6-5759.1	621.6-631.1	9.5	2.10	22	Chalk and limestone	U. Haut.-L. Barr.
40	5 – 1300	5759.1-5768.6	631.1-640.6	9.5	2.33	25	Limestone and chalk	U. Haut.-L. Barr.
41	5 – 1505	5768.6-5778.2	640.6-650.2	9.6	1.08	11	Limestone, marly chalk, and chert	M. Haut.
42	5 – 1725	5778.2-5787.7	650.2-659.7	9.5	1.10	11	Limestone, marly chalk, and chert	L. Haut.
43	5 – 2005	5797.2-5806.7	669.2-678.7	9.5	0.10	1	Limestone	L. Haut.
44	5 – 2245	5806.7-5816.2	678.7-688.2	9.5	0.70	7	Limestone, marly chalk, and chert	L. Haut.
45	6 – 0140	5825.7-5834.9	697.7-706.9	9.2	0.5	5	Limestone, calcareous claystone, and chert	U. Valang.-Haut.
46	6 – 0500	5854.0-5863.4	726.0-735.4	9.4	2.25	24	Limestone, sideritic limestone, and chert	U. Valang.-Haut.
47	6 – 0750	5872.9-5882.4	744.9-754.4	9.5	1.00	11	Limestone and sideritic limestone	M. Valang.
48	6 – 1107	5891.7-5901.1	763.7-773.1	9.4	1.45	15	Limestone, sideritic limestone, and chert	M. Valang.
49	6 – 1532	5910.4-5919.9	782.4-791.9	9.5	6.60	69	Limestone, marly limestone, sideritic limestone, and chert	U. Berr.-L. Valang.
50	6 – 2040	5919.9-5922.5	791.9-794.5	2.6	2.9	112	Basalt	U. Berr.-L. Valang.
Total			Total cored	467.9 m				
			Total recovered		178.15 m			

% recovery in intervals cored = 38.1%
% recovery of depth drilled = 22.4%
% of depth drilled which was cored = 58.9%

---

[a] From rig floor, 10 meters above sea level.

[b] U = upper, L = lower.

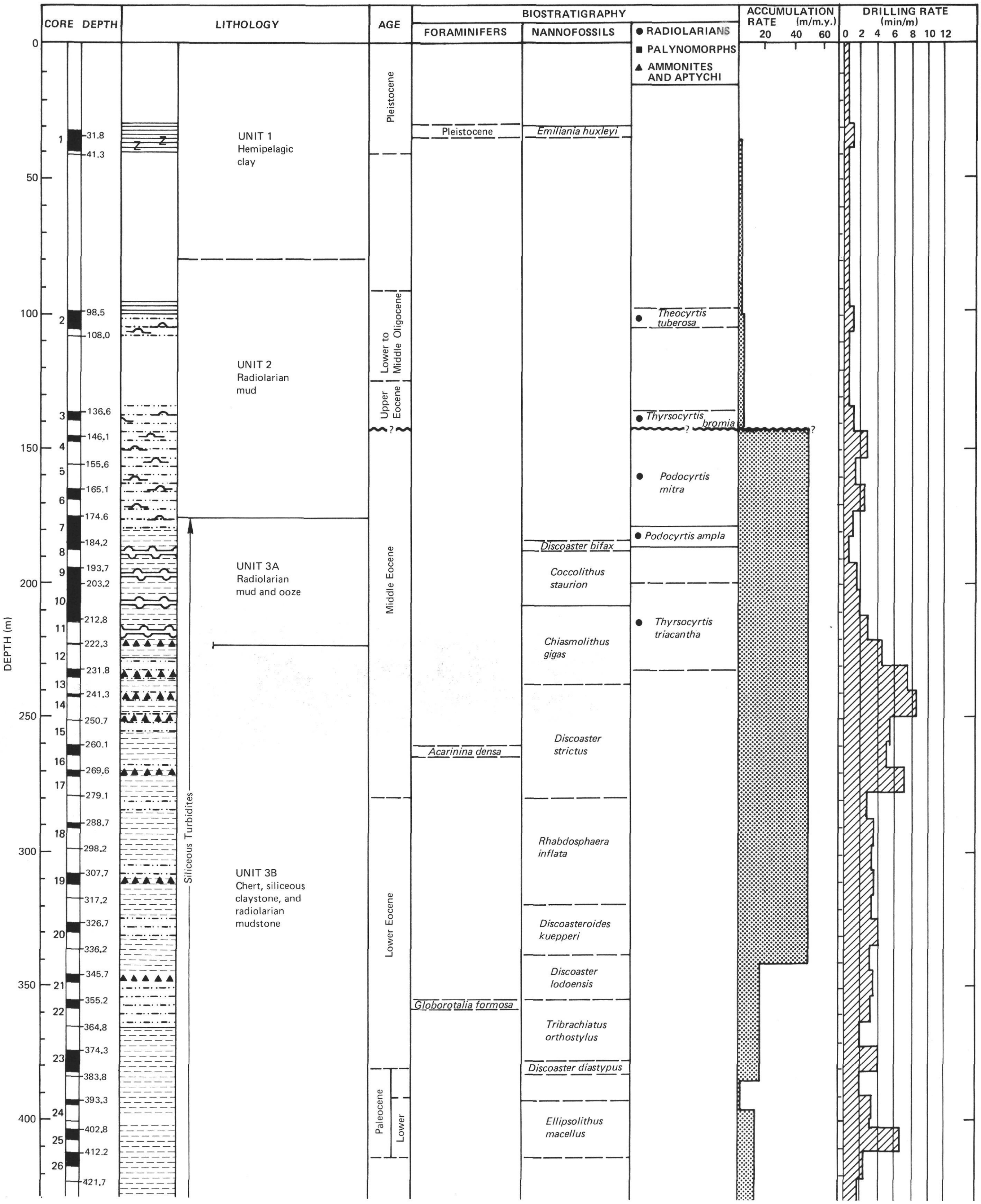

Figure 5. *Graphic hole summary, Site 387.*

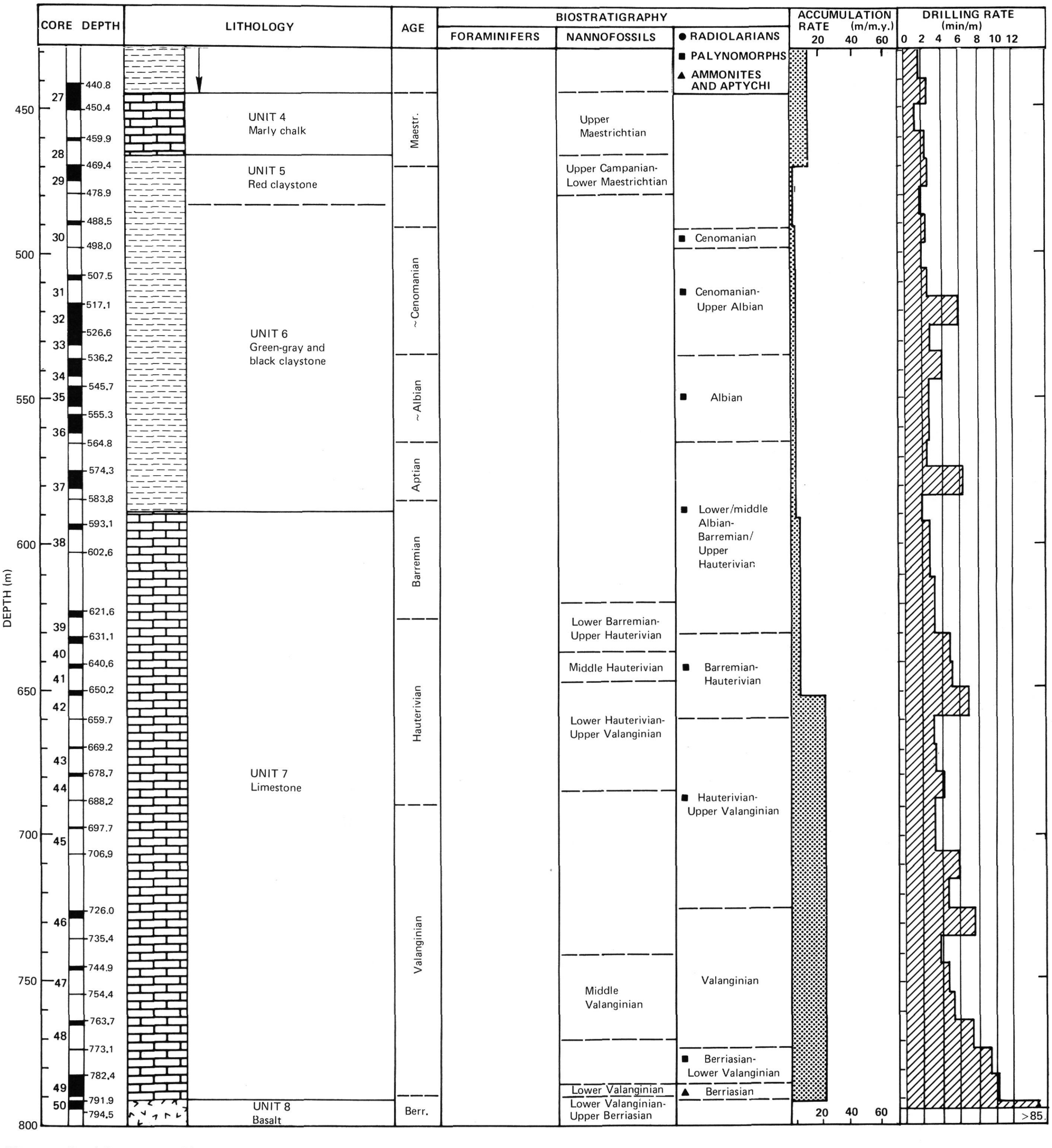

Figure 5. *(Continued).*

grained chips of basalt in the core catcher indicated that basaltic basement lay immediately beneath Core 49. Core 50 was drilled for 218 minutes, and penetrated 2.56 meters into basalt. The actual 2.9-meter recovery of hard basalt in this core was surprising and presumably includes a 30+ cm basalt column drilled during Core 49 coring but not trapped in the core catcher. Core 50 arrived on deck at 2040 hours, 6 August, and the drill string was immediately pulled; at this point, about 4.5 days of on-site time remained for Leg 43, and we planned to drill Site 388 near 33°04′N, 69°42′W.

The seal on the swivel above the Bowen sub ruptured when the unit was removed from the drill string, and large quantities of metal chips were found in the leaking oil. The unit could not be dismantled to check the damage until the entire drill string was pulled. Thus, early on the morning of 7 August, the swivel was dismantled, and the roller bearings and bearing race were found to be so severely damaged that further drilling without repair was out of the question. Because no spare parts nor spare swivel were on board, we were forced to cancel our plans for drilling Site 388 on the westernmost Bermuda Rise.

In lieu of drilling our final site, we conducted a detailed seismic survey around Site 387 on 7 August. We departed east-southeast from Site 387 at 1130Z, 7 August, making a Williamson turn to come west-northwest across Site 387 and make a sonobuoy recording; the sonobuoy record was of marginal quality. A second sonobuoy recording was attempted about 1800Z on a south-southwest track which took us just west of the site; interference from the ship's radio forced cancellation of the attempt. A third, successful sonobuoy recording was made early on 8 August along a southwest course across the site (Figure 3). One of the two EDO recorders became inoperable at this time, so that further surveying utilized only one recorder with a 10-second sweep. On 8 and 9 August we ran seismic lines eastward toward Site 386 and westward back through Site 387. These tracks are sub-parallel to the original profile between Sites 386 and 387 and are about 10 to 30 miles north and south of it. Because we had no satellite navigation, these surveys are mostly controlled by celestial fixes, with a few Loran C fixes of marginal quality and radar fixes on the Argus Island Tower near Bermuda. *Glomar Challenger* arrived in Norfolk, Virginia, early on the morning of 12 August 1975.

LITHOLOGY

Sediments

The main objectives of Site 387, like Site 386, were to determine the age and lithofacies of several regional seismic reflectors as well as the nature and age of the underlying basaltic crust. Nearly continuous coring through the 791.6-meter-thick sediment cover above basalt provided an excellent opportunity not only for geological interpretation of seismic data, but also for investigation of the sedimentary history from Early Cretaceous to Holocene time in the western North Atlantic Ocean. The section at Site 387 is comparable with those recovered in several previous holes in both the western and eastern basins of the ocean, providing the opportunity for broad lateral correlations of oceanic sedimentary formations.

The sedimentary sequence at Site 387 is divided into eight lithologic units, the deepest unit being basalt (Table 2); one of these (Unit 3) is sub-divided into two sub-units on the basis of differences in sediment diagenesis. Unit 3 at Site 387 correlates with Unit 4 of Site 386, and Units 5 and 6 at each site are correlative.

A graphic summary of smear-slide analyses of sediment composition is given in Foldout VI in the back cover pocket.

Unit 1—Hemipelagic Clay (0 to >41.3 m)

The sediments of this unit were recovered in Core 1 and were found in Section 1 of Core 2 as an intensely disturbed drilling slurry that is probably downhole contamination. Thus, the lower boundary of the unit is placed in Core 2, Sec. 1, 150 cm, rather than at the apparent contact Sample 2-1, 150 cm. Absolute thickness of the unit is unknown but is between 41.3 meters and 98.4 meters, assuming the hemipelagic clay extends upward to the present sea floor. Numerous piston cores from this region contain hemipelagic clay and support the assumption.

Unit 1 is composed of Quaternary and older homogeneous pale brown clay with scattered black spots of iron-manganese oxide. In the uppermost part (1-1, 80-110 cm) it contains up to 10 per cent nannofossils and 1 per cent foraminifers. Calcareous biogenic debris is absent in the lower part of the core. The calcareous clay may be either downhole contamination or a disturbed interbed in the clay section.

Smear-slide analysis shows that the hemipelagic clay consists almost entirely of a clay-size matrix (96% clay from grain-size analysis) with a minor admixture of zeolites, terrigenous clastic minerals (quartz, feldspar, mica), manganese micronodules, and rhodochrosite. In the lower part (1-5, 75 cm) radiolarians appear.

Total clay-mineral content, as determined by X-ray analysis, is about 80 per cent and consists of almost equal proportions of mica and montmorillonite. The relatively high quartz content (15%) is distributed in the silt- and clay-size fraction. The fraction coarser than 50 μm is less than 1 per cent of the sediment and consists of siliceous, calcareous, and phosphatic (bone) debris; authigenic rhodochrosite; and minor quartz, opaques, and clinopyroxene.

The organic carbon content is low (0.1%), iron is slightly enriched (5.5%), and manganese is low (0.1%).

Unit 2—Radiolarian Mud (41.3-98.4 to 175.2 m)

Unit 2 (Core 2 to Core 7, Sec. 1, 55 cm) differs from the overlying unit in both color and composition. The sediment is soft, homogeneous, radiolarian mud of middle Eocene to middle Oligocene age, and its color is pale olive to yellowish gray with pale green diffuse mottles. It is similar to the Holocene radiolarian mud that is widespread in the equatorial Pacific and Indian oceans. The mud consists dominantly of a clay matrix (70 to 85% from smear-slide determinations) and biogenic siliceous matter (radiolarians, diatoms, sponge spicules) ranging from 10 to 30 per cent. Biogenic silica tends to increase downward in the unit.

Total clay-mineral content was estimated by X-ray diffractometry as 80 to 90 per cent of the crystalline phase of the sediment. In the < 2 μm fraction, montmorillonite dominates over mica with a minor kaolinite and chlorite admixture (Koch and Rothe, this volume). Rare (1 to 2%) clinoptilolite was found, and fine-grained quartz ranges from 4 to 15 per cent.

In the coarse fraction (> 50 μm) the most abundant light mineral is biogenic opal; biogenic phosphate particles are common, and quartz and zeolites are rare. Heavy minerals are represented mainly by authigenic rhodochrosite and siderite (30 to 80% of the heavy fraction) and by unspecified opaques (10 to 20%).

TABLE 2
Lithologic Units at Site 387

Unit		Lithology	Age	Thickness (m)	Sub-Bottom Depth at Bottom of Unit (m)	Cores
1		Hemipelagic clay	Quaternary and older	41.3-98.4	41.3-98.4	1
2		Radiolarian mud	M. Oligocene to M. Eocene	75.7-133.9	175.2	2 to 7-1, 55 cm
3A	Siliceous turbidites	Radiolarian mud and ooze	M. Eocene	48.6	223.8	7-1, 55 cm to 12-1, 145 cm
3B		Chert, siliceous claystone, and radiolarian mudstone	M. Eocene to L. Paleocene	220.0	443.8	12-1, 145 cm to 27-2, 148 cm
4		Marly chalk	U. Maestrichtian	25.6	469.4	27-2, 148 cm to 28
5		Red claystone	L. Maestrichtian to U. Campanian (?)	9.5-19.1	>478.9	29
6		Greenish gray and black claystone	Cenomanian to Barremian	95.3-114.2	>583.8	30-37
7		Limestone	Barremian to L. Valanginian	198.9-208.1	791.9	38-49
8		Basalt		–	–	49, CC to 50

Low organic carbon (0.1%), and moderate iron (3.8 to 4.4%) and titanium (0.34 to 0.49%) content is common for this type of sediment. Manganese is rather high (0.24 to 0.31%) owing to the presence of rhodochrosite.

Unit 2 is probably pelagic, as is indicated by its composition and low accumulation rate (2-3 m/m.y.). It was deposited beneath surface waters with relatively high biological productivity compared with modern low productivity in the region.

The lower boundary of Unit 2 is moderately abrupt and is placed in Core 7, Section 1, at 55 cm (175.2 m sub-bottom), where clear turbidite stratification first appears below an interval of drilling disturbance.

Unit 3—Siliceous Turbidites (175.2 to 443.8 m)

As a whole, this unit (Core 7, Sec. 1, 55 cm to 27-2, 148 cm) represents a thick rhythmically stratified sequence of siliceous (radiolarian) clay and ooze of turbidite aspect. The turbidite rhythms are similar in appearance and thickness throughout the unit despite significant variation in composition and lithification. The 269-meter-thick unit was deposited very rapidly (48 m/m.y.) in the late early and early middle Eocene time.

The unit is composed of numerous rhythmically alternating layers, each consisting in the ideal case of five sublayers, indicated by the characters (from bottom to top), α, β, γ, δ, and ϵ, as at Site 386 (Figure 6). Thickness of a single rhythmic layer ranges from 10 cm to as much as 200 cm, but most layers are 30 to 40 cm thick. From top to bottom the sublayers are:

ϵ—dark greenish gray with abundant mottles and streaks elongated sub-parallel to bedding; very fine-grained.

δ—lighter greenish gray with dark burrow mottles, fine-grained.

γ—light greenish gray, homogeneous, fine-grained; size-grading is recognized by Coulter-counter grain-size analysis (McCave, this volume).

β—greenish gray or olive, thinly laminated, sometimes cross-laminated, in other cases faintly laminated, coarser, enriched in radiolarians and sponge spicules.

α—greenish gray to olive-gray, coarser, massive, commonly graded from silty clay or silt in the upper part to sandy silt or fine sand in the basal part, rich in sponge spicules and large radiolarians; in some cases, contains carbonate clasts or terrigenous silt. The basal contact with the underlying ϵ sublayer is sharp.

The complete sequence, just described, is seldom developed in each rhythm. The α sublayer is frequently missing, and in some cases both α and β are absent. The visually homogeneous, but finely graded γ, as well as the mottled ϵ sub-layers, are usually best developed. Although in several rhythms only the ϵ and basal γ sublayers are present, cyclic sedimentation is evident.

Unit 3 is sub-divided into two sub-units on the basis of lithification; Sub-unit 3A is less lithified radiolarian mud and ooze, whereas 3B is silicified claystone, mudstone, and porcelanite. The boundary between the two sub-units is placed in Core 12, Section 1, at 145 cm, at the first downhole appearance of porcelanite, although a distinct change from radiolarian mud to stiff mudstone occurs in Core 11. This change corresponds to a decrease in core recovery, starting in Core 11, and to a decrease in drilling rate (Figure 5).

Sub-Unit 3A—Radiolarian mud and ooze

This sub-unit comprises the interval between Core 7, Section 1, 55 cm and Core 12, Section 1, 145 cm, spanning a thickness of 48.6 meters. It was cored almost continuously with good core recovery and minor drilling

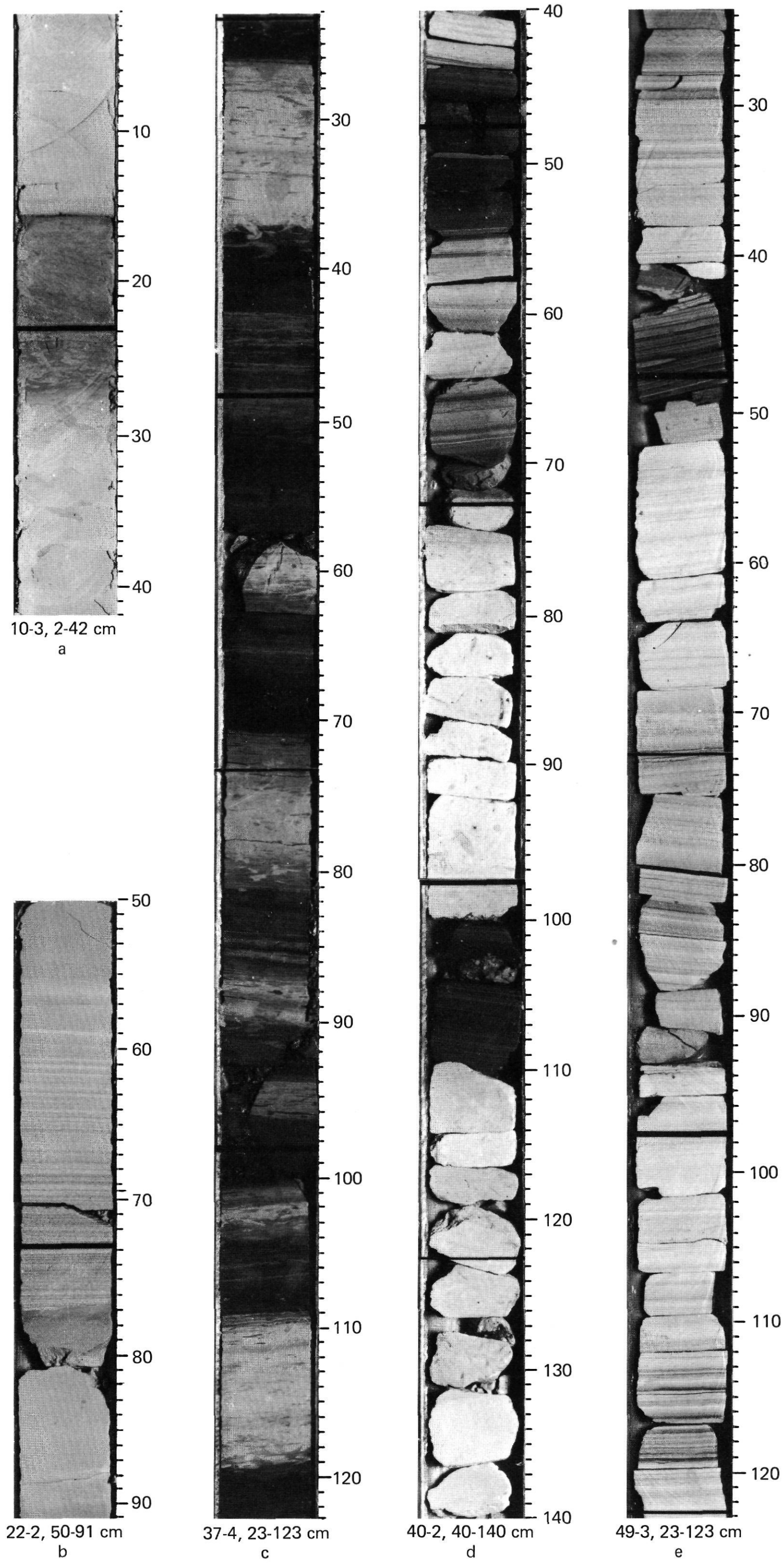

10-3, 2-42 cm
a

22-2, 50-91 cm
b

37-4, 23-123 cm
c

40-2, 40-140 cm
d

49-3, 23-123 cm
e

Figure 6. *Examples of lithofacies at Site 387. (a) Siliceous turbidites in lithologic Sub-unit 3A; from bottom: δ (light, calcareous homogeneous to mottled), ϵ (dark, bioturbated), overlain by β (light, laminated). (b) Siliceous turbidites in Sub-unit 3B; from bottom: gradation from β (laminated) through ϵ (dark, mottled), overlain in erosional contact by α (coarse-graded, laminated) through β (finer, laminated) and δ (homogeneous). (c) Green-gray and black claystones of Unit 6. (d) Massive, bioturbated limestone and laminated limestone of Unit 7. (e) Laminated limestones of Unit 7.*

disturbance through Core 10. The sediments are clayey radiolarian ooze, radiolarian mud, and calcareous radiolarian mud with sponge-spicule mud interbeds, including about 30 rhythmic layers. The main constituents of the sediments are clay matrix and siliceous microfossils (radiolarians, diatoms, sponge spicules). Calcareous biogenic matter (nannofossils and foraminifers) are common only in carbonate-rich sublayers. The relative abundance of constituents varies within each rhythmic layer and from one layer to another. At the same time, broad compositional changes occur downhole, so that the upper part of the sub-unit (Core 7) is rich in radiolarians (smear-slide average is 45%), the middle part (Cores 8 to 10) contains calcareous interbeds, and the lower part (Cores 11 and 12) is non-calcareous with a matrix consisting mainly of clay. Within each rhythmic layer the top, ϵ sublayers are the finest grained, non-calcareous, and relatively high in radiolarians, and they probably represent pelagic deposition. The δ and the γ sublayers contain the highest carbonate (up to 22%), radiolarians are less abundant, and clay is more abundant. Grading in grain size in the δ and γ sublayers can be determined only by detailed grain-size analysis. The basal α and β sublayers are enriched in radiolarians (radiolarian sand interbeds), sponge spicules, and rarely in foraminifers. Where the basal sublayer is a γ sublayer, the lower contact is sometimes marked by a thin (1-2 mm) coarse interbed of spicule mud or terrigenous (quartzose) silt with glauconite.

X-ray diffraction analysis generally confirms the compositional variations noted in smear slides. Quartz content ranges from 4 to 15 per cent and is higher in the basal sublayers, even where these are not represented clearly by a γ or β sublayer. For example, in the calcareous and homogeneous γ sublayer in Sample 8-2, 15-18 cm, quartz ranges up to 15 per cent. The uppermost sublayers (including ϵ) usually contain less quartz (4 to 7%) and more clay minerals (90 to 93%). Mica and montmorillonite are the dominant clay minerals in the <2 μm fraction. Mica tends to be enriched in the γ sublayers, whereas montmorillonite predominates in the pelagic ϵ sublayers.

The sediments of Sub-unit 3A are low in organic carbon (0.1 to 0.3%). Iron (1.77 to 2.41%) and titanium (0.19 to 1.25%) values are those common for siliceous mud and ooze. Manganese appears to be slightly enriched in several samples (e.g., 0.45% in Sample 7-3, 83-85 cm), where some rhodochrosite occurs.

Sub-Unit 3B—Silicified Claystone, Radiolarian Mudstone, and Chert

Sub-unit 3B spans the interval from Core 12, Section 1, 145 cm, to Core 27, Section 2, 148 cm, and has a total thickness of 220.0 meters (Table 2). It was cored continuously or alternately. Core recovery was relatively low, especially in the upper part of the sub-unit, where porcelanitic chert interbeds are common. Many softer layers were undoubtedly washed out in this interval.

Lithology of Sub-unit 3B is not uniform. In the upper part (Cores 12 to 18) it is greenish gray or olive-gray siliceous claystone with chert and calcareous mudstone interbeds; in Cores 19-20 and 23-24 greenish gray claystone predominates; in Cores 21-22 it is mostly greenish gray radiolarian mudstone. Brown or olive-brown interlayers occur in Cores 22 and 23. In the lowermost part (Core 24 to Core 27, Section 2, 148 cm) black carbon-enriched claystone alternates with greenish gray claystone; these cores are similar to the Unit 6 lithology, described below.

The main constituents of the sediments as determined from smear slides are: (1) clay matrix (including altered siliceous debris, which was not separately identified in smear slides); clay ranges from about 40 to 95 per cent, being highest in the lowermost part of the sub-unit; (2) recrystallized radiolarians, partly replaced by pyrite, ranging from rare occurrences in claystone layers to abundant (up to 50 per cent) in the basal sublayers of the rhythmic beds where altered radiolarian sand and silt was observed; (3) sponge spicules, also recrystallized and in some cases pyritized, ranging from nil to 25 per cent or more in the basal sublayers (sponge-spicule mudstone); (4) calcareous debris, represented by nannofossils and unspecified carbonate, the latter being mostly micritic; foraminifers are rare, increasing only in some basal sublayers of the rhythmic beds; $CaCO^3$ content ranges from 0 to 40 per cent (average of 59 determinations is 11%); (5) other minor constituents are terrigenous clastic minerals (quartz, mica, feldspar, and some heavy minerals), pyrite, glauconite, rhodochrosite, and siderite. Pyrite was found in most smear slides, and in some of the basal sublayers the amount reaches 5 per cent or more.

Silicification is significant throughout Sub-unit 3B, as shown by the visual core descriptions (claystone, silicified claystone, and porcelanitic chert), physical properties, smear-slide analyses, and shore-laboratory investigations of X-ray diffraction, bulk chemistry, scanning electron microscopy, and thin-section descriptions (see Riech and von Rad, this volume). Disordered cristobalite was found by X-ray in most samples, ranging from 2 to 18 per cent (no cherts were X-rayed). The black layers in the lowermost part of Sub-unit 3B contain no cristobalite, but quartz increases sharply, being as high as 35 per cent in black claystone of Sample 26-1, 48-50 cm (Koch and Rothe, this volume). Probably the "quartz" is authigenic chalcedony, formed after cristobalite. Scanning electron microscopy shows abundant cristobalite (opal CT) lepispheres in several samples of the sub-unit, in some cases in association with clinoptilolite crystals. In thin sections one can distinguish an opal-cristobalitic matrix with very weak birefringence and low refraction index. SiO_2 content (H_2O-free basis) in two samples analyzed by X-ray fluorescence is 86.0 per cent in Sample 25-3, 144-146 cm (homogeneous grayish olive claystone), and 73.2 per cent in Sample 26-2, 0-2 cm (laminated olive-black claystone). The SiO_2/Al_2O_3 ratios are 13.1 and 5.8, respectively, and are higher than those common in hemipelagic clay.

Hard cherts are common only in the upper part (Cores 12 to 18) of Sub-unit 3B, being most abundant in

Core 17. When interbedded with softer claystone or silicified claystone, the cherts are usually within the ϵ sublayer adjacent to the overlying coarser, and usually radiolarian-rich, sublayers (α, β, γ). It is noteworthy that cherts do not occur in Cores 21 and 22, although radiolarians and other siliceous biogenic materials are abundant. No cherts are formed in the black carbon-enriched claystones in Cores 24 to 27.

Organic carbon content in Sub-unit 3B is variable, ranging from 0.1 per cent in greenish gray or olive silicified claystone and radiolarian mudstone up to 1.3 per cent in the black layers of cores 24 to 27. The average of 18 determinations is 0.3 per cent. Iron and titanium content is low in greenish gray silicified claystone (1.50 to 1.57% Fe; 0.12 to 0.15% Ti) and increases slightly in brown and black claystone (4.15 to 4.30% Fe; 0.31 to 0.32% Ti). Manganese is generally low (0.01 to 0.04%); a single higher value (0.21%) was determined in a brown interbed (Murdmaa et al., this volume).

Sub-unit 3B in the upper part (Cores 12 to 23) is presumed to represent fine-grained turbidites because of the similarity with Sub-unit 3A in α to ϵ sublayers (Figure 6). Rapid sediment accumulation in this part of the sub-unit provides supporting evidence. In the lower part of Sub-unit 3B the absence of the α to ϵ sublayers as well as the occurrence of black carbon-enriched interbeds suggests a hemipelagic depositional environment.

The lower boundary of Sub-unit 3B in Core 27, Section 2, 148 cm, is distinct and is indicated by a color change from dark to light greenish gray and by a sharp increase in $CaCO_3$ content.

Unit 4—Marly Chalk (443.8 to 469.4 m)

This unit consists of 25.6 meters of upper Maestrichtian chalk between the Unit 3 and Unit 5 claystone units (Table 2). It is homogeneous olive to light olive-gray marly chalk with minor greenish gray calcareous claystone interbeds. The main constituents of the sediments are a clay matrix (50 to 70%) and carbonate (29 to 50%, average 41%); the carbonate fraction is 25 to 35% nannofossils, the remainder being unspecified micritic carbonate. Rare foraminifers and terrigenous clastic minerals are present. Authigenic pyrite, rhodochrosite, and/or siderite are present in trace quantities. Low iron (1.66 to 2.67%) and titanium (0.24%) were determined in two samples. Manganese ranges from 0.09 to 0.22% (Murdmaa et al., this volume). Organic carbon is rather high (0.7 to 0.8%).

No primary sedimentary structures were observed in Unit 4, and the unit is interpreted as pelagic sediment deposited above the calcite compensation depth (CCD).

The lower boundary of Unit 4 is placed at the bottom of Core 28. Core 29, immediately underlying Unit 4, contains reddish brown claystones with no chalk.

Unit 5—Red Claystone (469.4 to >478.9 m)

Reddish claystone was recovered only in Core 29, but the total thickness of the unit could be as much as 19.1 meters because one joint was uncored between Cores 29 and 30. The unit is composed of dark reddish brown, moderately stiff claystone with several thin greenish gray and red interbeds and white streaks. Average composition as determined from smear slides is 91 per cent clay, 4 per cent zeolites, and 2 per cent altered volcanic glass with less than 1 per cent each of unspecified carbonate, radiolarians, clastic minerals, hematite, and palagonite. In a single sample (29-2, 64-66 cm), 30 per cent carbonate was determined, half of which is high-magnesian calcite (Koch and Rothe, this volume).

Iron content in the reddish brown claystone is relatively high (5.54 to 5.78%). Titanium content is rather low (0.40 to 0.48%) compared with volcaniclastic variegated claystones of Sites 382 and 385. Manganese is low (0.08%) in one sample and slightly enriched (0.53%) in another (Murdmaa et al., this volume).

The total SiO_2 content (H_2O free basis), in Sample 29-2, 12-15 cm is 59.5 per cent, and Al_2O_3 in the same sample is 21.4 per cent. In Sample 29-4, 101-106 cm Al_2O_3 reaches 23.0 per cent, exceeding values for common pelagic red clay.

The accumulation rate for the red claystones is poorly known, because the sediments are almost barren of microfossils. Provided there are no hiatuses in the section, the red claystones accumulated at about 1 m/m.y. between the deposition of middle Cenomanian-Turonian black clays (Core 30) and the upper Maestrichtian marly chalks (Core 28). These are true pelagic rates and are even less than the low rates (2 m/m.y.) calculated for the multicolored clays at Site 386.

Unit 6—Gray-green and Black Claystone (478.9-488.5 to 583.8-593.1 m)

This unit is represented in Cores 30 to 37; both the upper and lower contacts fall in uncored intervals where one joint was skipped. The total thickness is at least 95.3 meters (Table 2). The unit was cored almost continuously, and core recovery was relatively good so that a well-documented section was obtained. The unit corresponds both lithologically and stratigraphically with Unit 6 at Site 386, as well as with black clay lithofacies drilled in other western North Atlantic holes (5, 101, 105, and 391) and holes in the eastern and South Atlantic. At Site 387 the unit spans a stratigraphic interval from Cenomanian to approximately Barremian, and the average accumulation rate may be only 3-4 m/m.y. However, similar black carbon-rich beds were also found in the Paleocene (Cores 24 to 27), separated from Unit 6 by red clay (Unit 5) and marly chalk (Unit 4). Black carbon-rich marl interbeds also appear in the upper part of the underlying Unit 7 limestones (see below), indicating that sporadic reducing conditions both preceded and followed deposition of the bulk of the black clays.

Unit 6 is composed of claystone with minor amounts of radiolarian mudstone and radiolarite. The most prominent feature of the unit is an alternation of black to gray-black and dark green-gray colors (Figure 6). The proportion of black layers gradually increases downward, to as much as 70 per cent in Core 36, Sections 3 and 4. However, the proportion of black beds is still less than that in the black-clay unit at Site 386. The color banding displays more or less rhythmic behavior. As a rule, a black or very dark green-gray layer with sharp upper contact grades downward to a lighter greenish gray layer with abundant and distinct black burrow mottles, and then to an almost homogeneous gray layer that has a sharp basal contact. Changes in sedimentary structures and texture are also rhythmic, but these do not correspond simply to color stratification. Distinct coarse layers, usually laminated like the β sublayers of Unit 3, consist of altered (recrystallized, pyritized) radiolarians and spicules with abundant pyrite, and in some cases siderite. Radiolarian content drops to trace quantities outside these beds. Some of these layers are calcareous and contain foraminifers, nannofossils, and unspecified carbonate. The coarse layers are several millimeters to centimeters thick and have sharp boundaries. They are found both in gray and, more commonly, in black layers.

The mottled, green-gray claystones have uniformly low organic carbon content, but gray and black layers have wide ranges of organic carbon (0.5 to 14%). Black layers differ from the gray intervals in that they tend to contain abundant finely disseminated pyrite. In laminated intervals, thin sections show an alternation of distinct, wavy, dark carbon-rich and lighter claystone laminae. Burrow mottling is most extensive in the gray and green-gray layers, but it also occurs locally in the thinner black layers in the upper part of the unit.

X-ray data (Koch and Rothe, this volume) show a very high quartz content throughout both the black and gray intervals in Unit 6 (18 to 50%; average of 13 analyses is 39%). Much of the "quartz" is authigenic chalcedony, visible in thin sections of the radiolarite and claystone as a weakly birefringent poikiloblastic matrix. This observation is supported by quartz to feldspar ratios which range from 6.2 to 25.0 (average of 12 analyses is 14.6); these ratios are much higher than those of other units (Unit 2—3.2; Sub-unit 3A-3.5; Sub-unit 3B—4.1). A single bulk analysis of greenish gray claystone in Sample 37-2; 101-103 cm (which exhibits no radiolarians in thin section) yields 76.7 per cent SiO_2, 10.3 per cent Al_2O_3, and an SiO_2/Al_2O_3 ratio of 7.45. These values are in the same range as the claystones of Sub-unit 3B and are higher than the values in common hemipelagic clay (Murdmaa et al., this volume). These data suggest diagenetic silicification wherein the chalcedony (or quartz) probably was formed by the recrystallization of cristobalite.

The lower contact of Unit 6 was not recovered; it lies somewhere in the 9.5-meter uncored interval between Cores 37 and 38.

Unit 7—Limestone (583.8-593.1 to 791.9 m)

Unit 7 contains more than 198.8 meters of upper Berriasian/lower Valanginian to upper Hauterivian/lower Barremian limestones and chalk. The unit is encompassed by Cores 38 to 49. On the basis of core recovered, the contact with underlying basaltic basement is in the core-catcher sample of Core 49, at a depth of 37 cm (791.9 m sub-bottom). However, the recovery of 2.9 meters of basalt in Core 50, which penetrated only 2.65 meters, suggests that basalt may occur at 791.6 meters sub-bottom (see Operations).

Limestones dominate the unit, and there are minor interbeds of finely laminated olive-gray to black marly chalk, marl, or calcareous claystone. Cores 38 and 39 at the top of the unit contain chalk with minor limestone interbeds. Chert fragments occur in nearly every core and dolomitized marls appear in the lower part of the unit.

Prominent stratification is distinguished as alternating beds, from several centimeters to 30-40 cm thick, of the following lithofacies:

1)White, very light gray, or bluish gray, hard, massive limestone, usually bioturbated (Figure 6). Carbonate content in the limestone is very high, usually more than 90 per cent (up to 99.5%). The limestone consists of unspecified micritic calcite with minor admixtures of clay minerals (1 to 6%) and quartz (1 to 2%) (Koch and Rothe, this volume). In Cores 45 to 49 the limestone is slightly dolomitized (1 to 10% dolomite). The bioturbated limestones first appear as small pieces in Core 39, Section 2, and increase in abundance downward; they are especially prominent in Cores 40 to 47.

2) Light gray, thinly laminated and in some cases rhythmically laminated limestone, grading to marly limestone (see below). The limestone is composed of alternating darker (marly) and lighter laminae less than one mm thick. Carbonate content is somewhat lower (82 to 88%) than in the bioturbated limestones. This lithofacies is well developed mostly in the lower part of the unit, and it dominates Core 49, which is extensively dolomitized (Figure 6). Wood fragments and ammonite fragments (Renz, this volume) occur in this limestone facies.

3) Olive-gray and dark greenish gray to olive-black marly chalk, marly limestone, or calcareous claystone which is dolomitic in the lower part of the unit and is distinctly laminated to thinly laminated. Parallel, horizontal, and sometimes slightly wavy laminae are alternately darker (carbon-rich, clayey) and lighter (more calcareous). Carbonate content of bulk samples ranges between 28 and 79 per cent, and the average is about 60 per cent. The dark laminae are enriched in organic carbon (1.1 to 4.8 %). Siderite and dolomite are present, the latter being as high as 54 per cent in Sample 46-1, 119-121 cm (Koch and Rothe, this volume). Thin sections show more dolomite rhombs in dark marly layers than in the lighter limestones. Pyrite is common in the dark layers, locally as sand-size crystals and micronodules. Dark laminae are more abundant in the upper part of the unit (Cores 38 and 39).

4) Light olive-gray graded limestone with faint carbonate clasts at the base, alternating with the laminated marly chalk (type 3) in Cores 38 and 39. Carbonate content is about 90 per cent.

5) Siliceous limestone with relics of altered radiolarians (20 to 30%) replaced by chalcedony forms thin interbeds in Core 41 and may occur in other cores as well.

6) Hard gray chert was found as small pieces in the limestone and marly limestone.

Lithofacies described above form a rhythmically alternating sequence. In the upper part of the unit (Cores 38 and 39) the succession consists of basal layers of graded chalk with carbonate clasts and sharp basal contacts (type 4), overlain by laminated marly chalk (type 3), and in turn overlain by bioturbated chalk layers. These sequences resemble the pelagic turbidites cored on DSDP Leg 11 (Lancelot et al., 1972). In Cores 40 through 48, dark (?basal) laminated marly chalk layers (type 3) grade upward into laminated limestones (type 2) and alternate with light bioturbated limestone (type 1) (Figure 6). Sediment reworking in the laminated members is probable, whereas bioturbated interbeds represent a purely pelagic depositional environment. Core 49 consists entirely of laminated limestone and marly limestone (types 2 and 3), and it is dolomitized except in the lowermost part (Core 49, Sec. 5, 135 cm to 49, CC) where bioturbated limestone occurs with minor cherts.

In the bottom of Core 49, core catcher pieces of altered basalt, together with chert fragments, occur in a highly disturbed reddish brown calcareous clay matrix. The clay contains 20 per cent unspecified carbonate, 12 per cent authigenic carbonate rhombs (dolomite and ?siderite), and minor quantities of nannofossils, radiolarians, and mica. Although the reddish clay was recovered only as a disturbed plastic mass, the uphole absence of any similar lithology indicates the sediment was in place. The composition of the clay is virtually identical to dark marly interlayers in the overlying limestone sequence and is similar to that of sediment enclosures in the underlying basalt. Therefore, the clay may represent the remnant of a baked contact with the underlying basalt.

Depositional History — Summary

Deposition at Site 387 began in early Valanginian to late Berriasian time with relatively fast accumulation (23 m/m.y.) of calcareous and marly sediments. The lowermost sedimentary layers were probably intruded by a basalt sill (see discussion of basalt, below). A thin, basal calcareous claystone was baked and oxidized at the basalt contact, and fragments of the soft sediment were incorporated in the basalt.

Sedimentary structures in the calcareous sediments are indicative of both pelagic sedimentation and near-bottom lateral sediment transport. The bioturbated limestones are pelagic members of the sequence, whereas lamination and grading are more likely produced by turbidity currents. Bottom currents (tidal?) may provide an alternative explanation of the fine laminae. High carbonate content in the pelagic members demonstrates deposition above the CCD. The laminated marly interbeds indicate either fluctuations in the level of the CCD or, more likely, rapid influxes of clays and organic matter. Local reducing conditions in the darker interbeds are indicated by pyrite.

The sudden cessation of carbonate accumulation in Barremian time, when deposition of non-calcareous black and gray claystone began, may be attributed to increasing depth or, more likely, to the effect of a shoaling CCD as the deep basin became stagnant. It is significant that the Unit 6 claystones as a whole do not contain much more organic matter than marly chalk interbeds in Unit 7. Thus, the supply of organic matter was roughly comparable in both units.

Possible environments leading to deposition of the Cretaceous "black clays" are discussed elsewhere in this volume (Kendrick; Tucholke and Vogt) as well as in several papers based on DSDP Legs 11, 40, and 41. A stagnant-basin model is preferred here, although at first this interpretation appears to be at odds with the presence of burrow mottling in thin black layers within the upper part of Unit 6. The discrepancy may be explained by burrowing activity in the aerobic environment which immediately followed the black "stagnant" cycles.

Very slow sediment accumulation or a hiatus between middle Cenomanian/Turonian black claystones (top of Unit 6) and upper Campanian/lower Maestrichtian red claystones (Unit 5) marks the cessation of anoxic basin conditions. The red claystone of Unit 5 may be interpreted as a stratigraphically compressed pelagic bed or it may include several hiatuses. Deposition was well below the CCD.

In late Maestrichtian time depression of the CCD resulted in deposition of a uniform hemipelagic marly ooze (Unit 4). The CCD rose again in the Paleocene, and non-calcareous clay and radiolarian mud were deposited with sporadic pulses of euxinic black clays.

By early Eocene time, significant siliceous hemipelagic sediments began to accumulate, and extremely rapid sedimentation dominated the late early and early middle Eocene. Clastic silt and sand is rather rare in these sediments, and an abundant supply of terrigenous clay must have contriubted to the high accumulation rate; high productivity of siliceous organisms was responsible for abundant biogenic silica in the sediments. The mechanism of deposition is presumed to be turbiditic, as indicated by subtle size-grading in the rhythmic sequences (McCave, this volume). However, in contrast with common turbidites, the basal members of these rhythmic sequences do not contain coarse, shallow-water material. The basal layers consist of biogenic pelagic (radiolarian) or deep water benthic (sponge spicule) siliceous particles that apparently are redeposited. Unlike the turbidites at Site 386, those at Site 387 seldom contain calcareous layers. The limited number of adjacent topographic highs and the unusual thickness of the Eocene turbidites make it unlikely that the flows were a local phenomenon. Thus the turbidites may represent distal deposition from flows that originated along the North American continental margin; such an abyssal-plain environment prior to the uplift to the Bermuda Rise was suggested by Ewing et al. (1969).

An abrupt cessation of turbidite accumulation in the middle Eocene is marked by a possible hiatus within Unit 2 (radiolarian mud). This cessation may have been caused by the middle Eocene uplift of the Bermuda Rise; supporting evidence is given by volcaniclastic turbidites at Site 386 which first record the denudation of the Bermuda volcanoes in late middle Eocene time. High productivity of siliceous organisms in the surface water continued into at least the late Oligocene (Core 2), but prior to the Pleistocene a low productivity environment became established.

Two broad conclusions may be drawn from the sedimentary record at Site 387: (1) The entire sedimentary record represents a deep-water sequence, with deposition mostly below the CCD. Only in the early Cretaceous (Neocomian) and for a short period in Maestrichtian was the CCD depressed below the sea floor. (2) A substantial thickness of the sedimentary section (Units 3, 6, 7) displays clear evidence of cyclic sedimentation and lateral sediment transport, most likely by turbidity currents.

Basalt

At Site 387 basement was reached at a nominal sub-bottom depth of 791.9 meters and was penetrated to a total hole depth of 794.5 meters, resulting in a recovery of 2.96 meters of basalt (Core 50).

Megascopic and Petrographic Description

Immediately overlying the basalt at 791.8 to 791.9 meters (Sample 49, CC), a small quantity of pale grayish red calcareous clay, intensely disturbed and containing fragments of chert and basalt, was recovered. The basalt fragments are mineralogically and texturally consistent with the underlying section. Except for its color, the calcareous clay is virtually identical in composition to the overlying limestone sequence.

Basalt recovered in this hole is generally a grayish black, holocrystalline, fine-grained, amygdaloidal phyric basalt characterized by a variable groundmass texture and by local enclosures of grayish red to dark reddish brown calcareous claystone. Phenocryst phases consist of common, partially corroded, subhedral, prismatic plagioclase (An 70 to An 80; 0.072-3.24 mm, averaging 0.75 mm) twinned according to the albite law, and rare, corroded, sub-angular pyroxene crystals. Slight alteration of plagioclase phenocrysts to montmorillonite and sericite gives the crystals a turbid appearance. Pyroxene phenocrysts display variable optic angle, always positive and less than 20°, suggesting compositions between pigeonite and sub-calcic augite. Corroded phenocrysts of both phases display optical strain. The dearth of alteration products associated with corroded phenocrysts suggests the corrosion reflects resorption of these early formed crystals.

Glass occurs at two distinct levels. Scarce dark basaltic glass was scattered throughout the uppermost 0.1 meter of basalt, and a concentration of selvedge and basalt clasts occurred in a mushroomed portion of a calcite vein at a sub-bottom depth of 791.9 meters. A second appearance of glass was noted in an intensely fractured and chloritized zone within the basalt at a sub-bottom depth of 793.68 meters (1.78 below the top of the basalt). Elsewhere the rock is holocrystalline.

Groundmass in all cases consists of a complex network of randomly oriented plagioclase (An 65 to An 76) microlites with intergranular pyroxene. Disseminated, granular to skeletal crystals of magnetite also appear in the groundmass. Groundmass texture varies widely throughout the basalt but generally increases in complexity downward in two steps. The upper 0.5 meter of basalt is very fine grained, displaying a random groundmass pattern of single microlites. As the texture coarsens gradually downward, plagioclase microlites show a tendency toward congregating into crude crystal sprays. Immediately below the second glass horizon, alteration to montmorillonite and chlorite partially obscures the textures; simplicity of pattern once again appears to dominate the remainder, although the fabric remains relatively coarse. The remaining basalt displays complex combinations of feather duster (as described from Site 386), true feather (Bryan, 1972; Site 100), variolitic, and shock (stook) groundmass textures (Figure 7). An average mineralogical composition for the basalt as determined from thin section is given in Table 3.

Amygdules of calcite, montmorillonite (nontronite?), and chlorite, in decreasing order of importance, account for less than 1 per cent of the cross-sectional area. Chlorite is important only in the sheared zone. No local vesicle concentrations were noted. Calcite veins up to 3 mm in width are abundant in the upper 1.5 meters of basalt and common below.

Numerous enclosures of grayish red to dark reddish brown slightly calcareous claystone appear throughout the basalt, ranging in size from 0.3 × 0.3 mm to 20 × 60 mm. Other enclosures of similar sediment occur only within the confines of calcite veins and appear to have been "intruded" into the basalt from below. Compositionally the enclosed claystone is very similar to that recovered immediately above the basalt (see Table 4). A subconchoidal fracture is well developed in the claystone indicating baking of the sediment has occurred. Nannofossils occurring rarely in the claystone im-

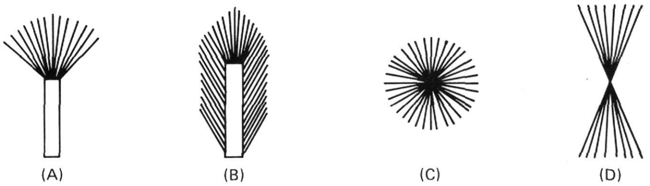

Figure 7. *Groundmass textures shown in basalt at Site 387. (A) Feather duster, (B) true feather, (C) variolitic, (D) shock (stook).*

TABLE 3
Average Mineralogical Composition of Site 387 Basalt Based on Thin-Section Analysis

Plagioclase phenocrysts	20-25%
Plagioclase groundmass	40-60%
Pyroxene phenocrysts	2-3%
Pyroxene groundmass	15-20%
Magnetite groundmass	1-5%
Calcite vein and vesicles	1-3%
Montmorillonite alteration	1-2%
Chlorite alteration and vesicles	1-5%
Glass	0-trace

TABLE 4
Smear-Slide Compositions of Sediments Within and Overlying Basalt at Site 387

	Calcareous Claystone Enclosures	Calcareous Claystone at Baked Contact
Clay	72%	57%
Unspecified carbonate	15%	20%
Siderite	8%	12%
Nannofossils	3%	5%
Radiolarians	2%	5%
Mica	trace	1%
Pyrite	trace	trace

mediately above and within the basalt date the unit as lower Valanginian to upper Berriasian in age.

Structure of the Igneous Unit

Structurally the basalt unit contains many of the characteristics of an extrusive flow, but the weight of evidence suggests it is an intrusive sill. The presence of glass and brecciated basalt at its upper surface could be taken as indications of a flow origin; however, the occurrence of this material in a calcite vein suggests that the glass may have been brought up by the vein fluids and concentrated at the top of the unit. Small quantities of glass in the basalt itself, though unusual for a sill, have been reported from several classic sills on land, including the Island of Mull sill complex (Thomas, 1922). Pillowed surfaces expected for a submarine flow are nowhere visible. The existence of a second "glassy" surface within the unit is puzzling, but glass concentrations are not sufficiently high to pose a barrier to the sill hypothesis. As the average flow drilled by DSDP has been 1 to 2 meters in thickness and the average sill 7 to 10 meters in thickness, establishment of a real boundary within the cored basalt would favor a flow origin. The extremely fractured nature of the internal "glass" zone suggests it also might be associated with a vein which was lost during coring. Chloritization halos surrounding the zone hint at, but do not require, minor hydrothermal activity along the sheared zone.

A baked sedimentary contact as we appear to have here has commonly been used as proof of an igneous body's intrusive nature. Leg 37, however, cored pillowed flows on the Mid-Atlantic Ridge intercalated with baked sediment. Sediment enclosures within a basalt flow may arise from the bulldozer action of a flow front encountering a sediment surface. Alternatively, a flow can override an earlier flow in whose corrugated upper surface sediment previously accumulated, resulting in interflow sediment inclusions. Thus, even the association of sediment enclosures within vein material, indicating a deeper source for the sedimentary material, is not conclusive proof of a sill origin.

Texturally, however, several features favor a sill origin for this basalt. A general increase in matrix grain size away from the upper contact, low vesicularity, and the wide variety of groundmass textures displayed are typical of most sills. Flows are periodically found to display a degree of grain-size grading and at ridge crest depths commonly have low vesicularity, but a single flow generally is typified by one groundmass texture. The corroded nature of most phenocrysts suggests pre-injection crystallization.

The occurrence of all these features together, some of which are rare in flows, suggests the structure drilled was a sill. The mineralogical and textural similarity of the basalt to ridge basalt recovered in nearby holes (Sites 100, 105, and 386), however, suggests it was emplaced at or near the ridge crest. Furthermore, if the basalt is a sill, it was probably intruded near the original extrusive/sediment contact because: (a) the age of the oldest sediment is not significantly younger than expected from previous dates on the *M*-series (see Vogt and Einwich, this volume) and (b) the basalt was encountered at a level for acoustic basement which is not anomalously shallow or in any way unusual (Figures 2 and 4). Its age is therefore considered approximately synchronous with basement age.

Summary

Basaltic rocks cored at Site 387 are fine-grained basalts commonly intruded by vein calcite and containing enclosures of calcareous claystone. Except for minor alteration to montmorillonite and lesser chlorite, the phenocrysts are affected only by resorption. The groundmass displays great textural variation. The absence of olivine, the presence of pigeonitic augite, and enrichment in groundmass iron as indicated by late-crystallized magnetite suggest a nearly saturated or oversaturated subalkaline basalt of the type that forms at present-day spreading ridges. A baked sediment contact and sediment enclosures, groundmass textural variety, and gradation to a coarser interior, low vesicularity, and general lack of glassy surfaces suggest the basalt is structurally a sill.

GEOCHEMISTRY

Carbon, Nitrogen

The results of the shipboard organic carbon and nitrogen measurements are summarized in Table 5 and the carbon data together with shore-lab analyses are plotted in Figure 8. Organic carbon values in the upper 490 meters of Site 387 (Units 1 to 5) are low, averaging about 0.2%. The underlying black claystones (Unit 6) and limestones (Unit 7), on the other hand, contain substantially greater amounts of organic matter. The distribution of organic matter in Units 6 and 7 is illustrated in Figure 9, where shipboard and post-cruise measurements of organic carbon are compared with pyrolysis fluorescence measurements. The sediments in Units 6 and 7 commonly contain 1.5 to 4.0% organic carbon, but values as high as 14% are observed. The profiles of organic carbon and pyrolysis fluorescence at Sites 386 and 387 are similar in that they display very high values near the top of the black claystone unit. More complete correlations are difficult, however, because the black claystone sequence at Site 387 has poorer age control and is about 100 meters thinner than at Site 386.

TABLE 5
Shipboard Organic Carbon, Nitrogen Measurements,[a] Site 387

Sample (Interval in cm)	Depth Below Sea Floor (m)	$C_{org.}$ (%)	N (%)	$\frac{C}{N}$
1-5, 150	39.3	0.1	0.06	2
2-4, 130	104.2	0.1	0.04	3
7-5, 150	182.1	0.2	0.03	7
14-2, 42-43	243.2	0.3	0.02	15
16-2, 130	262.9	0.3	0.02	15
20-2, 130	329.5	0.1	0.02	5
23-3, 150	378.8	<0.1	0.03	–
26-1, 48-50	412.7	0.7	0.05	14
26-2, 120	414.9	0.6	0.04	15
29-2, 150	472.4	<0.1	0.03	–
30-1, 142-143	490.0	14.0	0.52	27
32-4, 150	523.1	0.1	0.02	5
32-6, 41-42	525.0	1.5	0.06	25
35-3, 150	550.2	2.3	0.11	21
36-2, 150	558.3	2.9	0.14	21
37-1, 130	575.6	3.0	0.14	21
39-2, 43-44	623.5	2.8	0.14	20
44-1, 123-125	679.9	2.2	0.11	20
49-4, 0	786.9	0.5	0.02	25
49-4, 20	787.1	0.8	0.04	20

[a]Additional shore-lab data are given by Kendrick (this volume) and Cameron (this volume).

Values of C/N for Units 1 through 5 range from 2 to 15 and are similar to values measured at other Leg 43 sites. As was true at Site 386, however, the black and greenish gray claystones exhibit higher C/N ratios of 20 to 25. The uniformity of C/N values between Units 6 (black clays) and 7 (limestone) suggests that the organic matter in these two units is compositionally similar.

Calcium Carbonate

The results of the shipboard "carbonate bomb" measurements are tabulated in Table 6 and all shore-lab and shipboard values are plotted in Figure 8. $CaCO_3$ was measured in only one sample from the first six cores because smear-slide inspection indicated that no calcium carbonate was present. Calcium carbonate is moderately low in sediments from the upper 560 meters of Site 387. Sediments in Units 2 and 3 generally contain 10 to 20 per cent $CaCO_3$. No carbonate bomb measurements were made on the multicolored clay unit (Unit 5) or the upper part of the black claystone unit (Unit 6), but smear-slide observations indicate that this interval (460 to 560 m) contains only trace amounts of calcareous nannofossils and unspecified carbonate. In Core 36 (560 m) the amount of calcium carbonate increases sharply, and throughout the remainder of the hole the sediments contain 25 to 95 per cent $CaCO_3$.

Interstitial Water Chemistry

At Site 387 eleven interstitial water samples were taken between 40 and 575 meters. The results of the chemical analyses are summarized in Table 7 and Figure 10.

The chemistry of the interstitial waters is marked by trends of downward decreasing Mg^{++} and increasing Ca^{++} in the upper 375 meters of Site 387. These changes in dissolved calcium and magnesium do not appear to be related to the increased values of alkalinity between 100 and 175 meters.

The salinity of the pore waters decreases from about 35.2‰ near the sea floor to 33.8‰ at 400 meters. The decrease in salinity is independent of the chlorinity and reflects the removal of sulfate from the interstitial waters (Miller and Gieskes, this volume).

Interstitial Gases

Higher than normal gas pressures were noted in Cores 7, 8, and 9 at Site 387. Gas chromatographic analysis indicated the presence of 600 to 1500 ppm (by volume) CO_2, but no hydrocarbons were detected.

PHYSICAL PROPERTIES

At Site 387 the physical properties which were measured on-board ship include the undrained shear strength, thermal conductivity, compressional wave velocity, wet bulk density, and other bulk properties such as water content and porosity. These data are presented in Table 8, and the test methods and systems errors associated with the test techniques are listed in the Physical Properties section of the Site 382 Report, this volume. The objective of the test program was to determine these parameters on the least-disturbed specimens in each sedimentary unit. Thus, only cohesive sediment specimens with a minimum of visual distortion were selected for testing and only unfractured rock/chalk specimens were used.

In addition to the shipboard tests, three unsplit sediment samples were taken from the bottom sections of Core 1 and 2. These samples were subjected to strength and compression tests at a shore laboratory and the results are discussed by Demars et al. (this volume).

Shear Strength

The shear strength variation with sub-bottom depth is shown in Figure 11. Although the data are limited because of intermittent coring, a linear increase in strength with depth is apparent. Most of the data spread probably is caused by coring disturbance. However, at a sub-bottom depth of 105 meters (Core 2), two higher-than-average shear strengths were obtained which may indicate little coring disturbance. These high strengths are closer to *in-situ* conditions, as explained in the physical properties chapter of this volume (Demars et al.), but they are still significantly lower than *in-situ* values.

Vane shear tests were terminated on samples from deeper than 180 meters because the test specimens fractured upon vane insertion.

Water Content

Water content data are shown in Figure 12. Values generally decrease with sub-bottom depth as anticipated. However, there are significant changes that correlate closely with changes in lithology. The first zone contains brown, gray, and green clays and radiolarian clays to a depth of 224 meters (lithologic

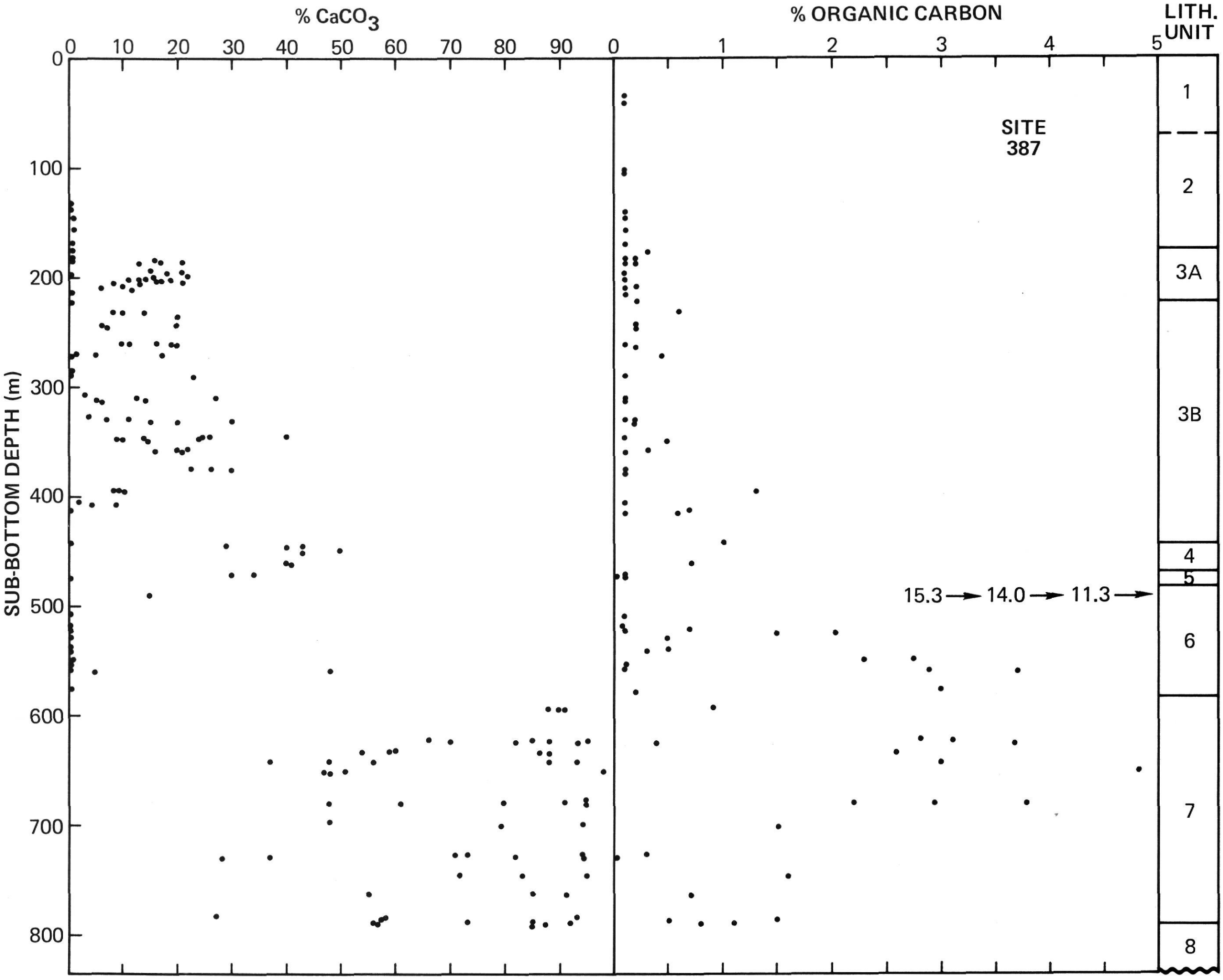

Figure 8. *Organic carbon and* $CaCO_3$ *versus depth at Site 387, based on all available data (shipboard data plus Koch and Rothe; Kendrick; and Cameron; all in this volume).*

Units 1, 2, and 3A). Water contents average about 46 per cent and vary little with sub-bottom depth in these sediments. Cherts, silicified claystones, and radiolarian mudstones were observed from 224 to 444 meters (Sub-unit 3B); water contents are low in the upper, cherty sediments and increase to about 30 per cent in the deeper, less silicified sediments. Water contents are fairly uniform throughout lithologic Units 4 (marly chalk), 5 (red claystone), and 6 (green-gray and black claystone), and in the upper, chalky limestones of Unit 7. The harder limestones in the lower part of Unit 7 average about 8 per cent water content. Water contents of the basalt are slightly lower than in the limestones.

Density and Acoustic Velocity

Wet bulk density, acoustic velocity, and acoustic impedance (density times velocity) also are plotted against sub-bottom depth in Figure 12. These parameters show the same kind of relationship to lithologic units as the water content and porosity data. In the upper 224 meters the wet bulk density averages about 1.52 g/cm³. Density ranges from 1.70 to 2.06 g/cm³ in cherts and silicified claystones in the upper part of Sub-unit 3B, down to 310 meters. From 310 to 444 meters (in Sub-unit 3B), the densities of the radiolarian mudstones average about 1.72 g/cm³ and have little variation. Densities are more erratic in Unit 4 and down through the chalky limestones at the top of Unit 7 (1.68 to 2.22 g/cm³), but they cluster around 1.95 g/cm³. The limestones below about 630 meters have an average density of about 2.35 g/cm³, and the basalts exhibit a density of about 2.60 g/cm³.

Measured acoustic velocities in all lithofacies increase slightly with sub-bottom depth from 1.53 km/sec at 45 meters to about 1.80 km/sec at 645 meters. Deviations from this trend are caused mainly by variable diagenetic cementation. For example, acoustic velocities of silicified claystones and cherts range from 1.85 to 3.75 km/sec. Radiolarites in the black claystone at 490 meters have velocities up to 2.58 km/sec. The deeper,

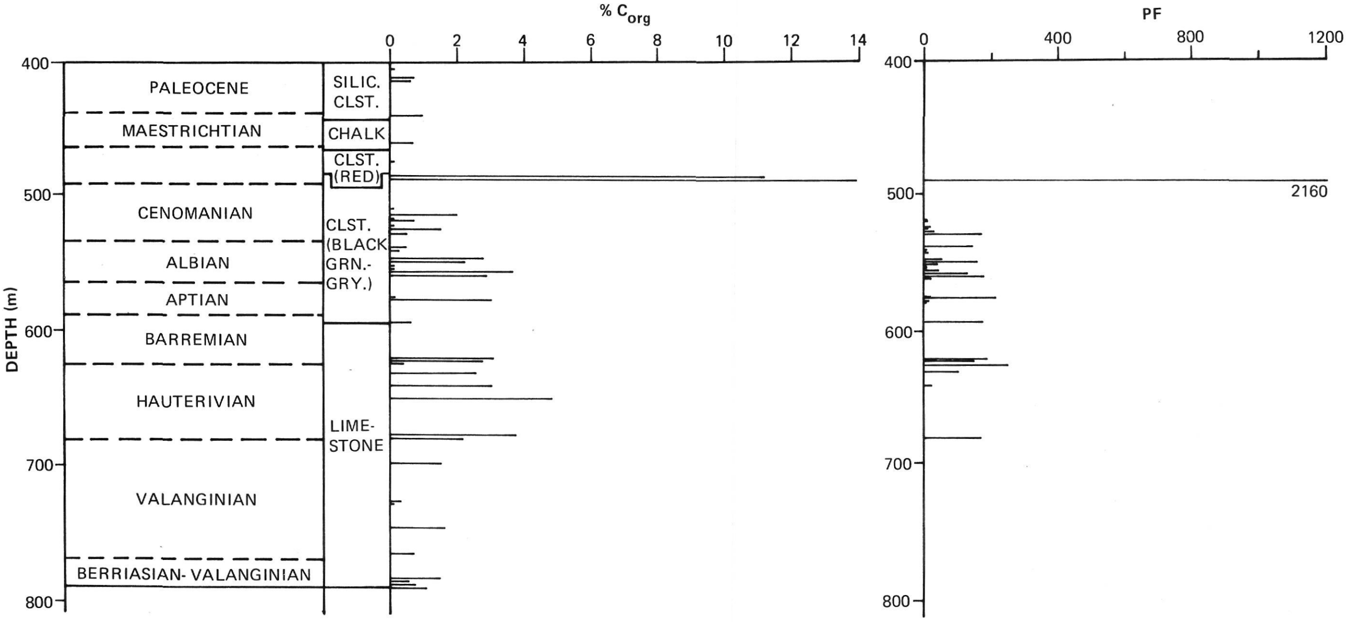

Figure 9. *Comparison of organic carbon content and pyrolysis fluorescence measurements of organic richness in black claystones and limestones, Site 387.*

harder limestones in Unit 7 have velocities of 2.50 to 4.85 km/sec, and basalt velocities range from 4.59 to 4.96 km/sec.

Significant changes in acoustic impedance occur near 224 meters between the siliceous turbidites and underlying cherty sediments, near 625 meters where indurated limestones were first measured, at the top of basalt at 792 meters. Correlation of measured impedance and velocity with the seismic profile at Site 387 is discussed later in this chapter.

BIOSTRATIGRAPHY

The location of Site 387 promised to provide linking information on biostratigraphy, acoustic stratigraphy, lithostratigraphy, and basement age for several sites, the western North Atlantic Basin in general, and the Bermuda Rise in particular. Except for the first above, valuable results were obtained, but the fossil record at this site proved to be very poor, both in continuity and quality.

As at Site 386 and elsewhere in the basin, the sedimentary succession includes Tertiary clays with relatively abundant radiolarians, a siliceous Eocene section, and barren red-gray clays that grade into barren dark gray and black clays. Also like Site 386, The Tertiary radiolarians, the persistently low level of carbonate, and the poor fossil record indicate persistent deposition mostly well below the CCD, except for the initial period of deposition of limestones during the Neocomian.

There were no intervals having exceptional contribution to taxonomic or biostratigraphic information, except for Core 49, the last before basalt, which yielded remains of ammonite aptychi and ammonites (see Renz, this volume).

Cenozoic Foraminifers

Cenozoic foraminifers were observed in only two samples of the sediments cored at Site 387. The upper occurrence is the top of the first core taken at this site and comprises a typical Pleistocene assemblage showing moderate dissolution effects. This assemblage is notable for the common occurrence of *Globorotalia hirsuta*, in addition to other typically Pleistocene forms. The second occurrence of foraminifers is in silicified sand laminae in Core 22, where a poorly preserved fauna of early Eocene (P.7) age was found. The poor preservation probably results partly from the disaggregation technique used to separate the foraminifers from the silicified matrix. The assemblage includes *Globortalia formosa* and abundant acarininids.

Mesozoic Foraminifers

Mesozoic foraminifers are rare and of little stratigraphic value at Site 387. A few samples from Core 28 near the top of the Cretaceous yielded sparse assemblages of low diversity, unusual specific content, and small specimen size. The planktonics are mainly hedbergellids and heterohelicids, the latter of which included *Guembelitria cretacea* Cushman. Globotruncanids, which are typically rich, diverse, and dominant in these Maestrichtian rocks, are absent or confined to rare, apparently immature specimens. The associated benthics are also an unusual assortment in that the few occurring are species such as *Tappanina costifera* Cushman, which are infrequently reported.

The red clays of Site 387 (Core 29) occasionally yielded small numbers of primitive agglutinated species, such as were encountered in similar red clays at Sites 385 and 386 and as have been described by Krasheninnikov

TABLE 6
Shipboard $CaCO_3$ Measurements,[a] Site 387

Sample (Interval in cm)	Depth Below Sea Floor (m)	$CaCO_3$ (%)
2-5, 122-123	105.7	0
7-2, 75-76	176.9	0
8-1, 130-131	185.5	16
8-2, 15-16	185.9	21
8-2, 60-61	186.3	0
8-2, 135-136	187.1	13
9-1, 40-41	194.1	15
9-1, 120-121	194.9	21
9-3, 17-18	196.9	18
9-4, 74-75	198.9	22
9-5, 75-76	200.5	16
9-6, 30-31	201.5	14
9-6, 74-75	201.9	11
9-6, 129-130	202.5	13
9, CC	202.8	13
10-1, 108-109	204.3	8
10-2, 40-42	205.1	21
10-4, 25-26	208.0	10
13-1, 111-112	232.9	10
13-2, 147-148	234.8	20
14-1, 146-147	242.8	20
14-2, 58-59	243.4	6
16-1, 80-81	260.9	19
16-1, 108-109	261.2	11
16-2, 64-65	262.2	20
17-1, 129-130	270.9	17
17-2, 129-130	272.4	0
18-1, 45-46	289.2	0
18-1, 145-146	290.2	23
19-2, 70-71	309.9	27
19-3, 113-114	311.8	5
19, CC	312.3	14
20-2, 56-57	328.8	11
20-3, 114-116	330.9	20
21-1, 85-86	346.6	14
21-1, 114-115	346.8	15
21-1, 144-145	347.1	24
21-2, 71-72	347.9	24
22-2, 79-80	357.5	22
22-3, 67-68	358.9	21
23-1, 75-76	375.1	22
24-1, 135-136	394.7	10
25-2, 127-128	405.6	9
27-3, 73-74	444.5	29
27-4, 75-76	446.1	40
27-5, 75-76	447.6	43
27-6, 75-76	449.1	43
35-4, 77-78	551.0	0
36-2, 108-109	557.9	0
36-4, 44-45	560.2	48
38-1, 65-66	593.8	90
39-1, 140-141	623.0	85
39-2, 96-97	624.1	88
39-2, 137-138	624.5	95
40-1, 113-116	632.2	87
40-1, 136-137	632.5	54
40-2, 70-71	633.3	88
41-1, 61-62	641.2	37
41-1, 113-114	641.7	88
42-1, 69-70	650.9	48
42-1, 70-71	650.9	94
43, CC	669.3	95
44-1, 122-123	679.9	91
44-1, 123-124	679.9	61
45-1, 125-126	669.3	48
46-1, 120-121	727.2	71
46-2, 37-38	727.9	28
46-2, 51-52	728.0	82
46-2, 82-83	728.3	37
47-1, 102-103	745.9	95
48-1, 93-94	764.6	91
49-1, 128-129	783.7	27
49-1, 133-134	783.7	85
49-1, 146-147	783.9	88
49-2, 71-72	784.6	58
49-3, 70-71	786.1	85
49-4, 122-123	788.1	73
49-5, 140-141	789.8	92

[a] Carbonate bomb method. Additional shore-lab data are given by Koch and Rothe (this volume) and Cameron (this volume).

(1973, 1975) from Leg 20 and Leg 27. Although these clays are generally found in the upper part of the Cretaceous at Sites 385, 386, and 387 and were reported by Krasheninnikov to be younger than Coniacian, the agglutinated foraminiferal fauna from these clays is a reflection of a depositional environment, well below the CCD. The agglutinated fauna of the red clays are too poorly known to be employed for age determinations.

A few samples from Core 37 yielded rare, poorly preserved benthics, mostly lagenids, of a Lower Cretaceous aspect. Below Core 38 limestones are fairly common, but no foraminifers were observed in untreated samples, and little disaggregation of samples was possible, despite repeated and diverse efforts to process them.

Nannofossils

Nannofossils of Quaternary and middle Eocene through Early Cretaceous age occur at this site. Preservation generally is moderate, and the recovery was rather poor.

A 30-cm-thick calcareous clay was recovered at the top of Core 1. A well-preserved assemblage of the *Emiliana huxleyi* Zone (late Pleistocene or Holocene) is recognized in these sediments. Core 1, Section 2 through Core 7 is barren of calcareous nannoplankton.

Cores 8 through 23 represent a seemingly continuous sequence of the early and middle Eocene. Preservation of nannofossils is generally good to moderate in the upper portion and poor in the lowest portion of this interval. Unlike Site 386, effects of overgrowth are sporadic and far less significant. Core 8, Section 1, yields assemblages of the middle middle Eocene (*Discoaster bifax* Sub-zone). Three sub-zones within the *Nannotetrina fulgens* Zone (early middle Eocene) occur between Sample 8, CC, and Core 17, Section 2. The two sub-zones of the *Discoaster sublodoensis* Zone (late early Eocene) are recognized within Cores 18 to 20. Cores 21 through 23, Section 2, are attributable to the *Discoaster lodoensis* and *Tribrachiatus orthostylus* zones of middle early Eocene. Sections 3 and 4 of Core

TABLE 7
Interstitial Water Chemistry, Site 387

Sample (Interval in cm)	Depth Below Sea Floor (m)	*p*H	Alkalinity (meq/l)	Salinity (°/₀₀)	Chlorinity (°/₀₀)	Ca^{++} (m mole/l)	Mg^{++} (m mole/l)
Surface seawater	–	8.80	2.44	36.3	19.9	10.8	56.3
1-5, 124-130	39.1	7.80	3.14	35.2	19.6	12.1	51.5
2-4, 124-130	104.3	7.80	4.25	35.2	19.5	17.3	47.7
3-2, 144-150	139.6	7.80	6.42	34.9	19.9	20.8	45.4
6-2, 144-150	168.1	7.80	7.84	35.2	19.4	23.1	45.1
16-2, 120-130	262.9	–	3.25	34.4	19.2	25.4	35.9
19-1, 140-150	309.2	8.10	3.10	34.1	20.0	–	–
23-3, 120-130	378.6	7.80	2.80	33.8	19.7	30.1	32.4
26-2, 140-150	415.2	–	–	33.8	19.6	29.1	31.1
29-3, 140-150	470.9	7.80	3.76	35.2	20.0	32.3	34.6
32-1, 140-150	518.6	–	–	31.9	19.2	32.1	38.3
37-1, 120-130	575.5	8.20	2.12	34.1	20.0	33.3	30.3

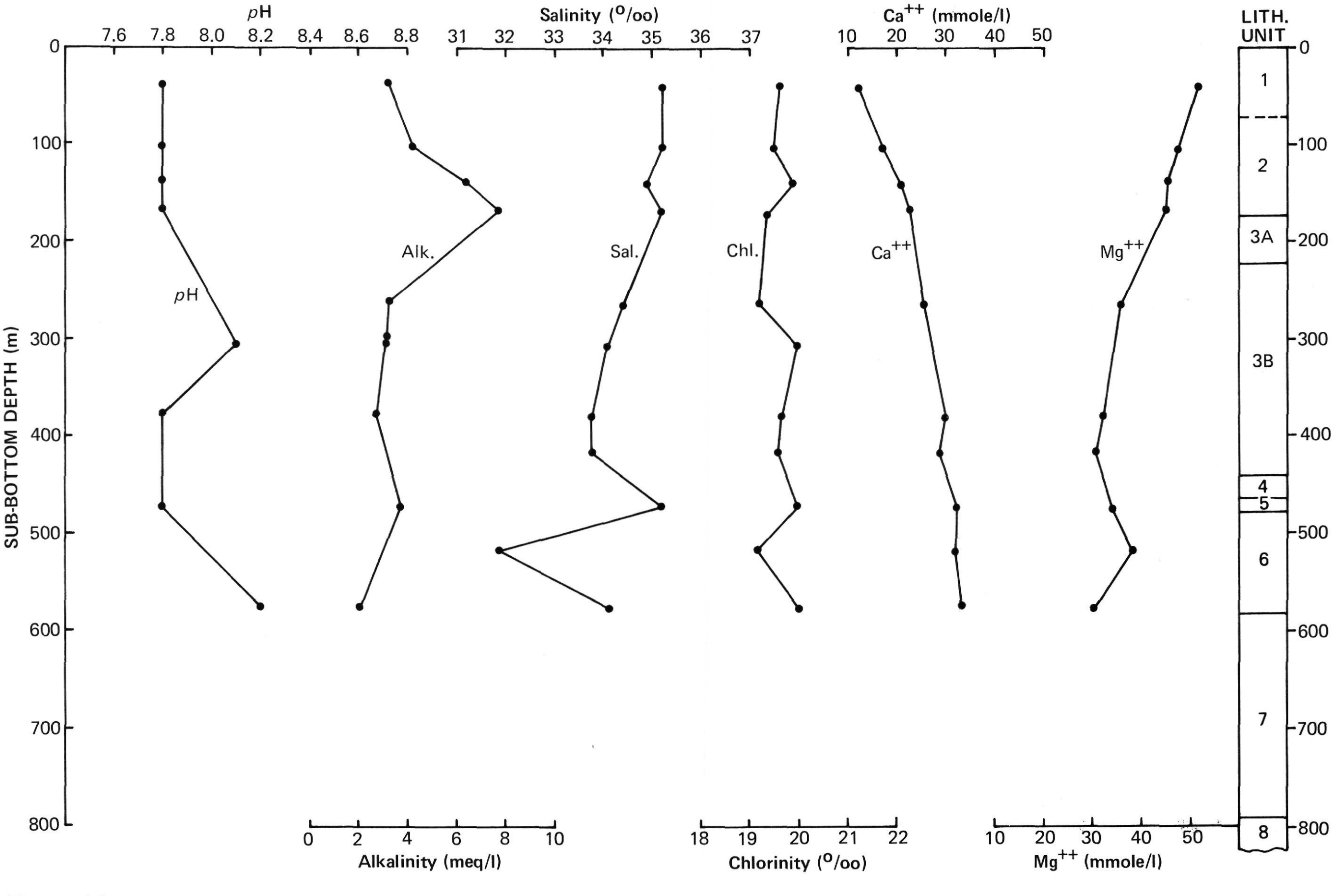

Figure 10. *Interstitial water chemistry versus depth, Site 387.*

23 yield poorly preserved assemblages of the earliest Eocene *Discoaster diastypus* Zone.

Because of poor preservation, age identification of these sediments at sub-zone level is difficult. However, abundant occurrence of *Tribrachiatus bramlettei* and *Tribrachiatus contortus* in these sediments suggests the presence of the *T. contortus* Sub-zone and, consequently, absence of the *Discoaster binodosus* Subzone at this site. Thus a short hiatus within the early Eocene is suspected. Cores 24 to 26 contain poor to moderately preserved assemblages of the *Ellipsolithus macellus* Zone (late Danian).

Cores 27 and 28 belong to the latest Maestrichtian *Micula mura* Zone with sporadic *Nephrolithus frequens* present. One poorly preserved assemblage of the latest Campanian/early Maestrichtian *Tetralithus trifidus* Zone was encountered in Core 29, Section 2. Cores 30 through 37 are barren of nannofossils. The stratigraphic overlap of the ranges of *Lithraphidites bollii* and *Cruciellipsis cuvillieri* in Core 38 through Core 40,

TABLE 8
Physical Properties Data, Site 387

Sample (Interval in cm)	Sub-Bottom Depth (m)	Velocity (km/sec)		GRAPE Routine[a,b,c]		Thermal Conduct.[d] (mcal/cm-sec-°C)	Shear Strength Undist./Rem. (g/cm^2)	Syringe or Rock Chunk			Impedance (g/cm^2-sec) × 10^5	Lithology
		Para. Beds	Perp. Beds	Wet Bulk Density (g/cm^3)	Poros. (%)			Water Content (%)	Wet-Bulk Den. (g/cm^3)	Porosity (%)		
1-5, 12, 42, 70, 102	37.8-38.8			1.40	77	X						Light brown clay
1-5, 60-120	38.67			1.40	77		73/	47	1.49	69		Light brown clay
1-6, 102	40.3			1.48	72		285/121					Light brown clay
1-6, 106-108	40.4	1.53		1.48	72		314/125	45	1.55	69	2.37	Light brown clay
1-6, 114	40.5			1.48	72		283/116	44	1.53	67		Light brown clay
2-5, 14, 43, 75, 112	104.6-105.6			1.51	70	X						Pale olive rad. mud
2-5, 84	105.3			1.51	70		1178/					Pale olive rad. mud
2-5, 88-98	105.4	1.57		1.51	70		682/260	45	1.60	72	2.51	Pale olive rad. mud
2-5, 101-103	105.5	1.57		1.51	70		1127/311	47	1.52	71	2.39	Pale olive rad. mud
2-5, 108	105.6			1.51	70		612/					Pale olive rad. mud
3-2, 125-128	139.4	1.54	1.54	1.43	75		593/195	47	1.53	72	2.36	Gray-brown clay
3-2, 136	139.5			1.43	75		760/222	48	1.47	71		Gray-brown clay
4-1, 56	146.7			1.49	71		853/	46	1.52	70		Gray-green rad. mud
4-1, 139	147.5			1.49	71		941/					Gray-brown rad. mud
4-1, 143-145	147.5	1.56	1.55	1.49	71		612/	40	1.60	64	2.48	Gray-brown rad. mud
6-3, 40, 70, 95, 120	168.5-169.3			1.59	65	X						Olive-gray rad. mud
6-3, 125	169.4			1.59	65		1136/					Olive-gray rad. mud
6-3, 131-133	169.4	1.63	1.62	1.59	65		1247/	34	1.78	61	2.88	Olive-gray rad. mud
7-2, 30, 60, 90, 122	176.8-177.7			1.44	74	X						Pale grn. rad. mud
7-4, 78-82	180.3	1.57	1.59	1.41	77		912/	49	1.44	71	2.29	Pale grn. rad. ooze
7-4, 101	180.5			1.41	77		882/					Pale grn. rad. ooze
8-2, 143	187.1	1.61	1.58	1.39	77			50	1.42	72	2.24	Pale grn. rad. mud
9-5, 29, 60, 93, 123	200.4-201.3			1.51	70	X						Grn-gry nanno rad. mud
9-6, 45	202.0	1.68	1.62	1.46	73			43	1.50	65	2.43	Green-gray spicule rad. mud
9-6, 86	202.4	1.60	1.59	1.46	73			48	1.43	69	2.27	Green-gray rad. mud
10-5, 25, 58, 102, 140	209.9-211.0			1.47	73	X						Rad. ooze & rad. mud
11-1, 143	214.2	1.61	1.58					47	1.45	69	2.29	Green-gry muddy rad. ooze
12-1, 112	223.4	1.65	1.62					43	1.51	65	2.45	Olive rad. mud
12-1, 127	223.6	2.09	1.87					32	1.61	51	3.01	Green-blue rad. mudst.
12-1, 147	223.8	-3.78-						8	2.01	16	7.60	Olive-gray chert
13-2, 148	234.8	2.29	2.05					22	1.86	40	3.81	Pale grn nanno clayst.
14-2, 29	243.1	2.72	2.47	1.65	61			22	1.86	42	4.59	Blue-grn silicified clayst.
14-2, 116	244.0	3.37	2.67	1.65	61			10	2.03	21	5.42	Olive chert
15, CC	(250.7)	-3.37-						17	1.97	33	6.64	Gray-brown chert
15, CC	(250.7)	-3.32-						18	1.88	33	6.24	Gray-brown chert
16-3, 23	263.3	2.03	1.87	1.53	69			20	1.72	35	3.22	Gray-green claystone
17-2, 50	271.6	2.38	2.19	1.57	66			25	1.78	45	3.90	Silicified claystone
17-2, 148	272.6	-3.55-		1.57	66			12	1.97	24	6.99	Gray chert
18-1, 115	289.8	2.11	1.96	1.46	73			28	1.74	48	3.41	Blue-green siliceous claystone
19-2, 55	309.8	2.96	2.73	1.48	72			14	2.06	29	5.62	Olive spicule mudst.
19-2, 72	309.9	1.98	1.80	1.48	72			26	1.83	47	3.29	Pale green claystone
20-2, 4	328.2	1.97	1.82	1.50	71			28	1.76	49	3.20	Olive siliceous claystone
20-2, 68	328.9	2.13	1.96	1.50	71			28	1.71	49	3.35	Olive siliceous claystone
21-2, 144	348.6	2.21	2.04	1.51	71			29	1.72	50	3.51	Green calc. claystone
22-2, 30	357.0	2.32	2.12	1.51	70			29	1.72	50	3.65	Gray-green rad. mudstone
22-2, 67	357.4		1.84	1.51	70			32	1.69	55	3.11	Green rad. mudstone
23-1, 95	375.2	2.18	2.00	1.49	71			28	1.73	49	3.46	Green claystone
23-5, 90	381.2	1.86	1.74					27	1.84	50	3.20	Brown claystone
24-1, 128	394.6	1.80	1.70					31	1.72	53	2.92	Gray-olive claystone
25-2, 74	405.0	1.89	1.73	1.53	69			31	1.72	53	2.98	Black claystone
25-2, 103	405.3	2.13	2.00	1.53	69			25	1.82	46	3.64	Blue-gray claystone
26-2, 45	414.2	1.87	1.70	1.55	68			30	1.79	53	3.04	Olive-gray claystone
26-2, 100	414.7	–	1.70	1.55	68			29	1.78	51	3.03	Black claystone
27-5, 148	448.7	1.83	1.76	1.85	49			22	1.97	44	3.47	Lt. gray marly chalk
28-1, 112	461.0	1.79	1.69					22	1.96	43	3.31	Lt. gray marly chalk
29-2, 17	471.1	1.85	1.70	1.76	55			23	1.98	45	3.37	Red claystone
29-2, 70	471.6	2.70	2.04	1.76	55			15	2.22	33	4.53	Blue-gray claystone
30-1, 90	489.4	2.20	1.97	1.63	63			19	2.06	38	4.06	Gray-green claystone
30-1, 130	489.8		2.22	1.63	63			22	1.65	36	3.66	Black claystone
30-1, 145	490.0		2.58	1.63	63			20	1.91	38	4.93	Black siltstone
31-1, 122	508.7	1.97	1.84	1.67	61			26	1.87	50	3.44	Brown claystone
32-3, 148	521.9	2.09	1.88	1.70	58			22	1.97	41	3.70	Blue-gray claystone
32-4, 35	522.3	1.96	1.82	1.71	58			23	1.94	46	3.53	Olive claystone
33-2, 27	528.4	2.10	1.88	1.65	62			24	1.93	46	3.63	Gray-blue claystone
34-2, 55	538.2	2.09	1.96	1.62	64			23	1.94	45	3.80	Gray-green mottled claystone
34-2, 106	538.8	2.26	2.04	1.62	64			20	2.07	42	4.22	Dark gray claystone
35-3, 89	549.6	2.32	2.16	1.70	58			20	2.02	40	4.36	Black-gray claystone
35-3, 114	549.8	2.10	1.91	1.70	58			23	1.90	43	3.63	Black rad. mudst.
36-3, 126	559.6	1.84	1.76	1.69	59			24	1.89	45	3.33	Black claystone
37-3, 48	577.8	1.85	1.75	1.67	60			23	1.99	45	3.48	Blue-gray mottled claystone
37-3, 82	578.1	1.97	1.80	1.67	60			23	1.69	39	3.04	Black rad. mudstone
38-1, 27	593.4	1.86	1.74	1.52	70			22	1.97	42	3.43	Gray-brown marly chalk
39-2, 67	623.8	1.91	1.79	1.72	57			20	1.96	40	3.51	Olive marly chalk
39-2, 148	624.6	3.52	3.57	1.72	57			7	2.43	18	8.68	Light gray limestone
40-1, 97	632.1	2.67	2.30					14	2.19	31	5.04	Light gray chalk

TABLE 8 – *Continued*

Sample (Interval in cm)	Sub-Bottom Depth (m)	Velocity (km/sec)		GRAPE Routine[a,b,c]		Thermal Conduct.[d] (mcal/ cm-sec-°C)	Shear Strength Undist./ Rem. (g/cm^2)	Syringe or Rock Chunk			Impedance (g/cm^2-sec) × 10^5	Lithology
		Para. Beds	Perp. Beds	Wet Bulk Density (g/cm^3)	Poros. (%)			Water Content (%)	Wet-Bulk Den. (g/cm^3)	Porosity (%)		
40-2, 94	633.5	3.32	3.63					8	2.43	18	8.82	Light gray limestone
41-1, 73	641.3	3.10	3.06					10	2.35	22	7.19	Light gray limestone
41-1, 114	641.7		1.78					19	2.05	38	3.65	Lt. gray marly chalk
42-1, 103	651.2	3.13	3.44					9	2.35	21	8.08	Light gray limestone
43, CC	(669.2)	3.10	2.75					11	2.28	25	6.27	Light gray limestone
44-1, 74	679.4		3.45					9	2.37	22	8.18	Light gray limestone
44-1, 111	679.8	3.91	3.82					5	2.54	13	9.70	Light gray limestone
45-1, 131	699.0		3.43					8	2.38	20	8.16	Light gray limestone
45-1, 145	699.2		4.74					3	2.47	8	11.70	Gray chert
46-1, 105	727.0	-4.85-						4	2.42	9	11.74	Gray chert
46-2, 9	727.6		4.03					8	2.36	20	9.51	Light gray cherty limestone
46-2, 99	728.5	2.47	2.49					11	2.31	26	5.75	Olive gray limestone
47-1, 135	746.2	3.29	3.00					7	2.34	21	7.02	Light gray limestone
48-1, 51	764.2	3.01	2.65					11	2.26	26	5.99	Light gray limestone
48-1, 112	764.8	3.88	3.50					6	2.29	15	8.02	Light gray limestone
49-2, 10	784.0	3.78	3.22					7	2.41	47	7.76	Light gray limestone
49-4, 125	788.2	3.00	2.77					10	2.33	24	6.45	Light gray limestone
50-1, 40	792.3	4.59-		2.11	33			5	2.60	14	11.93	Dark gray basalt
50-1, 58	792.5	-4.89-		2.11	33			5	2.59	13	12.67	Dark gray basalt
50-1, 95	792.8	4.98	4.96	2.11	33							Dark gray basalt

[a] No special 2-min. counts made at Site 387.

[b] Routine GRAPE values are averages for entire core section, normally based on 8 measurements between 10 and 140 cm in section. A complete listing of routine GRAPE data is given in the Appendix.

[c] Assumed grain density = 2.65 g/cm^3.

[d] Conductivity data not processed. Location of measurement indicated by X.

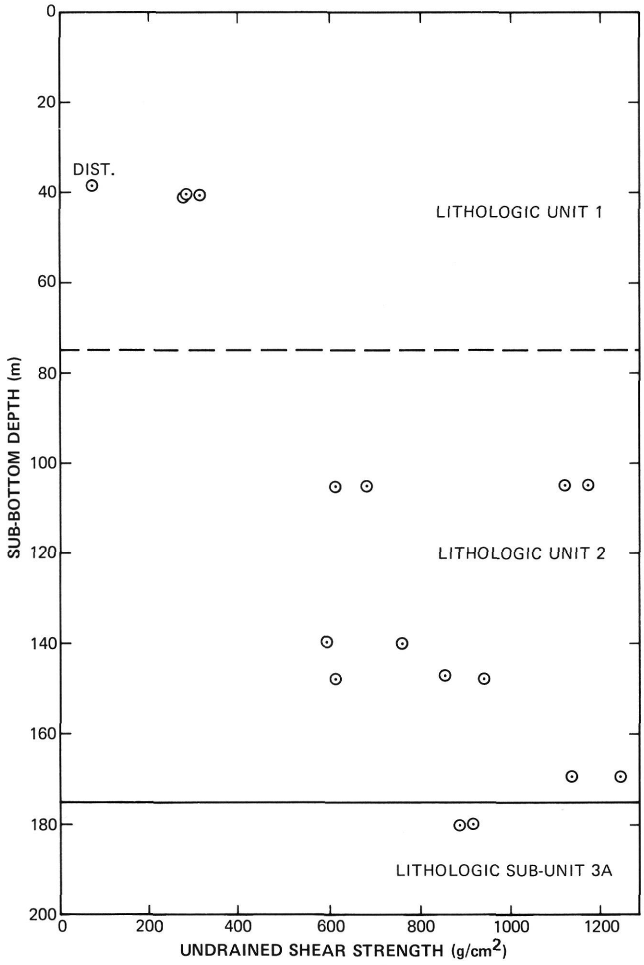

Figure 11. *Sediment shear strength data, Site 387.*

Section 2, dates these sediments as middle Hauterivian. The interval between Cores 40 and 46 yields moderately to poorly preserved nannoliths of late Valanginian to early Hauterivian age. Middle Valanginian assemblages occur in Cores 47 and 48 and early Valanginian nannoliths are present abundantly in Core 49, Sections 2 through 5. The lowermost nannofossils encountered in Samples 49, CC and 50-2, 88 cm (pocket in basalt) correlate with the late Berriasian to early Valanginian *Cretarhabdus angustiforatus* Zone. The best estimate for the age of the crust here is therefore 134 m.y. (Thierstein, in press) or about 131 m.y. on the van Hinte (1976) time scale. The overall succession of nannofossil assemblages at this site appears very similar to that at Site 105 (Thierstein, 1975).

Radiolarians

The radiolarian zonations are included in Figure 5.

SEDIMENT ACCUMULATION RATES

Patterns of sediment accumulation at Site 387 (Figure 13) are grossly similar to those at Site 386, and in particular, many major changes in accumulation rate occur near the same time at both sites.

The basal limestone sequence at Site 387 accumulated at an average rate of about 20 m/m.y. that is typical of pelagic carbonates. The accumulation rates for the overlying black clays (3-5 m/m.y.) are much lower, mostly in response to the reduced carbonate input. These reduced rates appear to be typical for black clays in most of the deep basin, but they are much lower than at Site 386 where black clays were rapidly deposited in a local topographic depression.

At Sites 387 and 386 there is a sharp reduction in accumulation rates beginning in the Turonian. Typical pelagic clay rates of 1-2 m/m.y. characterize the

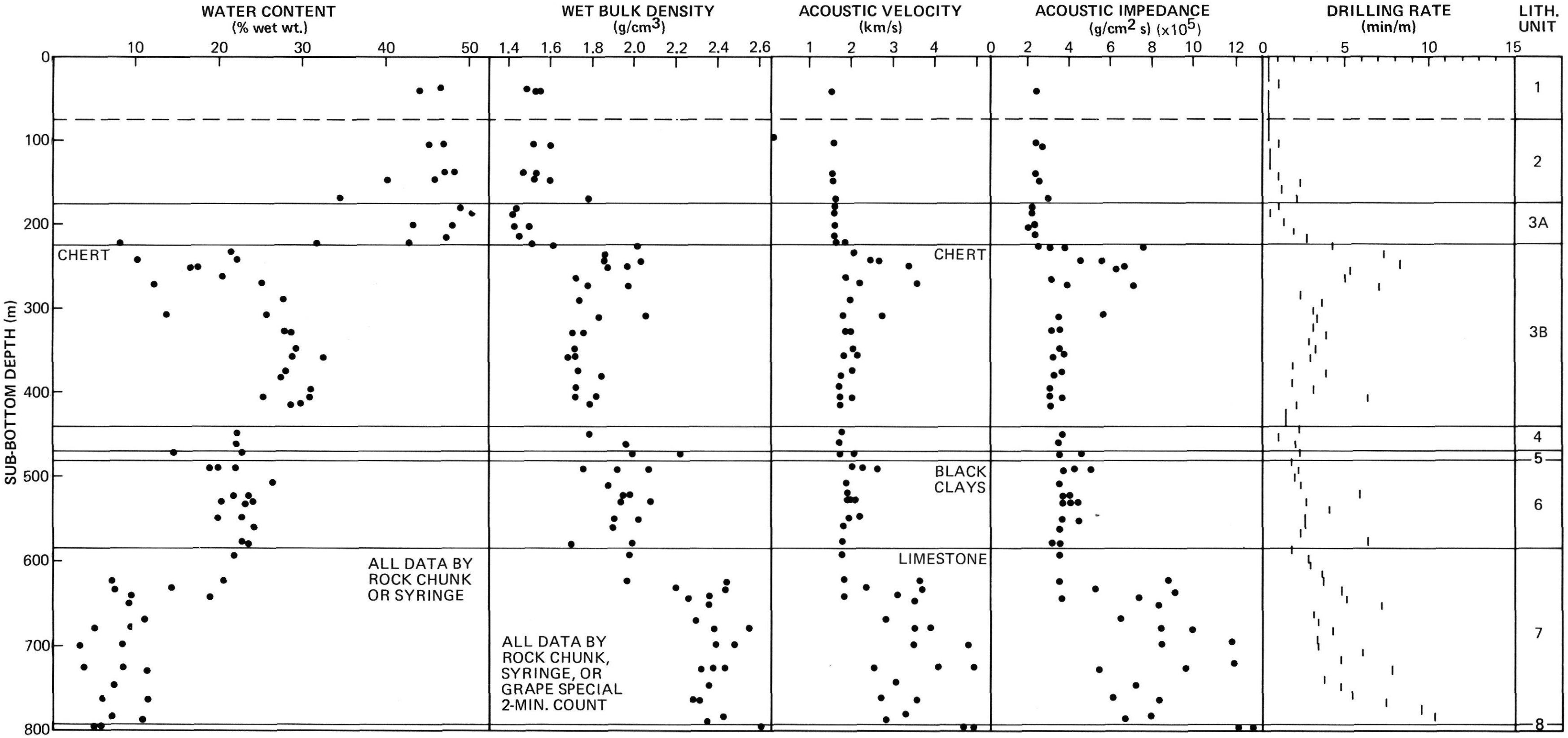

Figure 12. *Physical properties versus depth, Site 387.*

multicolored clays deposited through Maestrichtian time at Site 387 and possibly through Paleocene time at Site 386. Increased rates occur in the Paleocene at Site 387 and they may reflect initial turbidite influx to the area of the present Bermuda Rise. Because of minimal biostratigraphic control and uncertainties in the time scale, absolute accumulation rates are difficult to determine for this interval.

Dramatically increased accumulation rates (>35 m/m.y.) are observed beginning at the base of the Eocene at both Sites 387 and 386, and a sharp reduction in rates also occurs at both sites in the middle of the middle Eocene. This pulse of rapid sedimentation probably results from increased surface productivity of biogenic silica and an influx of distal turbidites from the continental margin.

Post-middle Eocene accumulation rates at Site 387 are low, about 2-3 m/m.y., but because of intermittent coring in this part of the sedimentary record we cannot resolve possibly significant fluctuations in Neogene accumulation rates. There is almost no indication of rapid sedimentation in the late Paleogene at Site 387; thus, the rapid accumulation of Bermuda-derived turbidites in this stratigraphic interval at Site 386 must have been restricted to the central Bermuda Rise. The sharp middle Eocene reduction in sediment accumulation rates at Sites 387 and 386 probably correlates with uplift that formed the Bermuda Rise and isolated these sites from turbidites derived along the continental margin.

CORRELATION OF SEISMIC PROFILE WITH DRILLING RESULTS

Site 387 was drilled on the western Bermuda Rise where the major acoustic Horizons A^T, A^C, A^*, and β (Tucholke, this volume) are well defined and where their lithofacies correlations and ages could be determined with reasonable confidence. The profiler record at the site shows that Horizon A^T is a relatively weak reflector at 0.22 sec (two-way travel time) sub-bottom (Figures 4, 14). Horizon A^C is better defined 0.05 sec deeper (0.27 sec sub-bottom) where it marks the top of a reverberant layer extending down about 0.1 sec in the section. A weak unidentified horizon is observed between Horizons A^C and A^* at about 0.435 sec sub-bottom. Horizon A^* is a very prominent reflector with a weak initial return at 0.515 sec. Horizon β at 0.675 sec sub-bottom is relatively weak in all profiler records obtained in this area, the *Challenger* record included. The horizon drapes irregularly over acoustic basement, and its locally "steep" upper surface is not conducive to reflecting a strong signal. Acoustic basement, interpreted as Layer 2 basalt, is also poorly defined; it is very irregular, exhibiting apparent crest-to-trough amplitudes in excess of 0.2 sec (nominally 200 m).

The correlations between drilling results and the profiler record are shown in Figures 14 and 15, along with calculated interval velocities and reflection times. The first certain correlation that can be made is between Horizon A^C and the top of measured high-velocity middle Eocene cherts from 224 meters sub-bottom. The calculated interval velocity of sediments between the sea floor and Horizon A^C is 1.66 km/sec. This velocity places Horizon A^T at about 183 meters depth in the section, or slightly below the top of lithologic Sub-unit 3A which consists of siliceous middle Eocene turbidites and radiolarian ooze (Figure 15). The only notable impedance contrast which was measured in the sediment recovered near this level occurs at about 168 meters within the Unit 2 radiolarian muds; this is much too shallow to correlate with Horizon A^T and still obtain reasonable interval velocities between the sea floor and Horizon A^T, and between Horizons A^T and A^C. Thus, with available data, we cannot specify the exact nature of the physical boundary representing Horizon A^T at Site 387.

Horizon A^* is correlated with a marked impedance contrast between upper Maestrichtian marly chalks (lithologic Unit 4) and red claystones (Unit 5). This correlation implies a 2.01 km/sec interval velocity between Horizons A^C and A^*, which is comparable to values measured on core samples from this interval (Figure 15). Although velocities and impedances measured on core samples do not show a contrast between the Sub-unit 3B siliceous claystones and the Unit 4 marly chalks, there is circumstantial evidence that Horizon A^* might better correlate with the top of the calcareous unit. First, the Horizon A^C-A^* interval velocity would be lowered and the Horizon A^*-B velocity raised; this would better accord with measured trends (Figure 15). Secondly, the correspondence of Horizon A^* to the top of the calcareous unit would match the lithologic correlation of Horizon A^* at Site 386. The 9.5-meter uncored interval at Site 387 between Cores 27 and 28 may have contained the high-velocity chalks necessary for this correlation. If a constant velocity of 2.01 km/sec is assumed for the A^C-A^* interval, the weak, unidentified reflector located between these horizons is placed at 390 meters depth, near the top of the chert-free siliceous claystones in the lower part of lithologic Sub-unit 3B. Contrasts of velocity and impedance measured on samples from this interval are not of sufficient magnitude to allow a more specific correlation.

It is obvious that Horizon β correlates with the transition from black claystones to limestones encountered in the Site 387 hole, but the exact sub-bottom depth at which the major acoustic impedance contrast occurs is somewhat problematical. The problem is complicated by discontinuous coring at the level of the reflector and by the relatively low and biased recovery. Chalks were first encountered in Core 38 (593.1 to 602.6 m) but unfortunately only a single sample was measured for velocity and impedance. The first established impedance contrast is at 624.6 meters in Core 39, where a limestone interbedded with clayey layers has a measured velocity of 3.57 km/sec. Correlating this level with Horizon B yields a Horizon A*-to-β interval velocity of 1.93 km/sec and a Horizon β-to-basement velocity of 1.91 km/sec; however, these values do not match the downhole increase of velocity measured on core samples (Figure 15). A more reasonable correlation with measured velocities would be established if β corresponded to limestones near 610 meters (Horizon

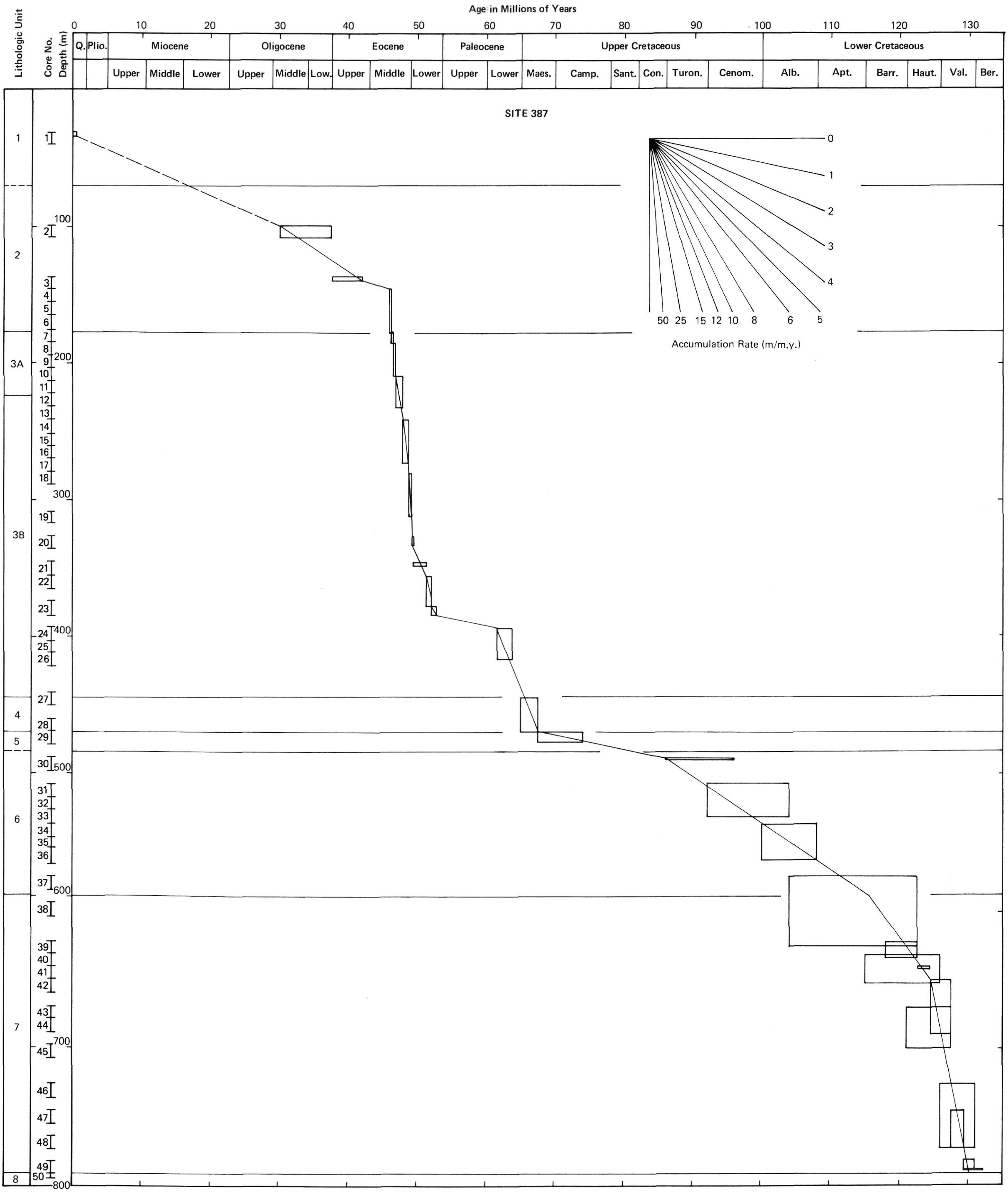

Figure 13. *Sediment accumulation rates, Site 387.*

A*-to-β, 1.75 km/sec; Horizon β-to-basement, 2.08 km/sec). In any case it is likely that the acoustic expression of Horizon β lies very close to the first downhole occurrence of limestone, below the chalk in Core 38 (593.1 to 602.6 m) and above the limestones in Core 39 (621.6 to 631.1 m). It is also significant that core recovery between Horizon β and basement was dominated by indurated limestone fragments and beds less than about 30 cm in length. The poor core recovery and the drilling record of alternate hard/soft drilling in this interval suggest that 75 per cent more of the pre-β section may consist of clayey, low-velocity interbeds. If this is the case, the average velocity of the pre-β section would be about 2.0-2.2 km/sec, comparable to the 2.08 km/sec calculated interval velocity, and much lower than the biased sampling of measured velocities shown in Figure 15.

Basement was reached at 791.9 meters sub-bottom, yielding an average velocity of 1.86 km/sec for the entire sediment column. This velocity is on the low end of, but still within, the range of velocities measured using sonobuoys in an area about 50 to 200 km west of the site (1.8-2.2 km/sec; R. Houtz, unpublished data). One sonobuoy of marginal quality was recorded aboard *Challenger* in our post-drilling survey; the calculated velocity, 2.03 ±0.15 km/sec, is high compared to the average determined by drilling at Site 387, but agrees with other sonobuoy data in the area.

SUMMARY AND CONCLUSIONS

Introduction

The main objectives at Site 387 were (1) to determine the age and lithofacies of Horizons A^T, A^c, $A*$, and β in an area with a well-defined seismic section; (2) to investigate the late Mesozoic and Cenozoic patterns of sedimentation and suface/abyssal circulation in an area likely to contain a continuous sedimentary record of the time interval following original crustal formation at the crest of the Mid-Atlantic Ridge; and (3) to sample and date basaltic crust and the sediment immediately overlying it in order to calibrate the Mesozoic magnetic-reversal chronology between anomalies *M*-15 and *M*-16.

Site 387 was located on the western Bermuda Rise, about 290 km north of Sites 6 and 7 drilled on DSDP Leg 1. At the time these earlier sites were drilled, diamond drag bits were used, and drilling generally failed to penetrate the siliceous and cherty Eocene section comprising Horizon A^c. However, at Site 7 an intrigu-

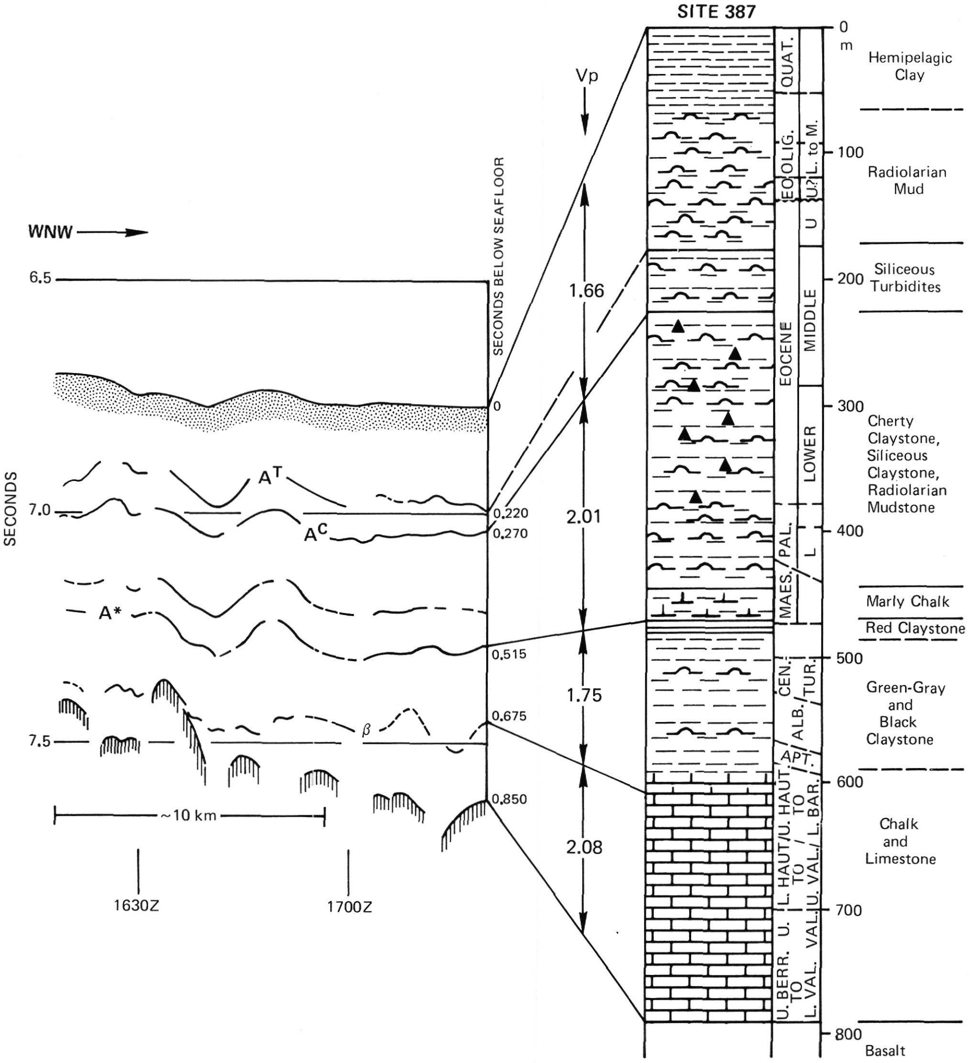

Figure 14. *Correlation between seismic profile and drilling results at Site 387.*

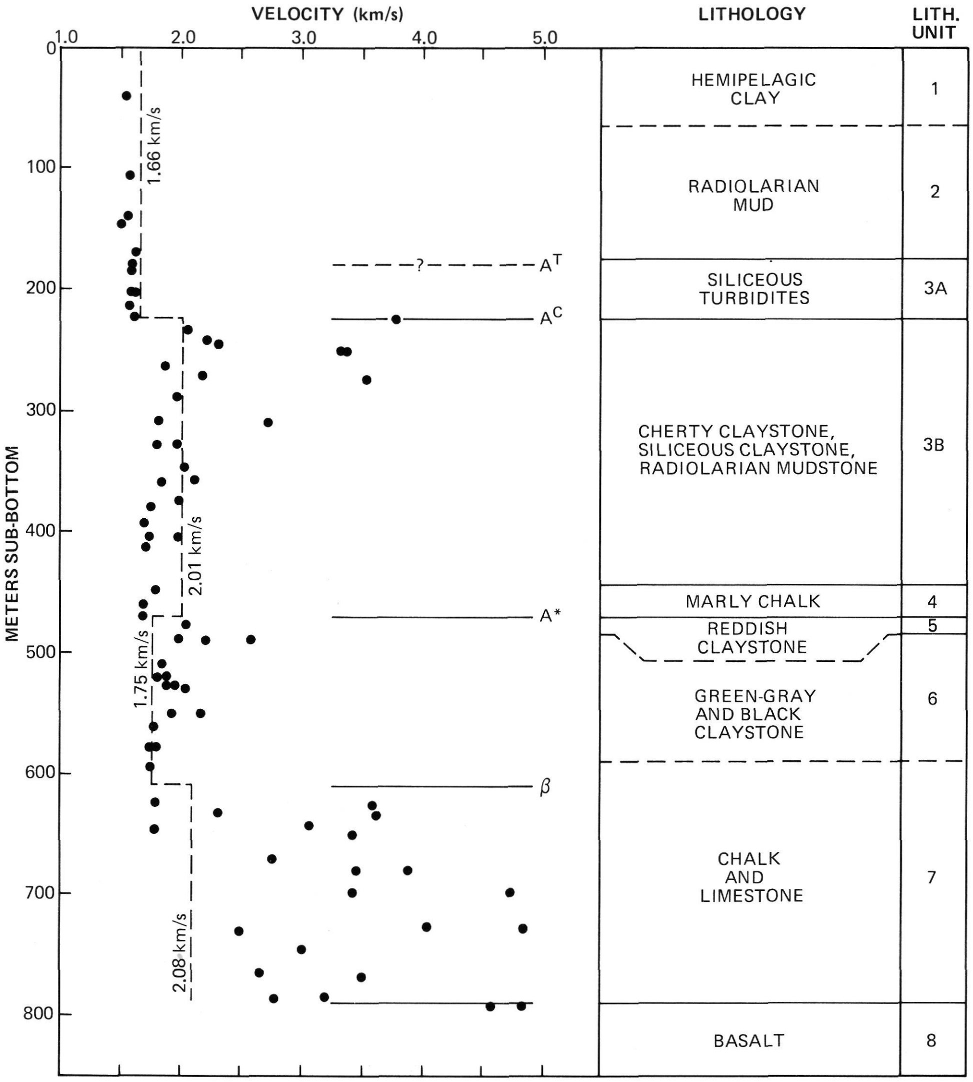

Figure 15. *Comparison of sonic velocities measured with the Hamilton-frame velocimeter (dots) and interval velocities calculated from correlation with seismic profile (dashed lines) at Site 387.*

ing glimpse of multicolored clays, lying just below Horizon A^C cherts, was obtained before drilling on Leg 1 had to be terminated for port call.

The calibration begun on Leg 1 with respect to age and lithofacies of the various reflectors comprising "Horizon *A*" has been a major ongoing objective in paleobasin analysis of the western North Atlantic. Drilling at Sites 386 and 387, with supplementary information from Sites 384, 385, and previously drilled sites, now provides a reasonably firm basis for such calibration, and we are confident that mapping of acoustic horizons (thickness, reflectivity, attitude, "acoustic texture," and relationship to other reflectors) will become a useful method of analyzing ancient patterns of sedimentation, ocean circulation at all depths, biologic productivity, and sediment source areas for the North American Basin.

Acoustic Horizons

Horizon A^T correlates approximately with the top of a sequence of middle Eocene siliceous turbidites (lithologic sub-unit 3A) which underlies upper Eocene radiolarian mud (Unit 2); this reflector correlation is identical to that at Site 386. Horizon A^T is the uppermost reflector of a series that has regional extent in the "Horizon-*A* complex." With the exception of Horizon A^C, most of the reflectors below Horizon A^T are poorly defined. The acoustic character of Horizon A^T, its probable correlation to the top of fine-grained siliceous turbidites, and its widespread distribution all suggest that middle Eocene and older Paleogene turbidites were deposited rapidly on the western Bermuda Rise. This lends support to the idea of Ewing et al. (1969), that the area now comprising the western Bermuda Rise was an abyssal plain (probably distal) prior to formation of the rise, and the continental margin of North America probably was the source area for the turbidites. The change to non-turbiditic radiolarian mudstones in the upper Eocene also demonstrates that broad uplift forming the Bermuda Rise occurred late in the middle Eocene. Provided Bermuda volcanism accompanied the uplift, the inferred time of uplift agrees with drilling results at Site 386, which indicate late Eocene through Oligocene denudation of the exposed summit of the Bermuda volcanic pedestal.

Horizon A^c at Site 387 clearly corresponds to the top of lower-middle Eocene cherts, and these are not masked by overlying calcareous turbidites like those found at Site 386. The carbonate sequence at Site 386 appears to be a local phenomenon caused by rapid redeposition of calcareous sediment from adjacent bathymetric highs.

Horizon A^* at Site 387 correlates with marly chalk at the top of Maestrichtian multicolored claystones, as it did at Site 386. It is unclear whether the actual correlation is with the upper or lower part of the chalk unit; correlation of A^* with the top provides more reasonable interval velocities between Horizons A^c to A^* and A^* to β, but the only marked impedance contrast that was measured in cored sediment occurred at the bottom of the unit. The discrepancy with the Site 105 correlation of A^* to the red-clay/black-clay transition (Hollister, Ewing, et al., 1972) is probably explained by the near convergence of Horizon A^* and "Horizon A" at Site 105; the 48-meter uncored interval at the level of these reflectors at Site 105 may have contained Paleocene and Maestrichtian siliceous and calcareous sediment which we observe at and above Horizon A^* at Site 386 and 387.

Horizon β, cored at Site 387 near the easternmost limit where it can be traced confidently in profiler records, corresponds to a Barremian transition from black claystones downward through chalks into limestones. The similarity of this correlation to that at Sites 101 and 105 provides evidence that Horizon β is essentially a lithostratigraphic horizon. Although somewhat variable from site to site, the age of Horizon β as determined by drilling at Sites 5, 99, 101, 105, 387, and 391 is consistently within the Hauterivian or Barremian. Lithologically it corresponds to the shallowest occurrence of high-impedance limestone beneath the Cretaceous black clays. Of all the drill sites in this area, high-carbonate sediments tend to persist longest in the sedimentary record at Site 99 near the Bahama Banks and at Site 387 in the Early Cretaceous ridge-flank province where carbonate deposition could be expected to continue for some time after black-clay deposition was initiated in the deeper basin.

Depositional History

The age of basaltic crust (acoustic basement) at Site 387 is established as Berriasian to Valanginian by dated nannoflora in pink clayey sediment both overlying the basalt and as baked inclusions in the basalt. Petrographic evidence suggests that the basalt cored is a sill; however, because similar basaltic material cored on DSDP Leg 37 consists of a thick (≅ 300 m) series of flows and sills all formed very near the spreading axis, it is likely that the late Berriasian/early Valanginian date is very close to the age of original ocean crust at Site 387. The age of crust between anomalies *M*-15 and *M*-16 is therefore about 129-133 m.y. on the van Hinte (1976) time scale.

The Neocomian limestones first deposited at Site 387 probably accumulated in a lower bathyal to upper abyssal, well-oxygenated environment above the contemporary CCD. Marly interbeds which contain mica and fine quartz (Koch and Rothe, this volume) probably reflect dispersal of terrigenous debris by surface currents and weak deep currents in the basin. Wood fragments and other (probably land-derived) materials containing organic carbon are common in these interbeds, as are aptychi of pelagic ammonites (Renz, this volume). The dark color of these marly interbeds suggests microreducing conditions were common within the sediments. Primary sedimentary structures of turbiditic connotation must result from deposition of local, pelagic turbidites (Lancelot et al., 1972) because the position of the site on the Neocomian Mid-Atlantic Ridge flank precludes a continental margin provenance. Interbedded hard gray cherts probably derived their silica from complete dissolution and reprecipitation of biogenic opal deposited with the calcareous sediments.

Reducing conditions became prevalent and the CCD rose abruptly late in the Barremian, resulting in the deposition of gray-green and black clays. Minor reducing pulses preceding this event are observed in the upper part of the limestones. Organic carbon content is uniformly low in the burrow-mottled gray-green clays and is highly variable (0.1 to 14%) in the unmottled gray and black claystones (Kendrick, this volume). Abundant humic (land-derived) carbon and quartz in the unit indicate significant terrigenous input, possibly as very fine-grained distal turbidites. Coarser layers of radiolarian ooze (and very minor nannofossil ooze) suggest high, possibly episodic, productivity in the surface waters. Episodic anoxic bottom-water conditions are indicated by the absence of burrow mottling and by excess sulfur in the sediment, the sulfur probably being derived from sulfate in the overlying water column (Kendrick, this volume).

The change to multicolored claystones, probably in the middle Cenomanian to Turonian or later, was accompanied by a sharp drop in sediment accumulation rates, a marked decrease in terrigenous input, and re-establishment of oxidizing conditions. Volcanic glass observed in smear slides form this interval suggests that a substantial proportion of the sediment was derived from alteration of volcanogenic debris; this volcanogenic component may represent essentially the background level of volcanism in this truly pelagic unit. Volcanism along the New England Seamount chain (Sites 382, 385) and possibly at Bermuda about 90-110 m.y.B.P. (Reynolds and Aumento, 1974) might have provided volcanogenic debris. Deposition was well below the contemporary CCD.

The late Maestrichtian drop in the CCD, which interrupted red-clay deposition, and which is suggested by calcareous sediments at Sites 384, 385, and 386 (Tucholke and Vogt, this volume), is substantiated at Site 387 by deposition of marly chalks. Shoaling of the CCD and deposition of minor black clays occurred in the Paleocene at Site 387.

By Eocene time siliceous biogenic sediments were being deposited in abundance, mostly below the CCD. The rapid accumulation rates probably result from the combined influences of high surface-water productivity and deposition of fine, distal turbidites. Sedimentation rates decrease in the upper Eocene radiolarian mudstones, presumably because the broad uplift forming the Bermuda Rise isolated the site from the influx of turbidites.

Surface-water productivity decreased markedly sometime after the late Oligocene, and hemipelagic clays, probably deposited largely from bottom currents, dominate the Quaternary sedimentary record.

REFERENCES

Bryan, W. B., 1972. Textural and mineralogical relations of basalts from Sites 100 and 105. *In* Hollister, C. D., Ewing, J. I., et al., *Initial Reports of the Deep Sea Drilling Project,* v. 11: Washington (U. S. Government Printing Office), p. 873-876.

Ewing, J. I. and Hollister, C. D., 1972. Regional aspects of deep sea drilling in the western North Atlantic. *In* Hollister C. D., Ewing, J. I., et al., *Initial Reports of the Deep Sea Drilling Project,* v. 11: Washington (U.S. Government Printing Office), p. 951.

Ewing, J., Windisch, C., and Ewing, M., 1970. Correlation of Horizon A with JOIDES bore-hole results, *J. Geophys. Res.,* v. 75, p. 5645-5653.

Ewing, M., Worzel, J. L., et al., 1969. *Initial Reports of the Deep Sea Drilling Project*, v. 1: Washington (U.S. Government Printing Office).

Hollister, C. D., Ewing, J. I., et al., 1972. *Initial Reports of the Deep Sea Drilling Project*, v. 11: Washington (U.S. Government Printing Office).

Krasheninnikov, V. A., 1973. Cretaceous benthonic foraminifera, Leg 20, Deep Sea Drilling Project. *In* Heezen, B. C., MacGregor, I. D., et al., *Initial Reports of the Deep Sea Drilling Project*, v. 20: Washington (U.S. Government Printing Office) p. 205-219.

________, V. A., 1975. Upper Cretaceous benthonic agglutinated foraminifera, Leg 27 of the Deep Sea Drilling Project. *In* Veevers, J. J., Heirtzler, J. R., et al., *Initial Reports of the Deep Sea Drilling Project*, v. 27: Washington (U.S. Government Printing Office) p. 631-661.

Lancelot, Y., Hathaway, J. C., and Hollister, C. D., 1972. Lithology of sediments from the western North Atlantic Leg 11 Deep Sea Drilling Project. *In* Hollister, C. D., Ewing, J. I., et al., *Initial Reports of the Deep Sea Drilling Project,* v. 11: Washington (U.S. Government Printing Office), p. 901-949.

Larson, R. and Hilde, T., 1975. Revised time scale of magnetic reversals for the Early Cretaceous, Late Jurassic, *J. Geophys. Res.*, v. 80, p. 2586-2594.

Reynolds, P. H. and Aumento, F., 1974. Deep Drill 1972. Potassium-argon dating of the Bermuda drill core, *Canadian J. Earth Sci.*, v. 2, p. 1269-1273.

Theirstein, H. R., 1975. Calcareous nannoplankton biostratigraphy of the Jurassic-Cretaceous boundary, *Mem. Bur. Tech. Geol. Min.*, v. 86, p. 85-94.

________, 1976, Mesozoic calcareous nannoplankton biostratigraphy of marine sediments, *Mar. Micropaleontol.*, v. 1, p. 324-362.

Thomas, H. H., 1922. On certain xenolithic Tertiary minor intrusions in the island of Mull (Argyllshire), *Quart. J. Geol. Soc. London*, v. 78, p. 229-259.

Tucholke, B. E. and Ewing, J., 1974. Bathymetry and sediment geometry of the Greater Antilles Outer Ridge and Greater vicinity, *Geol. Soc. Am. Bull.*, v. 85, p. 1789-1802.

van Hinte, J. E., 1976. A Cretaceous time scale, *Am. Assoc. Petrol. Geol. Bull.*, v. 60, p. 498-516.

Vogt, P. R., Anderson, C. N., and Bracey D. R., 1971. Mesozoic magnetic anomalies, sea-floor spreading, and geomagnetic reversals in the southwestern North Atlantic, *J. Geophys. Res.*, v. 76, p. 4796-4823.

Hole 387 Core 1 Cored Interval: 31.8-41.3 m

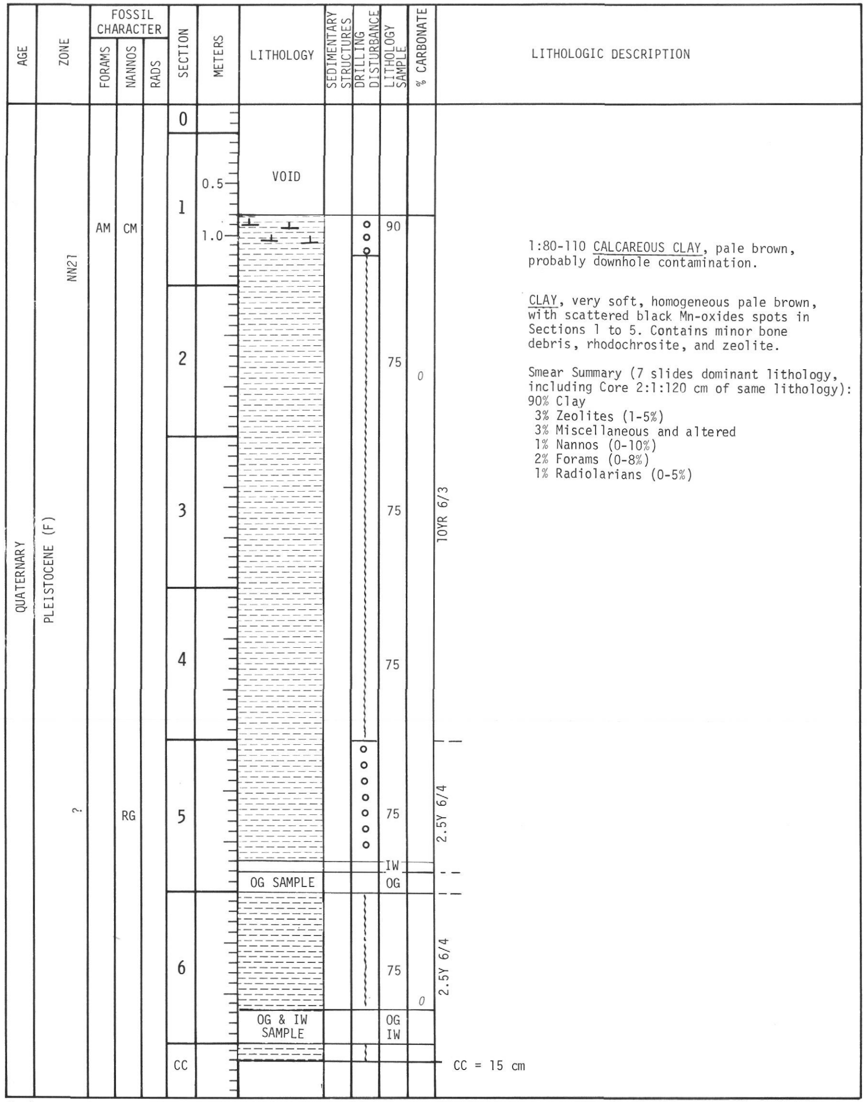

1:80-110 CALCAREOUS CLAY, pale brown, probably downhole contamination.

CLAY, very soft, homogeneous pale brown, with scattered black Mn-oxides spots in Sections 1 to 5. Contains minor bone debris, rhodochrosite, and zeolite.

Smear Summary (7 slides dominant lithology, including Core 2:1:120 cm of same lithology):
90% Clay
3% Zeolites (1-5%)
3% Miscellaneous and altered
1% Nannos (0-10%)
2% Forams (0-8%)
1% Radiolarians (0-5%)

Explanatory notes in Chapter 1

Hole 387 Core 2 Cored Interval: 98.4-108.0 m

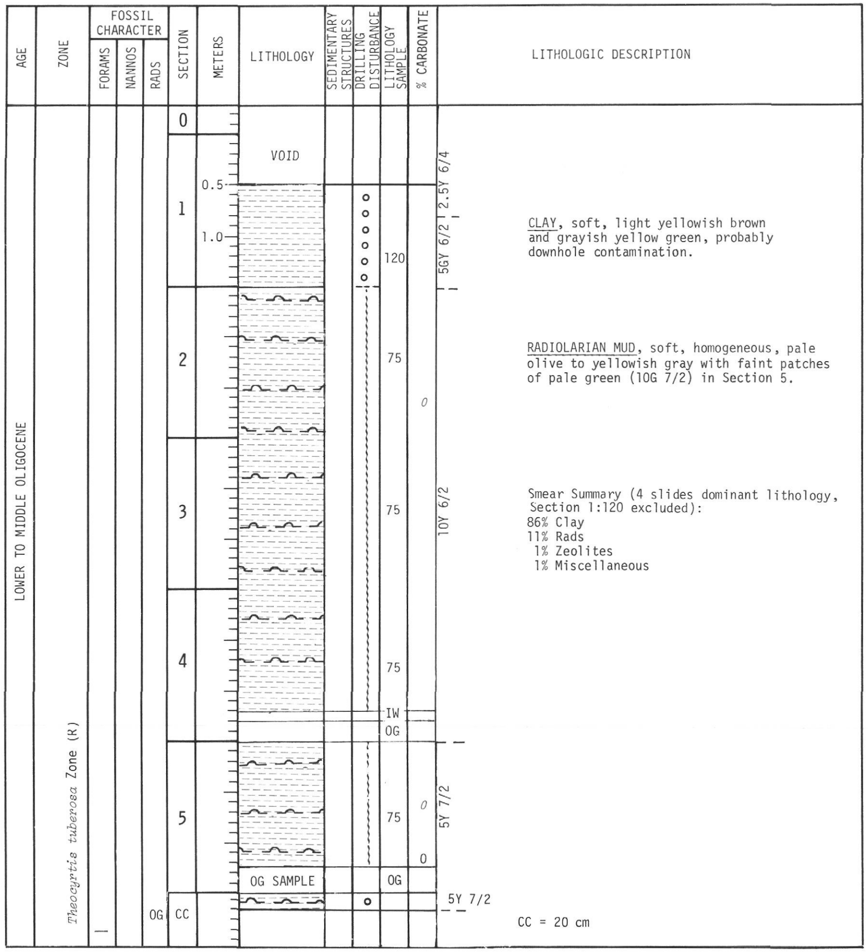

CLAY, soft, light yellowish brown and grayish yellow green, probably downhole contamination.

RADIOLARIAN MUD, soft, homogeneous, pale olive to yellowish gray with faint patches of pale green (10G 7/2) in Section 5.

Smear Summary (4 slides dominant lithology, Section 1:120 excluded):
86% Clay
11% Rads
1% Zeolites
1% Miscellaneous

Hole 387 Core 3 Cored Interval: 136.6-146.1 m

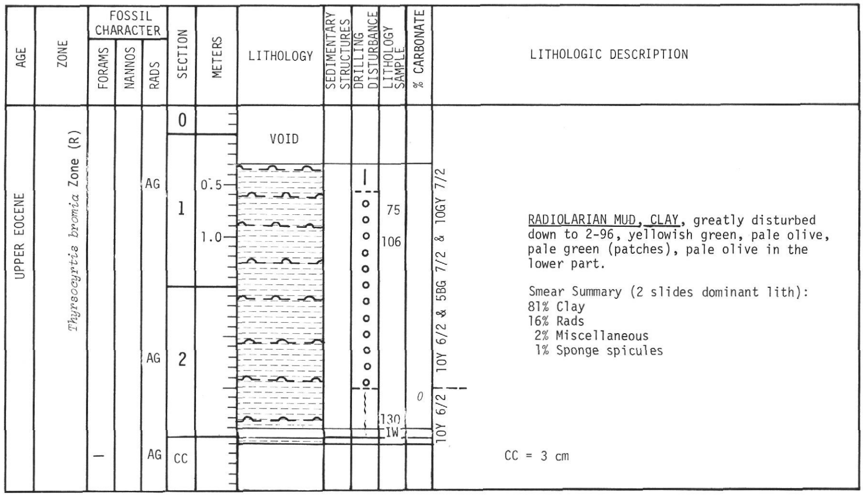

RADIOLARIAN MUD, CLAY, greatly disturbed down to 2-96, yellowish green, pale olive, pale green (patches), pale olive in the lower part.

Smear Summary (2 slides dominant lith):
81% Clay
16% Rads
2% Miscellaneous
1% Sponge spicules

CC = 3 cm

Hole 387 Core 4 Cored Interval: 146.1-155.6 m

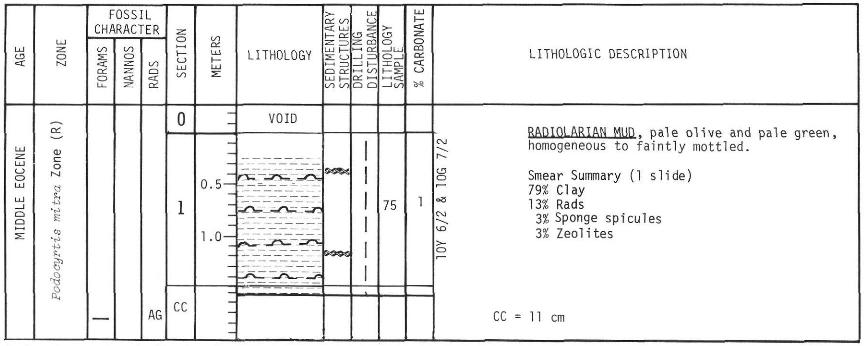

RADIOLARIAN MUD, pale olive and pale green, homogeneous to faintly mottled.

Smear Summary (1 slide)
79% Clay
13% Rads
3% Sponge spicules
3% Zeolites

CC = 11 cm

Explanatory notes in Chapter 1

Hole 387 Core 5 Cored Interval: 155.6-165.1 m

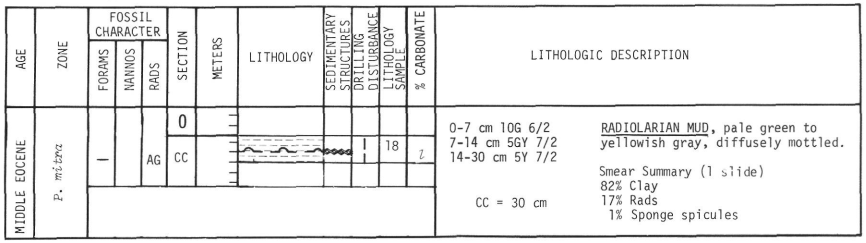

0-7 cm 10G 6/2
7-14 cm 5GY 7/2
14-30 cm 5Y 7/2

CC = 30 cm

RADIOLARIAN MUD, pale green to yellowish gray, diffusely mottled.

Smear Summary (1 slide)
82% Clay
17% Rads
1% Sponge spicules

Hole 387 Core 6 Cored Interval: 165.1-174.6 m

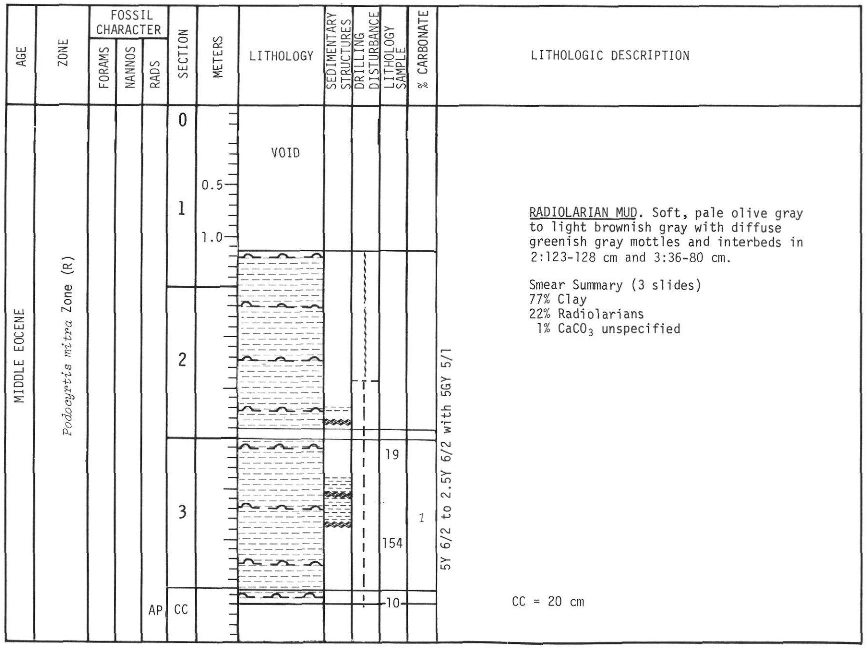

RADIOLARIAN MUD. Soft, pale olive gray to light brownish gray with diffuse greenish gray mottles and interbeds in 2:123-128 cm and 3:36-80 cm.

Smear Summary (3 slides)
77% Clay
22% Radiolarians
1% $CaCO_3$ unspecified

CC = 20 cm

Hole 387 Core 7 Cored Interval: 174.6-184.2 m

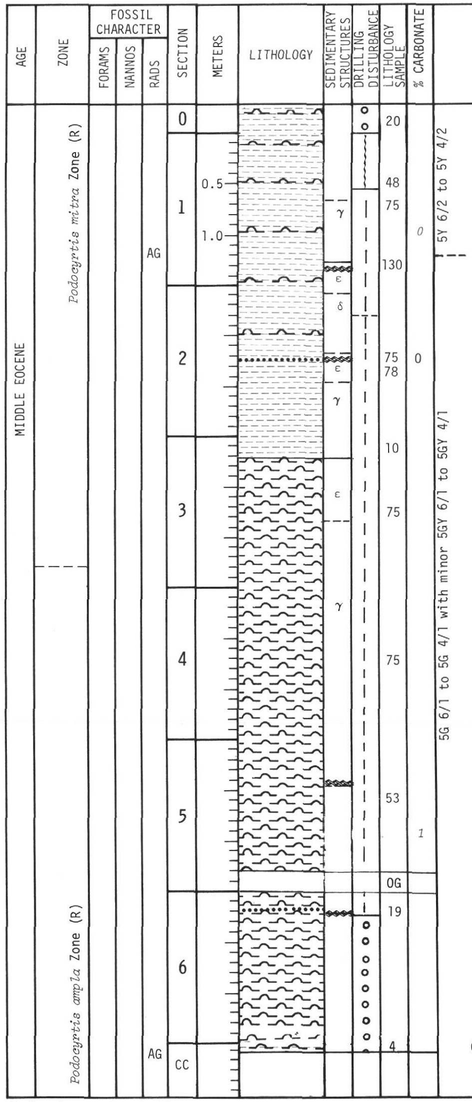

LITHOLOGIC DESCRIPTION

0 Sect. = 37 cm

RADIOLARIAN MUD, olive gray in upper part, *mostly greenish gray below 1:115 cm. In* both, alternation of darker and lighter colored layers.
ε-dark, with black streaks
δ-faintly mottled
γ-homogeneous
Sharp basal boundary, not in every unit.

Smear Summary (6 slides)
70% Clay
27% Radiolarians
2% Sponge spicules

sharp contact

RADIOLARIAN OOZE, greenish gray to dark greenish gray, alternation of darker and lighter layers (indistinctly rhythmic) as above. Boundaries are rather poorly defined, dark layers, "ε", with black streaks of hydrotroilite are not distinct. A thin interbed of sponge spicule mud occurs in Section 6, 19 cm (.....), containing ∿20% spicules, as well as ∿15% detrital silt-size minerals.

Smear Summary (4 slides)
46% Clay
45% Radiolarians
5% Sponge spicules
4% Miscellaneous

CC = 4 cm

Explanatory notes in Chapter 1

Hole 387 Core 8 Cored Interval: 184.2-193.7 m

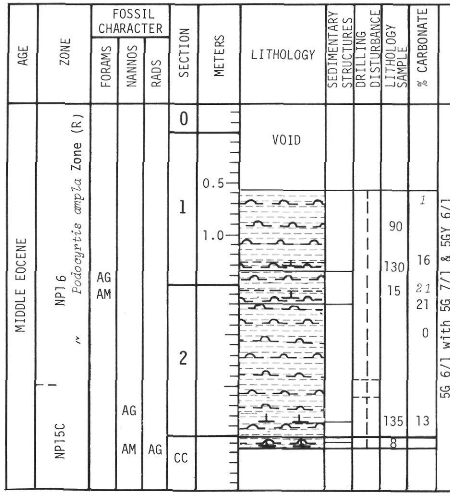

LITHOLOGIC DESCRIPTION

RADIOLARIAN MUD, firm to moderately firm, *greenish gray, with olive gray and yellow* greenish gray NANNO RAD MUD interlayers in:
Section 1, 128-134 cm
Section 2, 7-20 cm
Section 2, 133-137 cm
CC, 0-4 cm
The basal contacts of the calcareous interlayers are usually distinct or sharp; the upper contacts are rather transitional.

Smear Summary (5 slides)
57% Clay
29% Radiolarians
7% Nannos (0-18%)
3% Carb. unspec. (1-11%)
3% Sponge spicules
1% Glauconite

CC = 8 cm

5GY 6/1 & 5G 5/1

Hole 387 Core 9 Cored Interval: 193.7-203.2 m

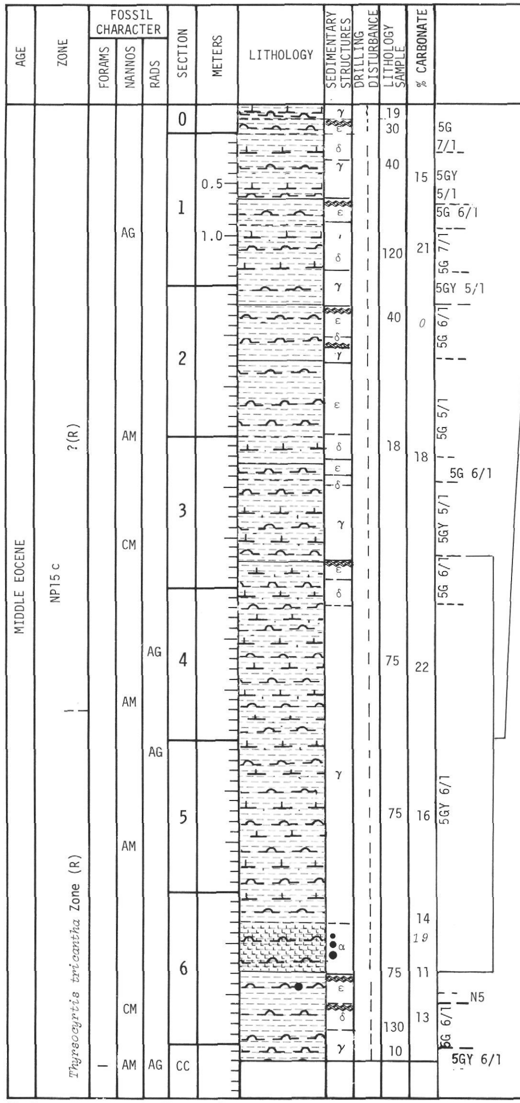

LITHOLOGIC DESCRIPTION

0 Sect. = 37 cm

RADIOLARIAN MUD AND CALCAREOUS RADIOLARIAN MUD: rhythmic sequence of distinct units 50 to 400 cm thick, most completely represented in Sections 3-6:

- ε - RAD MUD medium gray with abundant dark streaks, mottled;
- δ - RAD MUD, with more nannos, mottled, greenish gray (5G 6/1);
- γ - NANNO RAD MUD, greenish gray (5GY 6/1), homogeneous;
- α - SPONGE-SPICULE RAD MUD greenish gray, grading down from silty clay to coarse sandy silt; with sharp basalt contact.

Other units consist of γ, δ, ε, subunits, i.e. RAD MUD grading downward to CALCAREOUS (NANNO) RAD MUD or to RAD MUD with slightly higher $CaCO_3$. In the uppermost units, the downward transition from NANNO RAD MUD to CALCAREOUS (unspec. $CaCO_3$) RAD MUD is distinguished in smear slides.

Smear Summary (10 slides)
59% Clay
21% Rads
4% Sponge spicules
10% Nannos (2-19)
1% Glauconite
6% Other
1% Feldspar

CC - 21 cm

Explanatory notes in Chapter 1

Hole 387 Core 10 Cored Interval: 203.2-212.8 m

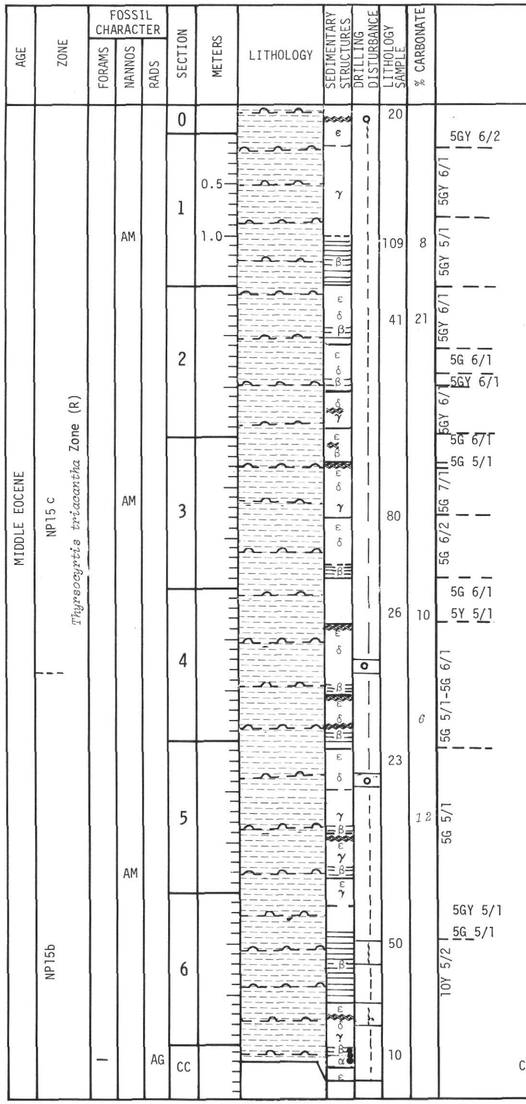

LITHOLOGIC DESCRIPTION

0 Section = 41 cm

MUDDY RADIOLARIAN OOZE and RADIOLARIAN MUD alternating in rhythmically bedded sequence, consisting of more or less distinct units with 2 to 5 subunits in each (α to ε) distinguished by color changes, partly by texture (coarser-finer) or by changes in compostiion (rad-clay-nanno content).

ε - darker greenish gray with dark streaks, mottled, rad mud.
δ - lighter greenish gray (5GY 6/1), mottled, more $CaCO_3$, less rads, rad mud.
γ - lighter greenish gray (5GY 6/1 or 5G 7/1), calcareous rad mud, homogeneous.
β - thinly laminated (faintly laminated), greenish gray (5GY 5/1) to olive (5Y 5/1) or greenish olive (10Y 5/2); in some units β_2 (upper) - greenish gray, light β_1 (lower) - olive gray, dark.
Rad mud to muddy rad ooze, high rad content, abundant sponge spicules (6-8%).
α - coarser, massive, graded, abundant spicules, poorly developed only in CC.
Thickness of single units in the core ranges from 30 cm to 150 cm.

Smear Summary (8 slides)
46% Clay
37% Radiolarians
6% Sponge spicules
2% Diatoms
4% Nannos
3% $CaCO_3$ unspec.
1% Glauconite
1% Feldspar

CC = 15 cm

Hole 387 Core 11 Cored Interval: 212.8-222.3 m

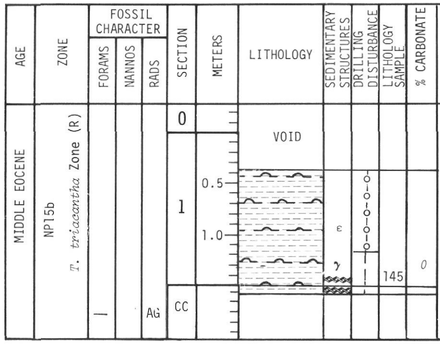

LITHOLOGIC DESCRIPTION

MUDDY RADIOLARIAN OOZE different shades of greenish gray (disturbed). In the lower part of Section 1 - transition between ε and γ subunits (see Core 10).

Smear Summary (1 slide)
47% Clay
50% Radiolarians
1% Sponge spicules
1%. Diatoms
1% Feldspar Tr Quartz

10Y 3/2

CC = 10 cm

Hole 387 Core 12 Cored Interval: 222.3-231.8 m

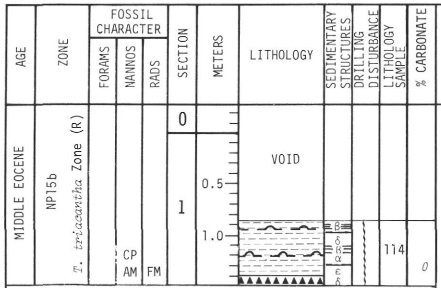

LITHOLOGIC DESCRIPTION

RADIOLARIAN MUDSTONE, greenish gray to medium olive gray. Three thin units grading from clay and silty clay (ε,γ) to laminated radiolarian siltstone (Radiolarite) in the basalt subunits α,β. CHERT with relict structure and appearance of the "ε" subunit.

5G 6/1
5Y 4/2

Smear Summary (1 slide)
43% Clay
45% Radiolarians
5% Sponge spicules
1% Diatoms
1% Nannos
1% $CaCO_3$ unspec.
1% Quartz
2% Feldspar
1% Miscellaneous

CC = empty

Explanatory notes in Chapter 1

Hole 387 Core 13 Cored Interval: 231.8-241.3 m

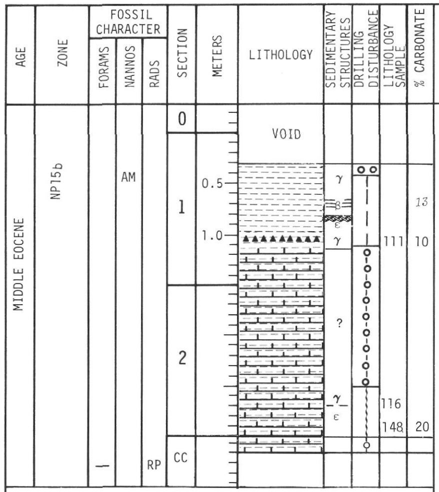

LITHOLOGIC DESCRIPTION

CLAYSTONE olive gray to greenish gray (2 indistinct units).
CHERT (PORCELANITE), medium greenish gray (5G 5/1), mottled.

5Y 4/2
5Y 3/2
5G 5/1

drilling breccia

NANNO CLAYSTONE, olive gray (γ), dark greenish gray (ε) to very light greenish gray.

5Y 4/2
5G 4/1
5G 8/1
5GY 6/1

Smear Summary (3 slides)
71% Clay*
14% Nannos
3% Radiolarians
2% Forams
2% $CaCO_3$ unspec.
5% Miscellaneous
1% Feldspar + Quartz
1% Opaques
*Includes recrystalized silica

CC = 19 cm of:
NANNO CLAYSTONE, greenish gray, homogeneous.

Hole 387 Core 14 Cored Interval: 241.3-250.7 m

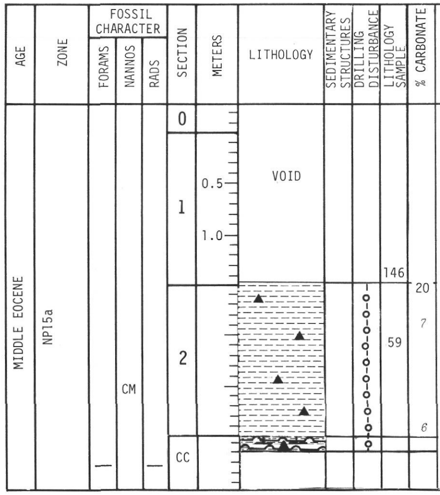

LITHOLOGIC DESCRIPTION

SILICIFIED CLAYSTONE and PORCELANITIC CHERT. Series of thin incomplete units (see Core 9, α-ε),10-20 cm each, represented mostly by subunits ε and β, whereas softer material of the sequence (γ and δ) has been washed out. Most silicified are greenish gray subunits "ε" below coarser interbeds.

Laminated subunit "β" is olive green (5YR 4/1) claystone. Thin (10 cm) top layer of calcareous siliceous mudstone occurs in Section 1 (140-150).

Smear Summary (2 slides)
57% Clay*
17% Radiolarians
9% Diatoms
1% Sponge spiculae
8% Nannos
3% Forams
3% $CaCO_3$ unspec.
2% Miscellaneous
*includes recrystallized silica
CC = 15 cm

Hole 387 Core 15 Cored Interval: 250.7-260.1 m

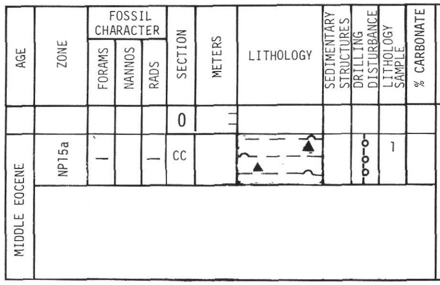

LITHOLOGIC DESCRIPTION

5Y 3/2 CC = 25 cm of PORCELANITIC CHERT and SILICIFIED RADIOLARIAN MUDSTONE. Chert is mottled greenish gray subunit "ε", mudstone is olive gray (5Y 3/2).

Smear Summary (1 slide)
79% Clay*
15% Radiolarians
5% Miscellaneous
1% Opaques *includes recrystallized silica

Hole 386 Core 16 Cored Interval: 260.1-269.6 m

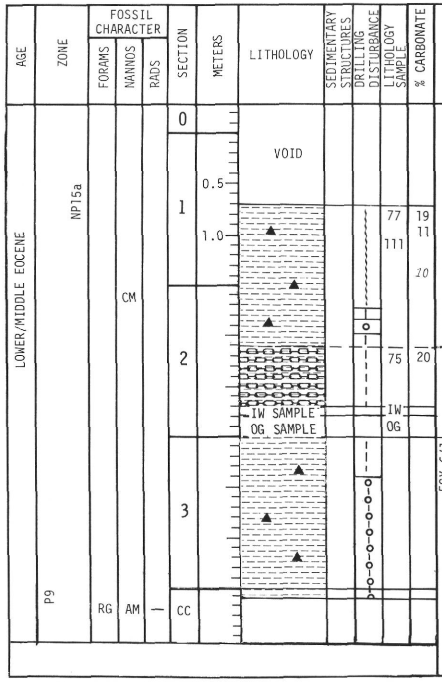

LITHOLOGIC DESCRIPTION

5G 7/1
5Y 4/1
5G 6/2
5G 4/1
5Y 4/1
5GY 6/1

SILICIFIED CLAYSTONE and PORCELANITIC CHERT, alternating layers of greenish gray (ε,δ) and olive gray (β,γ); cherts occur usually in ε and α (coarse) subunits.

CALCAREOUS SILICIFIED CLAYSTONE, homogeneous, greenish gray.

SILICIFIED CLAYSTONE, homogeneous, greenish gray.

Smear Summary (3 slides)
72% Clay*
10% Radiolarians
6% Nannos
2% Forams
9% $CaCO_3$ unspec.
1% Miscellaneous
*Includes recrystallized silica

5GY 6/1 CC = 10 cm of CLAYSTONE, greenish gray.

Explanatory notes in Chapter 1

Hole 387 Core 17 Cored Interval: 269.6-279.1 m

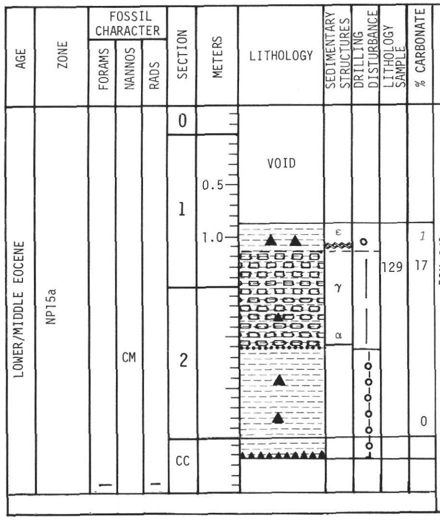

LITHOLOGIC DESCRIPTION

5GY 6/1

PORCELANITIC CHERT, SILICIFIED CLAYSTONE, and SILICIFIED CALCAREOUS CLAYSTONE: series of alternating subunits as above, but cherts are more abundant, being predominant in "ε" - greenish gray, mottled; and "β" - olive gray, thinly laminated. Lighter "γ" and "δ" subunits are silicified claystone or calcareous claystone, greenish gray, homogeneous. Thin interbed of calcareous muddy sandstone with mud clasts occurs in Section 2, 52-56 cm (α).

For symbols see Core 9.

Smear Summary (1 slide)
81% Clay*
14% $CaCO_3$ unspec.
2% Nannos
5GY 6/1 1% Forams
2% Miscellaneous
CC = 20 cm *Includes recrystallized silica

Hole 387 Core 18 Cored Interval: 288.7-298.2 m

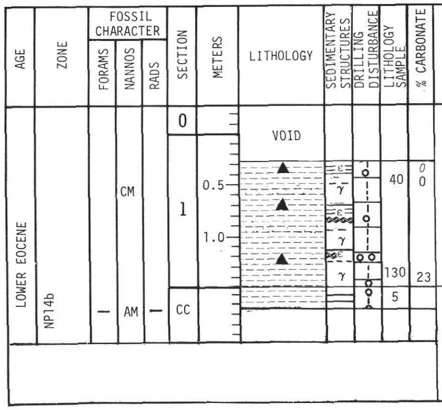

LITHOLOGIC DESCRIPTION

SILICIFIED CLAYSTONE and SILICIFIED CALCAREOUS CLAYSTONE, rhythmically alternating units:

5G 3/1-4/1 ε (incl. β?) - dark greenish gray, mottled & laminated, with cherts on the top (claystone
10Y 4/2 subunit).

γ - grayish olive, homogeneous (calcareous
5G 4/1 claystone with higher rad content).
10Y 4/2

5G 3/1-4/1 Smear Summary (3 slides)
10Y 4/2 78% Clay*
8% Carb. unspec. (1-20%)
9% Rads
10Y 5/2 2% Forams
5G 5/1 1% Nannos
1% Feldspar + Quartz
*Includes recrystallized silica
CC = 26 cm of
SILICIFIED CLAYSTONE, thinly bedded.

Hole 387 Core 19 Cored Interval: 307.7-317.2 m

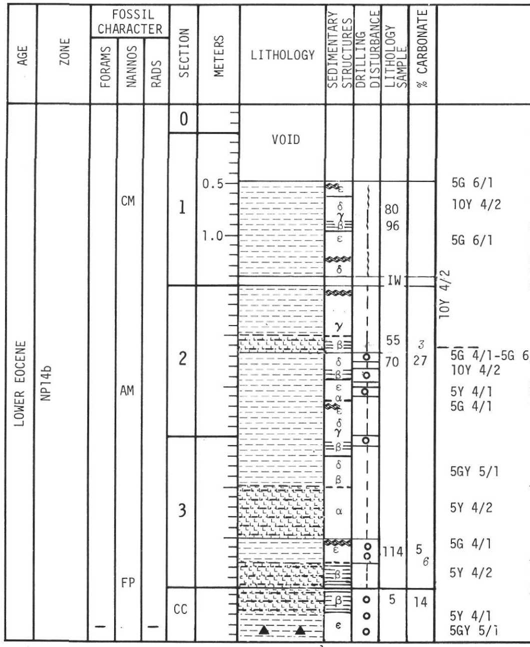

LITHOLOGIC DESCRIPTION

CLAYSTONE with SPONGE-SPICULE MUDSTONE interbeds, the latter being α and β subunits :

ε - claystone, dark greeenish gray to greenish gray, mottled, with dark streaks.
δ - claystone, grayish olive, mottled.
γ - claystone or calcareous claystone, grayish olive, homogeneous.
β - claystone or sponge spicule mudstone, grayish olive, laminated.
α - sponge spicule mudstone, grayish olive, graded (silt→silty clay).

Smear Slide Summary (6 slides)
74% Clay*
8% Sponge spicules (0-28%)
8% Unspec. carb. (2-22%)
6% Rads
2% Nannos
2% Mica
*Includes recrystallized silica

CC = 25 cm of SPONGE-SPICULE MUDSTONE, CLAYSTONE, and PORCELANITIC CHERT.

Explanatory notes in Chapter 1

Hole 387 Core 20 Cored Interval: 326.7-336.2 m

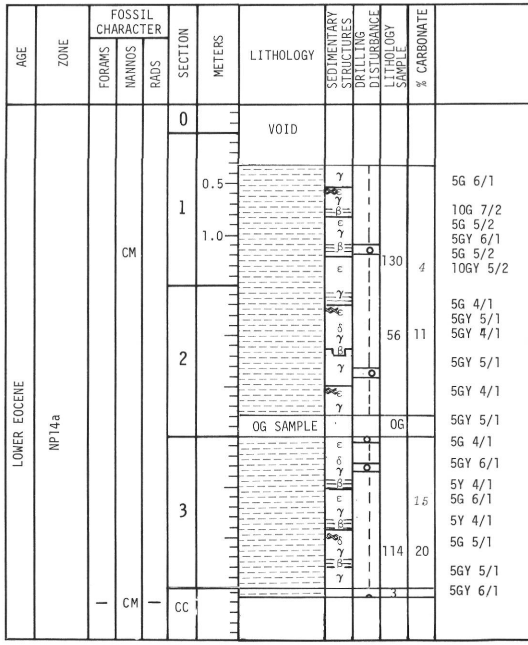

LITHOLOGIC DESCRIPTION

CLAYSTONE, in the upper part SILICIFIED, with *SILTY CLAYSTONE* and *NANNO CLAYSTONE* interbeds, the latter in γ and δ subunits.
ε - dark greenish gray, greenish gray, grayish green, mottled, with dark streaks.
δ - grayish green, greenish gray nanno claystone, burrowed.
γ - Same, homogeneous.
β - greenish gray, olive gray, laminated to faintly laminated claystone and silty claystone. At some levels homogeneous layer (α?) appears between β and underlying ε without distinct textural change.
From upper part to lower, firmness of the sediment decreases.
Smear Slide Summary (4 slides)
78% Clay*
8% Nannos
5% Rads (0-12%)
4% Unspec. carb.
3% Mica (0-10%)
1% Glauconite
1% Pyrite
*Includes recrystallized silica

CC = 5 cm

Hole 387 Core 21 Cored Interval: 345.7-355.2 m

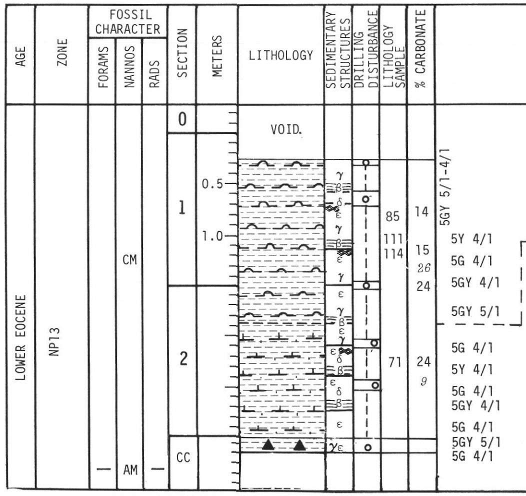

LITHOLOGIC DESCRIPTION

RADIOLARIAN MUDSTONE, rhytmically alternating color layers with less distinct textural and structural changes.
ε - dark greenish gray (5G 4/1) mottled.
γ,δ - greenish gray, homogeneous, higher $CaCO_3$.
β - laminated, olive gray, increasing rad content, spicules in basal part of subunit.

CLAYSTONE, CALCAREOUS CLAYSTONE, alternating layers, as above, but less radiolaria, more nannos and clay.

Smear Summary (4 slides)
62% Clay
22% Rads
8% Nannos
6% Unspec. carb.
1% Sponge spicules
1% Mica

CC = 20 cm of SILICIFIED CLAYSTONE, and PORCELANTIIC CHERT, greenish gray and dark greenish gray.

Hole 387 Core 22 Cored Interval: 355.2-364.8 m

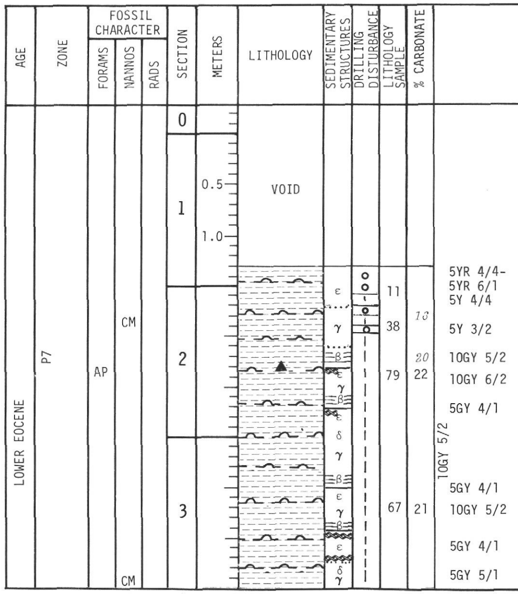

Explanatory notes in Chapter 1

LITHOLOGIC DESCRIPTION

RADIOLARIAN MUDSTONE with distinct rhythmic stratification (units: ε to β):

ε - dark, greenish gray (5GY 4/1) or grayish green (10GY 4/2); in the uppermost unit (Section 1) top layer is olive brown (5Y 4/4) to moderate brown (5YR 4/4) with green interbeds.

δ - poorly developed mottled zone (below ε) greenish gray.

γ - well developed thick subunits, homogeneous, grayish green (10GY 5/2) or olive gray (5Y 3/2) in the upper part of the core; higher $CaCO_3$.

β - thin, faintly laminated grayish green; well developed only in Section 2, 60-80 cm, (with silicified Foram-Rad Mudstone basal layer).

Smear Summary (4 slides)
59% Clay*
26% Rads (10-50%)
5% Nannos (0-15%)
4% Forams (0-17%)
4% Unspec. carb.
1% Sponge spicules
1% Glauconite
*Includes recrystallized silica

CC = empty

Hole 387 Core 23 Cored Interval: 374.3-383.8 m

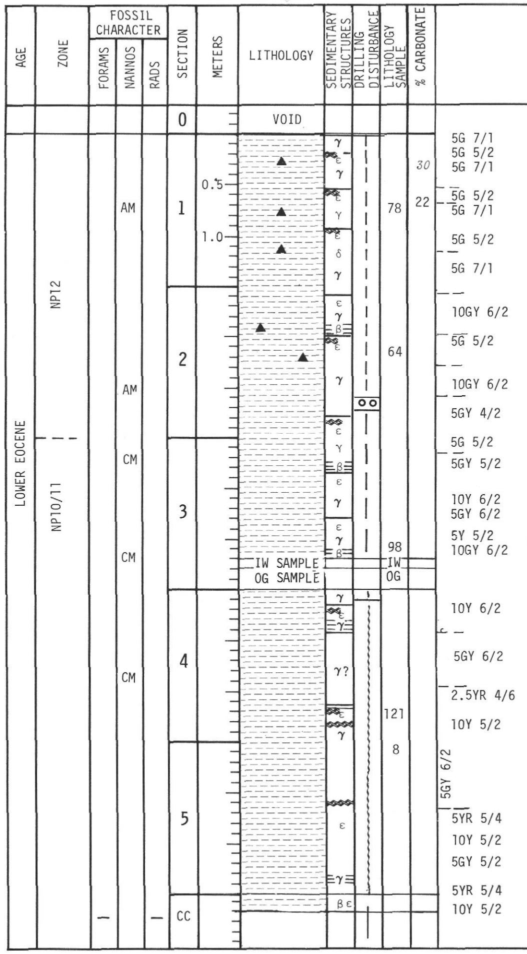

LITHOLOGIC DESCRIPTION

CLAYSTONE with silicified interbeds (PORCELANITE) and CALCAREOUS CLAYSTONE in Section 1. Alternating color layers without distinct textural changes: mainly ε and γ Subunits developed with minor δ (light, mottled) and β (laminated). In Sections 4-5, units are indistinct due to intense drilling disturbance and random color variations.

Dominant colors for "ε" subunits are greenish gray (5G 5/2, 5G 4/2, 5GY 4/2) in Sections 1-2; pale brownish greenish to greenish brown (5Y 5/2) and light brown (5YR 5/4) in Sections 3-5. For "γ" subunits (homogeneous): light greenish gray (5G 7/1) - in Section 1, grayish green (10GY 6/2), dusky yellow green (5GY 5/2), pale olive (10Y 6/2) in Sections 2-5.

Smear Summary (5 slides)
91% Clay*
2% Nannos (0-12%)
2% Unspec. carb. (0-10%)
2% Feldspar
1% Rads
2% Miscellaneous and altered
*Includes recrystallized silica

CC = 14 cm

Hole 387 Core 24 Cored Interval: 393.3-402.8 m

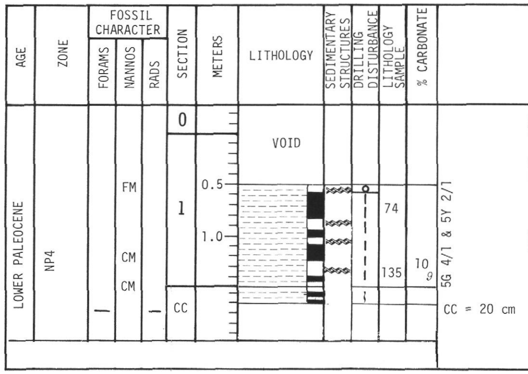

LITHOLOGIC DESCRIPTION

CLAYSTONE with alternating color layers of olive black (pyritic) and dark greenish gray (intensely mottled). Boundaries, originally sharp, are cut by burrows, filled with olive black clay. Thickness of the layers ranges from 10 to 25 cm, the black layers (as indicated) being somewhat thicker.

Smear Summary (3 slides)
85% Clay*
5% Rads
3% Unspec. carb.
3% Miscellaneous and altered
2% Nannos
1% Mica
1% Pyrite
*Includes recrystallized silica

Hole 387 Core 25 Cored Interval: 402.8-412.2 m

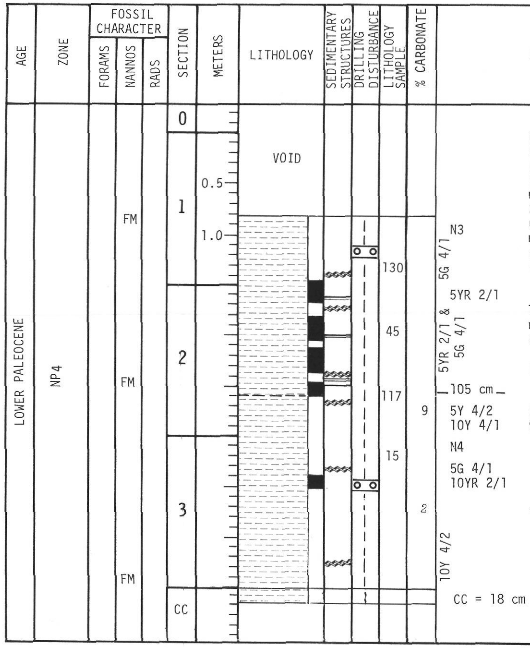

LITHOLOGIC DESCRIPTION

CLAYSTONE, with alternating color layers of brownish black, dark greenish gray and olive (medium olive gray (5Y 4/2) to light olive (10Y 5/2 - 10Y 4/2), the greenish being mostly in the upper part (Section 1, Section 2, 0-105 cm) and the olive in the lower. The upper part is in some intervals intensely mottled, burrows cutting color boundaries and laminae. Laminated intervals (═) in black as well as in gray layers.

The lower part (below Section 2, 105 cm) is more homogeneous, less burrowed, non-laminated.

NOTE: black layers are indicated.

Smear Summary (4 slides)
93% Clay*
2% Nannos
2% Rads
1% Unspec. carb.
1% Pyrite
1% Miscellaneous and altered
*Includes recrystallized silica

Explanatory notes in Chapter 1

Hole 387 Core 26 Cored Interval: 412.2-421.7 m

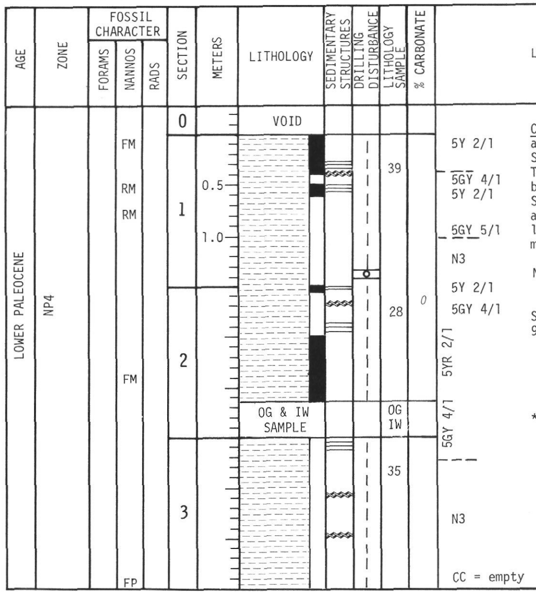

LITHOLOGIC DESCRIPTION

CLAYSTONE, alternating layers of olive black and dark greenish gray (or dark gray) in Sections 1-2, dark gray in Section 3. The upper part is thinly laminated and burrowed in some intervals (Section 1, Section 2, 0-47 cm), the middle part is almost homogeneous (Section 2) and the lower is faintly thinly laminated, or faintly mottled (Section 3).

NOTE: black layers are indicated.

Smear Summary (3 slides)
93% Clay*
2% Feldspar
2% Miscellaneous and altered
1% Rads
1% Glauconite
1% Pyrite
*Includes recrystallized silica

Hole 387 Core 27 Cored Interval: 440.8-450.4 m

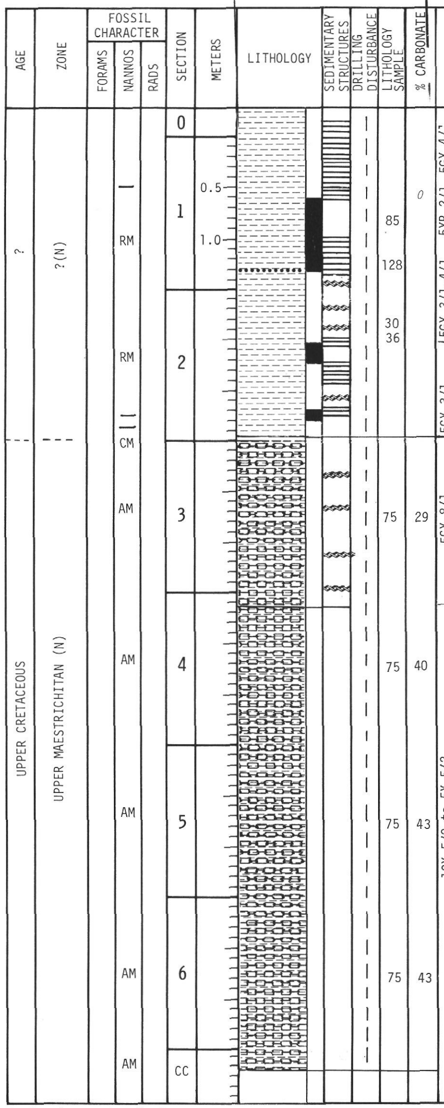

LITHOLOGIC DESCRIPTION

0 Sect. = 45 cm

CLAYSTONE, alternating dark greenish gray and brownish black layers with distinct boundaries, faintly laminated or faintly mottled, homogeneous in minor interbeds. Laminated layer in Section 1, 130-100 cm is enriched in silt (SILTY CLAYSTONE) grading up to less silt content.

5YR 2/1

Smear Summary (4 slides claystone)
82% Clay
8% Feldspar
3% Miscellaneous and altered
2% Quartz
2% Mica
2% Rads
1% Pyrite

NOTE: black layers are indicated.

CALCAREOUS CLAYSTONE light greenish gray, diffusely mottled. Calcareous material is mostly unspecified carbonate with minor nannos.

MARLY CHALK, moderate olive to light olive gray, homogeneous.

Smear Summary (4 slides marly chalk):
60% Clay
29% Unspec. carb.
10% Nannos
1% Miscellaneous and altered

CC = 24 cm
N4
5YR 6/4

Explanatory notes in Chapter 1

Hole 387 Core 28 Cored Interval: 459.9-469.4 m

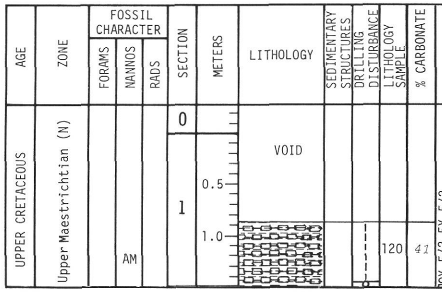

LITHOLOGIC DESCRIPTION

MARLY CHALK, moderate olive to light olive gray, homogeneous.

Smear Summary (1 slide)
67% Clay
20% Unspec. carb.
10% Nannos
2% Forams
1% Pyrite

CC = empty

Hole 387 Core 29 Cored Interval: 469.4-478.9 m

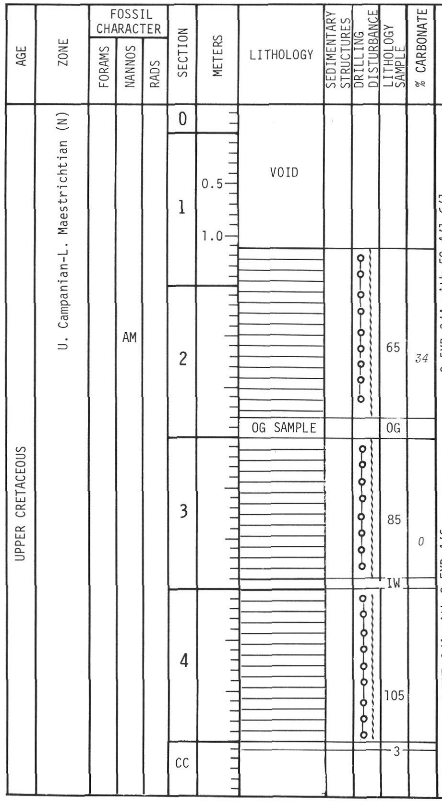

LITHOLOGIC DESCRIPTION

CLAYSTONE, dark reddish brown with several greenish gray to dark greenish gray layers (1 to 15 cm thick, with sharp boundaries) in the upper part of Sections 1 and 2. Some pieces are faintly laminated or mottled.

In the lower part (Sections 3-4) red and dark red (2.5YR 4/6-3/6) thin (1-2 cm) interbeds appear; with light gray to white irregular streaks or layers (1-3 mm) in central parts of some of the interbeds, containing more altered volcanic glass.

Smear Summary (3 slides)
91% Clay
4% Zeolites (0-10%)
2% Volcanic glass
1% Unspec. carb.
1% Rads
1% Glauconite

2.5YR 4/6
to 2.5YR 4/4
CC = 10 cm

Hole 387 Core 30 Cored Interval: 488.5-498.0 m

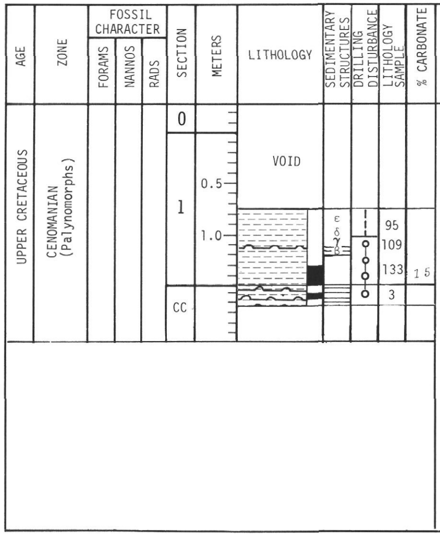

LITHOLOGIC DESCRIPTION

5G 4/1 with 5GY 2/1

CLAYSTONE, dark greenish gray, thinly laminated or mottled, with homogeneous interbeds. The sequence is comparable with ε-α units in upper part of the hole (see Core 9).
Distinct unit in 75-112 cm:
ε-dark, mottled claystone
δ-lighter, mottled, claystone
γ-homogeneous
β-laminated, with coarse light greenish gray RADIOLARITE in the bottom layer (α?) and sharp basal contact.

5G 4/1 with 5G 2/1

Other units are disturbed, but "β" subunits, as well as black coarse MUDDY RADIOLARITE pieces may be distinguished, in which very high organic C content was measured (30:1:136 = 11.3%). Radiolarians are completely altered, recrystallized, or replaced by pyrite.
Smear Summary (4 slides):
51% Clay (25-87%)
42% Rads (7-75%)
4% Organic matter (0-15%)
2% Pyrite
1% Unspec. carb.

CC = 23 cm of RADIOLARIAN MUDSTONE, dark greenish gray with black interbed.

Hole 387 Core 31 Cored Interval: 507.5-517.1 m

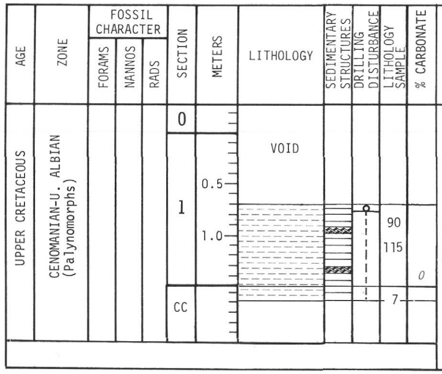

LITHOLOGIC DESCRIPTION

5Y 4/3

CLAYSTONE, thinly laminated and mottled, olive, with greenish gray mottles and laminae, with dark greenish gray interbed at 110-120 cm

Smear Summary (3 slides):
93% Clay
4% Mica
1% Feldspar
1% Rads
1% Heavy minerals

2.5Y 4/2
5Y 4/4

CC = 17 cm of CLAYSTONE, grading from dark grayish brown to olive.

Explanatory notes in Chapter 1

Hole 387 Core 32 Cored Interval: 517.1-526.6 m

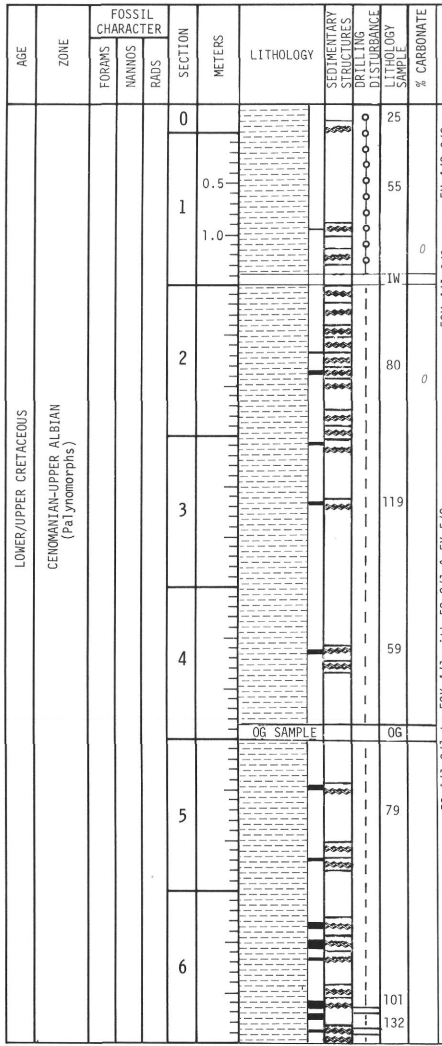

LITHOLOGIC DESCRIPTION

0 Sect. = 35 cm

5Y 4/2-3/2

CLAYSTONE:series of rhythmically alternating color layers with some silty basal layers (above the black "top" subunits).

Three distinct subunits may be compared with those described in Core 9 as ε,δ,γ:
ε-dark greenish gray or greenish black (5G 2/1), mottled,some irregularly laminated. (see black layers in lith. column).
δ-intensely mottled and burrowed, with distinct black mottles on the gray background (see structure column).
γ-homogeneous, with sharp basal contact, not found in every unit.

5GY 4/1-3/1

The greenish gray is irregularly shaded by bands and patches of olive gray in Sections 1-3.

Smear Summary (6 slides):
87% Clay
5% Mica
3% Rads
2% Heavy minerals (0-9%)
1% Feldspar
1% Unspec. carb.
1% Vol. glass

5G 4/1-3/1 to 5GY 4/1 with 5G 2/1 & 5Y 5/2

CC = empty

Hole 387 Core 33 Cored Interval: 526.6-536.2 m

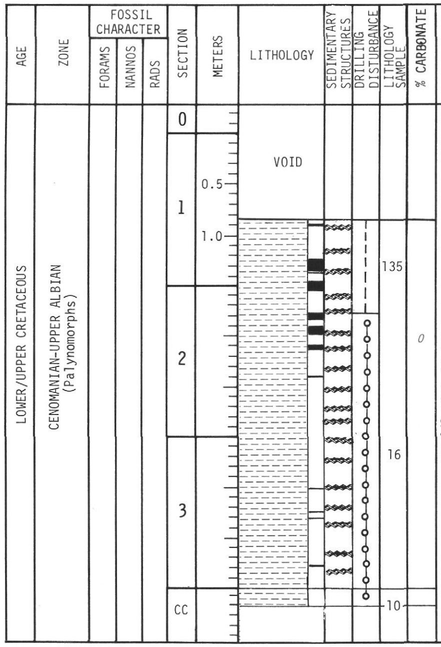

LITHOLOGIC DESCRIPTION

CLAYSTONE: alternating color layers of greenish gray (intensely mottled throughout the core with minor homogeneous interlayers increasing downward) and greenish black, usually with distinct upper contacts and mottled lower contacts.

NOTE: Shading in lithologic column = black layers. Markings in structures column = mottling).

Smear Summary (3 slides)
89% Clay
6% Rads
3% Mica
1% Pyrite
1% Heavy minerals

5G 4/1 with 5G 2/1

CC = 21 cm
5G 4/1

Explanatory notes in Chapter 1

Hole 387 Core 34 Cored Interval: 536.2-545.7 m

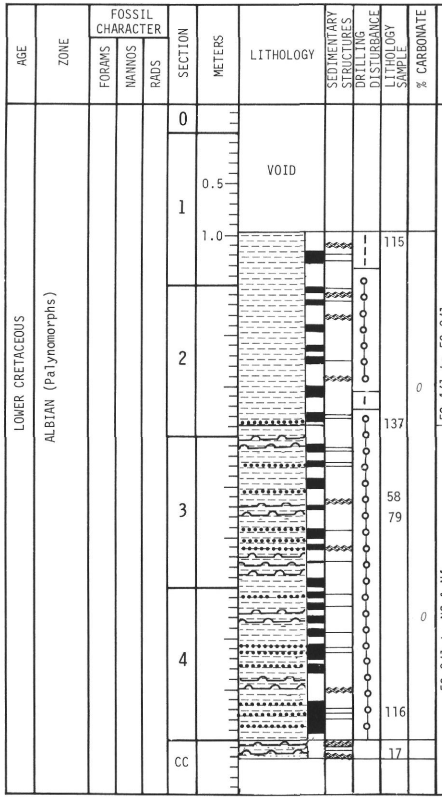

LITHOLOGIC DESCRIPTION

CLAYSTONE with thin interbeds of RADIOLARIAN MUDSTONE in black as well as in gray color layers. Alternating layers of dark greenish gray, intensely mottled, and greenish black, partly laminated, mottled.

RADIOLARIAN MUDSTONE with thin interbeds of coarser (silty) RADIOLARITE (dots), probably forming basal subunits of rhythmic sedimentary units, but not directly correlated with color variations. Radiolarians are strongly altered, poorly preserved.

NOTE: Shading in lithologic column = black layers.

Smear Summary (5 slides) :
76% Clay*
19% Rads
2% Mica
1% Pyrite
1% Heavy minerals
*Includes recrystallized silica

5G 4/1 to 5G 2/1

5G 2/1 to N2 & N4

N2
N3
CC = 21 cm

Hole 387 Core 35 Cored Interval: 545.7-555.3 m

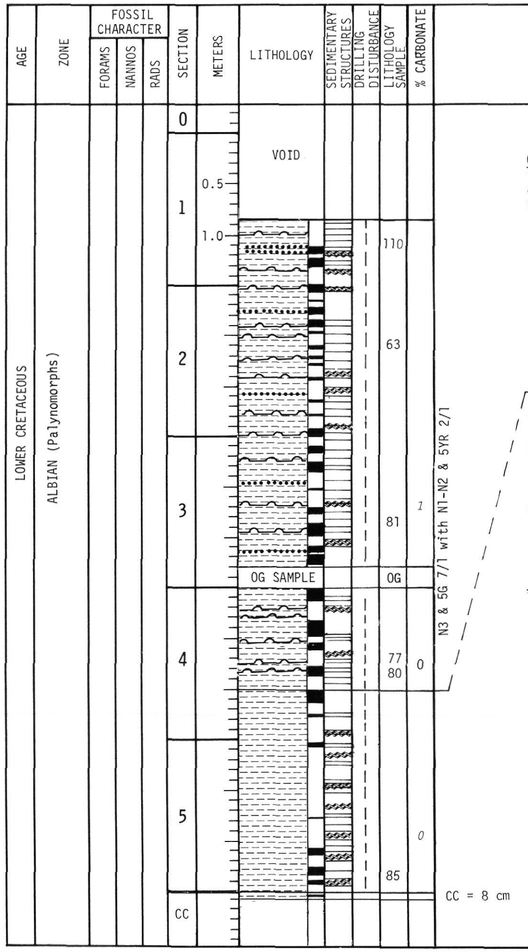

LITHOLOGIC DESCRIPTION

CLAYSTONE AND RADIOLARIAN MUDSTONE with thin interbeds of RADIOLARITE (radiolarian sand and silt-dotted lines) consisting of recrystallized, poorly preserved radiolarians.

Alternating layers in the rhythmic sequence are:
- black, homogeneous or thinly laminated, grading downward to:
- dark gray, wavy laminated, with small burrow mottles
- greenish gray with large black burrows, probably the basal layers of the units.

NOTE: Shading in lithologic column = black layers.

CLAYSTONE, mostly gray or greenish gray with minor black interbeds. Gray layers have less burrow mottling than above, mottles are lighter and smaller, no large black burrows.

Smear Summary (5 slides):
81% Clay*
14% Rads
2% Miscellaneous and altered
1% Feldspar + Quartz
1% Mica
1% Pyrite
*Includes recrystallized silica

Explanatory notes in Chapter 1

Hole 387 Core 36 Cored Interval: 555.3-564.8 m

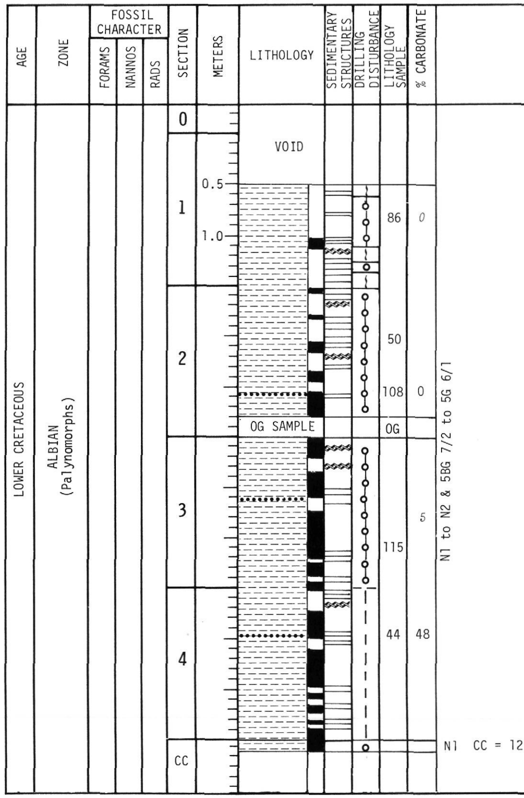

LITHOLOGIC DESCRIPTION

CLAYSTONE with alternating layers similar to those in Core 35. Black layers are thicker, and wavy laminated layers are less abundant in comparison with Core 35. Thin sandy-silt interbeds (dotted lines) are radiolarian- and calcareous-rich with siderite, radiolarians are altered, recrystallized.

NOTE: Shading in lithologic column = black layers.

Smear Summary (3 slides):
87% Clay
7% Rads
2% Miscellaneous and altered
2% Pyrite
1% Feldspar + Quartz
1% Mica

Hole 387 Core 37 Cored Interval: 574.3-583.8 m

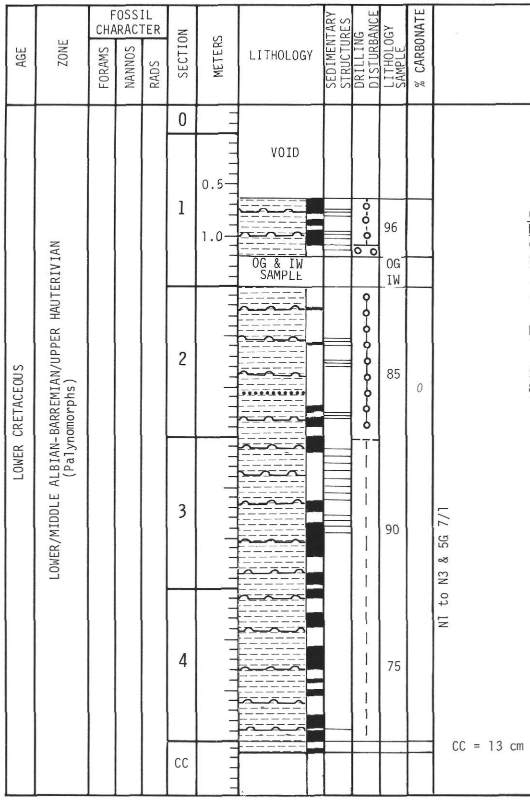

LITHOLOGIC DESCRIPTION

CLAYSTONE, greenish gray, and RADIOLARIAN MUDSTONE, black, with pyrite nodules and crystals, with thin radiolarian sand/silt interbed (dotted line). Alternating layers of black and gray as in Core 35 with less developed wavy laminated intermediate layers.

NOTE: Shading in lithologic column = black layers.

Smear Summary (4 slides):
80% Clay
13% Rads
3% Pyrite
1% Miscellaneous and altered
1% Unspec. carb.
1% Feldspar + Quartz
1% Mica

Hole 387 Core 38 Cored Interval: 593.1-602.6 m

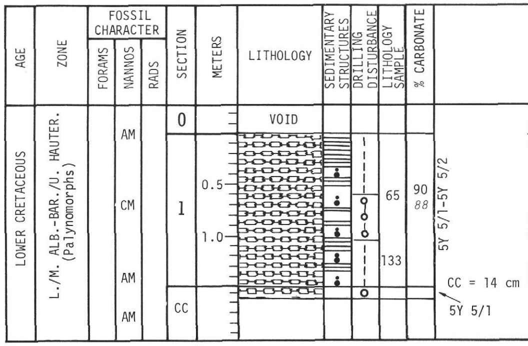

LITHOLOGIC DESCRIPTION

CHALK and MARLY CHALK, olive gray, alternating layers of 2 kinds:(light/dark laminae).
≡ - laminated or thinly laminated.
⁝ - graded, with flat carbonate clasts at the base.

$CaCO_3$ is "unspecified carbonate" with minor nannos.

Smear Summary (1 slide):
87% Unspec. carb.
10% Clay
3% Nannos

Explanatory notes in Chapter 1

Hole 387 Core 39 Cored Interval: 621.6-631.1 m

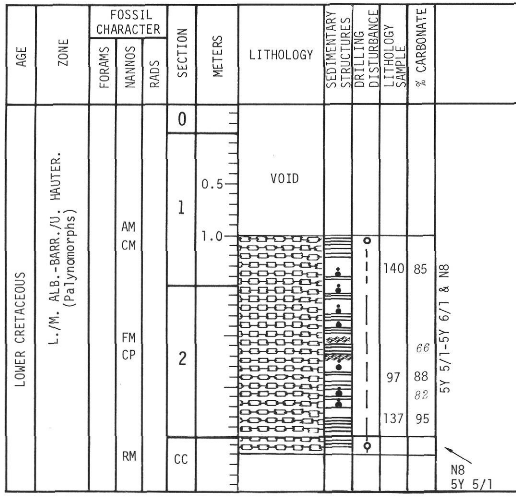

LITHOLOGIC DESCRIPTION

CHALK, olive gray with minor LIMESTONE layers (light gray [N8]) in the lower part. Alternating laminated and graded units are similar to those in Core 38. Limestone is burrow mottled.

NOTE: See Core 38 for symbols.

Smear Summary (3 slides):
81% Unspec. carb.
11% Clay
5% Nannos
1% Forams
1% Siderite
1% Miscellaneous and altered

CC = 20 cm of LIMESTONE AND CHALK

Hole 387 Core 40 Cored Interval: 631.1-640.6 m

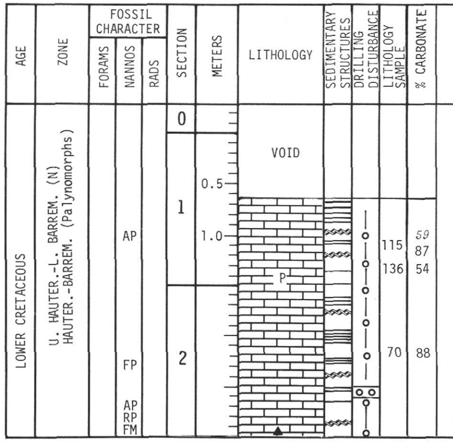

LITHOLOGIC DESCRIPTION

LIMESTONE, very light gray, burrowed, locally laminated, with interbeds of CHALK, olive gray, laminated. Two thin interbeds of PYRITIC CHALK, olive black, occur in Section 1 (135 and 150 cm), and a piece of CHERT in Section 2 (150 cm).

Smear Summary (2 slides):
85% Unspec. carb.
10% Clay
4% Nannos
1% Miscellaneous and altered

CC = empty

Hole 387 Core 41 Cored Interval: 640.6-650.2 m

AGE	ZONE	FOSSIL CHARACTER FORAMS	FOSSIL CHARACTER NANNOS	FOSSIL CHARACTER RADS	SECTION	METERS	LITHOLOGY	SEDIMENTARY STRUCTURES	DRILLING DISTURBANCE	LITHOLOGY SAMPLE	% CARBONATE
LOWER CRETACEOUS	MIDDLE HAUTERIVIAN (N) BARR.-HAUT. (Palyn.)		AP FM		0 1 CC	0.5 1.0	VOID			61 113	37 *48* 88

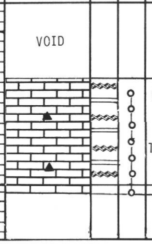

N8-N7 with 5Y 2/1

CC = 10 cm
N7

LIMESTONE, very light gray, massive, burrow mottled; with minor MARLY CHALK interbeds, black, laminated; and pieces of CHERT.

NOTE: No original orientation of the rock fragments in the drilling breccia.

Smear Summary (3 slides) :
54% Unspec. carb. (7-86%)
31% Clay (10-53%)
11% Nannos (0-30%)
2% Pyrite
1% Mica
1% Rads

Hole 387 Core 42 Cored Interval: 650.2-659.7 m

AGE	ZONE	FOSSIL CHARACTER FORAMS	FOSSIL CHARACTER NANNOS	FOSSIL CHARACTER RADS	SECTION	METERS	LITHOLOGY	SEDIMENTARY STRUCTURES	DRILLING DISTURBANCE	LITHOLOGY SAMPLE	% CARBONATE
LOWER CRETACEOUS	UPPER VALANGINIAN- LOWER HAUTERIVIAN (N) BARR.-HAUT. (Palyn.)		CP CP		0 1	0.5 1.0	VOID			72	48 94 *51*

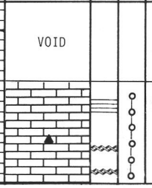

5B 7/1, N8, 5Y 2/1

CC = empty

LIMESTONE, light bluish gray, laminated (in the upper part of the section), or very light gray (N8), burrowed (in the lower part), with minor MARLY CHALK, olive black, and MARLY LIMESTONE, intensely burrowed with olive gray (5Y 4/1) mottles on light greenish gray background. Some pieces of CHERT, medium bluish gray (5B 5/1), mottled.

NOTE: No original orientation of the rock fragments in the drilling breccia.

Smear Summary (1 slide):
94% Unspec. carb.
6% Clay

Hole 387 Core 43 Cored Interval: 669.2-678.7 m

AGE	ZONE	FOSSIL CHARACTER FORAMS	FOSSIL CHARACTER NANNOS	FOSSIL CHARACTER RADS	SECTION	METERS	LITHOLOGY	SEDIMENTARY STRUCTURES	DRILLING DISTURBANCE	LITHOLOGY SAMPLE	% CARBONATE
LOWER CRETACEOUS	UPPER VALANGINIAN- LOWER HAUTERIVIAN (N) HAUT.-U. VAL. (Palyn.)		—		0 CC		VOID				95

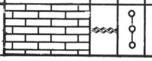

CC = 10 cm
5B 8/1

LIMESTONE, very light bluish gray, faintly laminated and burrowed.

Smear Summary (1 slide):
95% Unspec. carb.
5% Clay

Explanatory notes in Chapter 1

Hole 387 Core 44 Cored Interval: 678.7-688.2 m

AGE	ZONE	FOSSIL CHARACTER FORAMS	FOSSIL CHARACTER NANNOS	FOSSIL CHARACTER RADS	SECTION	METERS	LITHOLOGY	SEDIMENTARY STRUCTURES	DRILLING DISTURBANCE	LITHOLOGY SAMPLE	% CARBONATE
LOWER CRETACEOUS	UPPER VALANGINIAN- LOWER HAUTERIVIAN (N) HAUT.-U. VAL. (Palyn.)		CP CM		0 1	0.5 1.0	VOID			122 124	48 91 61

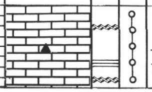

N7-N8 with 5GY 6/1 & 5GY 3/1

CC = empty

LIMESTONE of two varieties:
(1) medium light gray, thinly, faintly laminated, recrystallized;
(2) very light gray (N8), faintly burrowed, massive, fine grained (micritic);
minor interbeds of MARLY CHALK and CALCAREOUS CLAYSTONE, dark greenish gray (5GY 3/1 to 6/1), laminated to homogeneous in black. A single piece of CHERT, bluish gray (5B 5/1).

Smear Summary (2 slides):
73% Unspec. carb.
19% Clay
3% Nannos
2% Pyrite
1% Siderite
1% Mica
1% Rads

Hole 387 Core 45 Cored Interval: 697.7-706.9 m

AGE	ZONE	FOSSIL CHARACTER FORAMS	FOSSIL CHARACTER NANNOS	FOSSIL CHARACTER RADS	SECTION	METERS	LITHOLOGY	SEDIMENTARY STRUCTURES	DRILLING DISTURBANCE	LITHOLOGY SAMPLE	% CARBONATE
LOWER CRETACEOUS	HAUTERIVIAN- UPPER VALANGINIAN (Palynomorphs)		FM AP		0 1	0.5 1.0	VOID			130	48 *79*

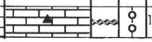

5B 8/1
with
5G 4/1 &
5Y 2/1

CC = empty

LIMESTONE, very light bluish gray, hard, burrowed, with minor CHERT (dark greenish gray) and CALCAREOUS CLAYSTONE, (olive black).

Smear Summary (1 slide):
45% Unspec. carb.
37% Clay
12% Siderite
3% Nannos
2% Mica
1% Pyrite

Hole 387 Core 46 Cored Interval: 726.0-735.4 m

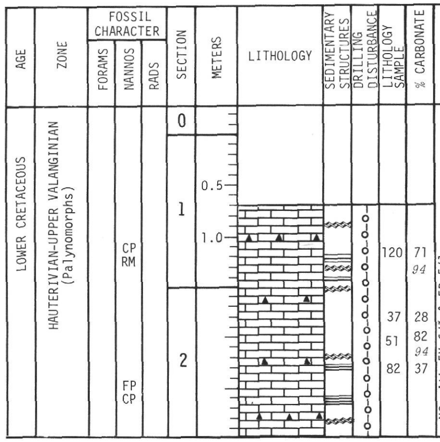

LITHOLOGIC DESCRIPTION

LIMESTONE, very light gray, homogeneous or burrowed, massive, with minor interbeds and loose pieces of: SIDERITIC MARLY LIMESTONE dark olive gray (5Y 4/1), laminated, relatively coarse (very fine sand and silt-size); MARLY CHALK, dark olive gray to black; CHERT, medium bluish gray (5B 5/1).

NOTE: Laminated sideritic limestone and chalk are ═ in "sediment structure" column; cherts ▲ in "lithology" column, according to their stratigraphic position in the core.

Smear Summary (3 slides):
56% Unspec. carb. (25-79%)
17% Clay
12% Siderite (0-21%)
8% Miscellaneous and altered (0-20%)
6% Nannos
1% Pyrite

CC = empty

Hole 387 Core 47 Cored Interval: 744.9-754.4 m

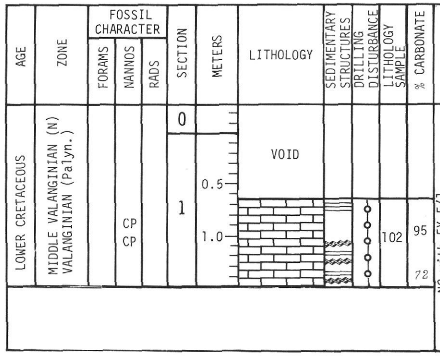

LITHOLOGIC DESCRIPTION

LIMESTONE, very light gray, burrow mottled, with some pieces of SIDERITIC LIMESTONE, medium olive gray, laminated. Sideritic bands and irregular laminae occur in some limestone pieces, probably produced by solution and concentration of siderite.

NOTE: Broken pieces of rock, without original orientation.

Smear Summary (1 slide):
65% Unspec. carb.
15% Nannos
15% Siderite
5% Clay

CC = empty

Hole 387 Core 48 Cored Interval: 763.7-773.1 m

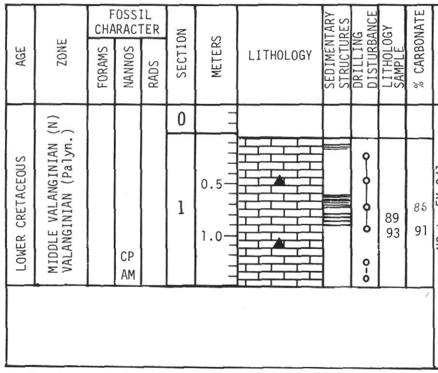

LITHOLOGIC DESCRIPTION

LIMESTONE, very light gray, to SIDERITIC LIMESTONE, dark olive gray (5Y 3/1) with most shades in between. Alternating layers of: homogeneous or burrowed limestone, laminated limestone and dark sideritic limestone containing fine laminae enriched in organic matter and pyrite.

Some pieces of chert occur, one with pyrite.

Smear Summary (1 slide):
89% Unspec. carb.
6% Clay
2% Nannos
2% Miscellaneous and altered
1% Siderite

CC = empty

Explanatory notes in Chapter 1

Hole 387 Core 49 Cored Interval: 782.4-791.9 m

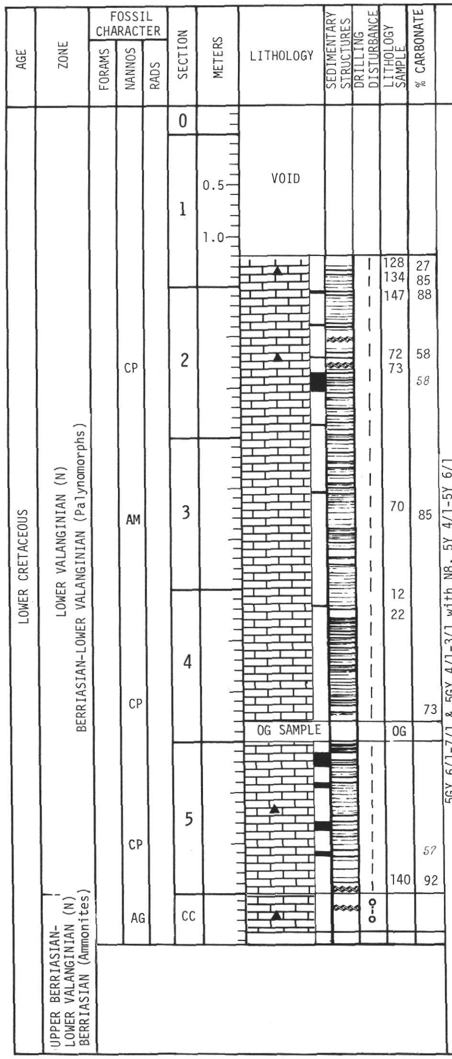

LITHOLOGIC DESCRIPTION

LIMESTONE with interbeds of MARLY (SIDERITIC) LIMESTONE grading to CALCAREOUS SIDERITIC MUDSTONE. Primary lithologies in the (rhythmic?) sequence are:
(1) Limestone - massive, burrowed, very light gray (N8 or 5B 8/1) with thin cherty(?) veinlets
(2) Limestone (to marly limestone) with minor siderite and pyrite, thinly laminated (rhythmic lamination with ~1 cm thick micro-units). Wood fragments occur.
Grades to:
(3) Marly (sideritic) limestone, distinctly laminated with alternating dark greenish gray (5GY 4/1) and light (5GY 7/1) laminae (less than 1 mm thick)
(4) Calcareous sideritic mudstone (minor interbeds, shown as black in "Lithologic" column), dark greenish gray (5GY 4/1 to 3/1 or to 5Y 4/1), thinly laminated, with pyrite nodules.

There are gradational transitions between (2)-(3)-(4) and sharp contacts between (4) and (1). Some CHERT occurs in Sections 1, 2, 5, CC.

Ammonites and aptychi are abundant in the laminated limestones.

Smear Summary (8 slides):
55% Unspec. carb. (7-90%)
26% Clay (5-66%)
12% Siderite (5-20%)
6% Nannos (0-15%)
1% Mica

CC = 40 cm

Hole 387 Core 50 Cored Interval: 791.9-794.5 m

AGE	ZONE	FOSSIL CHARACTER			SECTION	METERS	LITHOLOGY	SEDIMENTARY STRUCTURES	DRILLING DISTURBANCE	LITHOLOGY SAMPLE	% CARBONATE
		FORAMS	NANNOS	RADS							
					0						
					1	0.5 1.0					
					2						

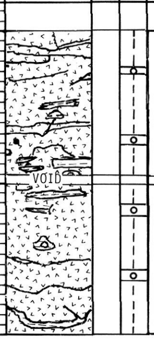

N2 to 5G 1/1

146

N2 to 5G 1/1

CC = empty

LITHOLOGIC DESCRIPTION

BASALT

Megascopic: grayish black, fine-grained, holocrystalline phyric basalt. Locally heavily veined with white (N9) calcite. Veins apparently walled with chlorite. Basalt grades to dark greenish black (5G 1/1) in veined regions, probably due to alteration. Phenocrysts of feldspar (<2 mm) comprise <5%. Enclosures of "baked" claystone (stippled) up to 6 cm long are locally important. Enclosures show signs of partial assimilation near edges and are commonly bounded on their upper surfaces either by grayish orange (10YR 7/4) sediment (leached claystone) or by vein calcite. Chlorite zones border calcite veins and sediment enclosures in basalt. Enclosures frequently "intruded" along calcite veins.

Microscopic: Holocrystalline, fine-grained, amygdaloidal phyric basalt. Phenocryst phases consist of common subhedral, prismatic plagioclase (An 70 to An 80; 0.072-3.24 mm, average 0.75 mm) and rare corroded, subangular pyroxene crystals. Slight alteration of plagioclase phenocrysts to sericite and montmorillonite gives crystals turbid appearance. Pyx. phenocrysts display variable optic angle, always positive and <25°, suggesting compositions between pigeonite and subcalcic augite. Both phases corroded and show optical strain. Groundmass consists of a complex network of randomly oriented plagioclase (An 65-76) with intergranular pyx. Disseminated granular to skeletal crystals of magnetite also appear in the groundmass. Groundmass texture varies widely throughout but generally increases in complexity downward. Fabric is combination of feather duster, true feather, variolitic, and shock (stook) groundmass textures. Amygdules of calcite, montmorillonite, and chlorite, in decreasing order of importance, account for <1%.

Explanatory notes in Chapter 1

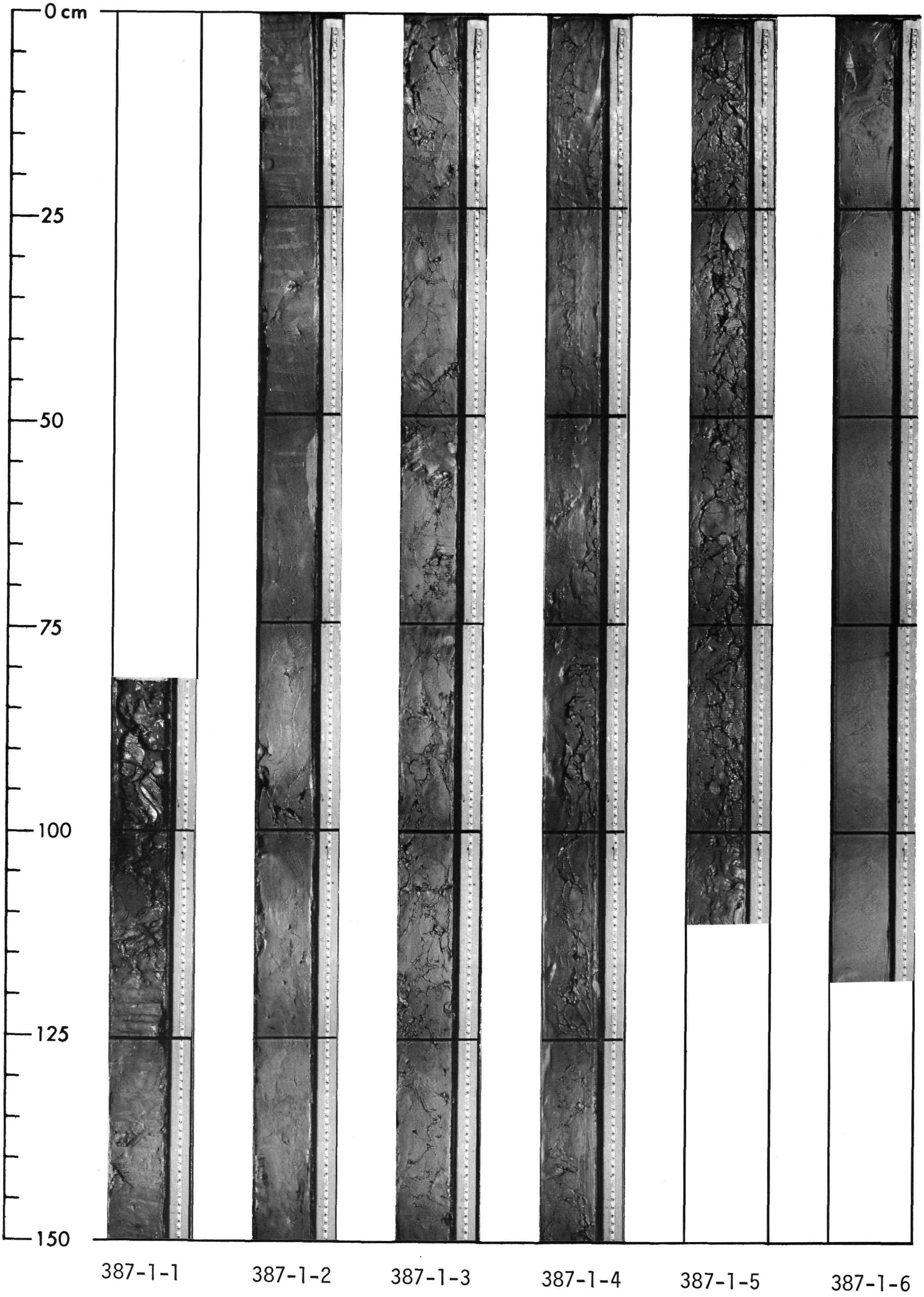
0 cm
25
50
75
100
125
150
387-1-1
387-1-2
387-1-3
387-1-4
387-1-5
387-1-6

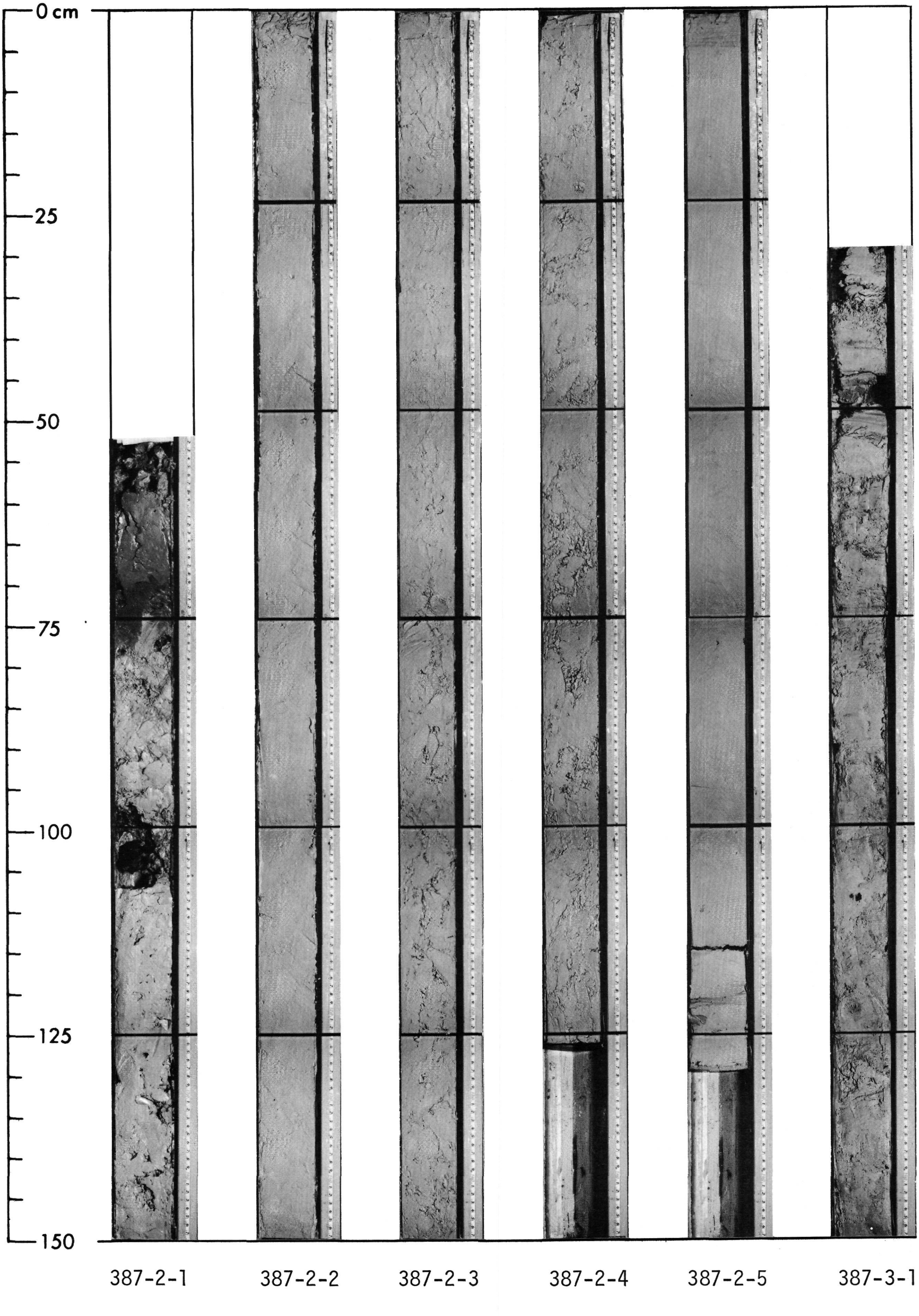
0 cm
25
50
75
100
125
150
387-2-1
387-2-2
387-2-3
387-2-4
387-2-5
387-3-1

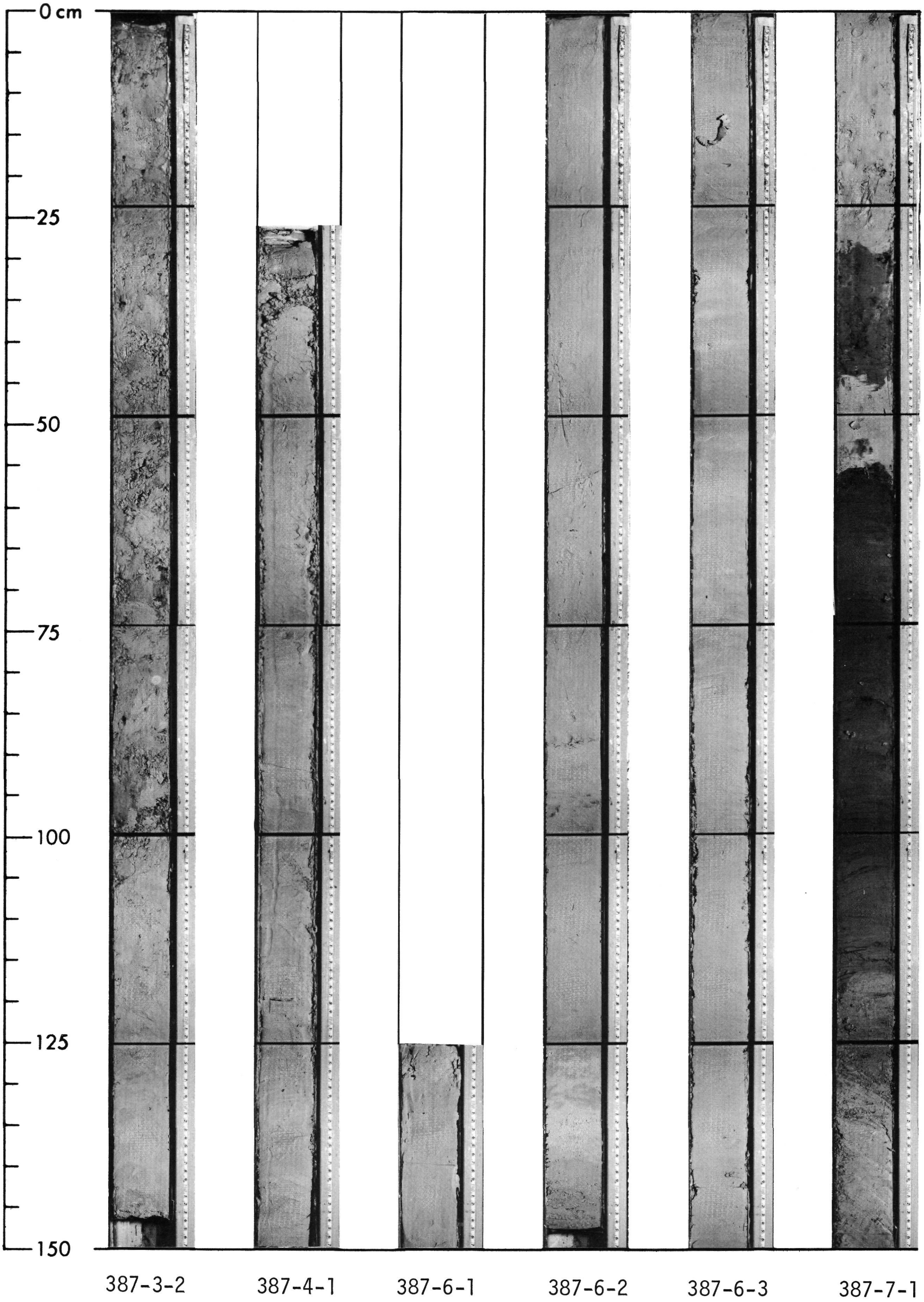
0 cm
25
50
75
100
125
150
387-3-2
387-4-1
387-6-1
387-6-2
387-6-3
387-7-1

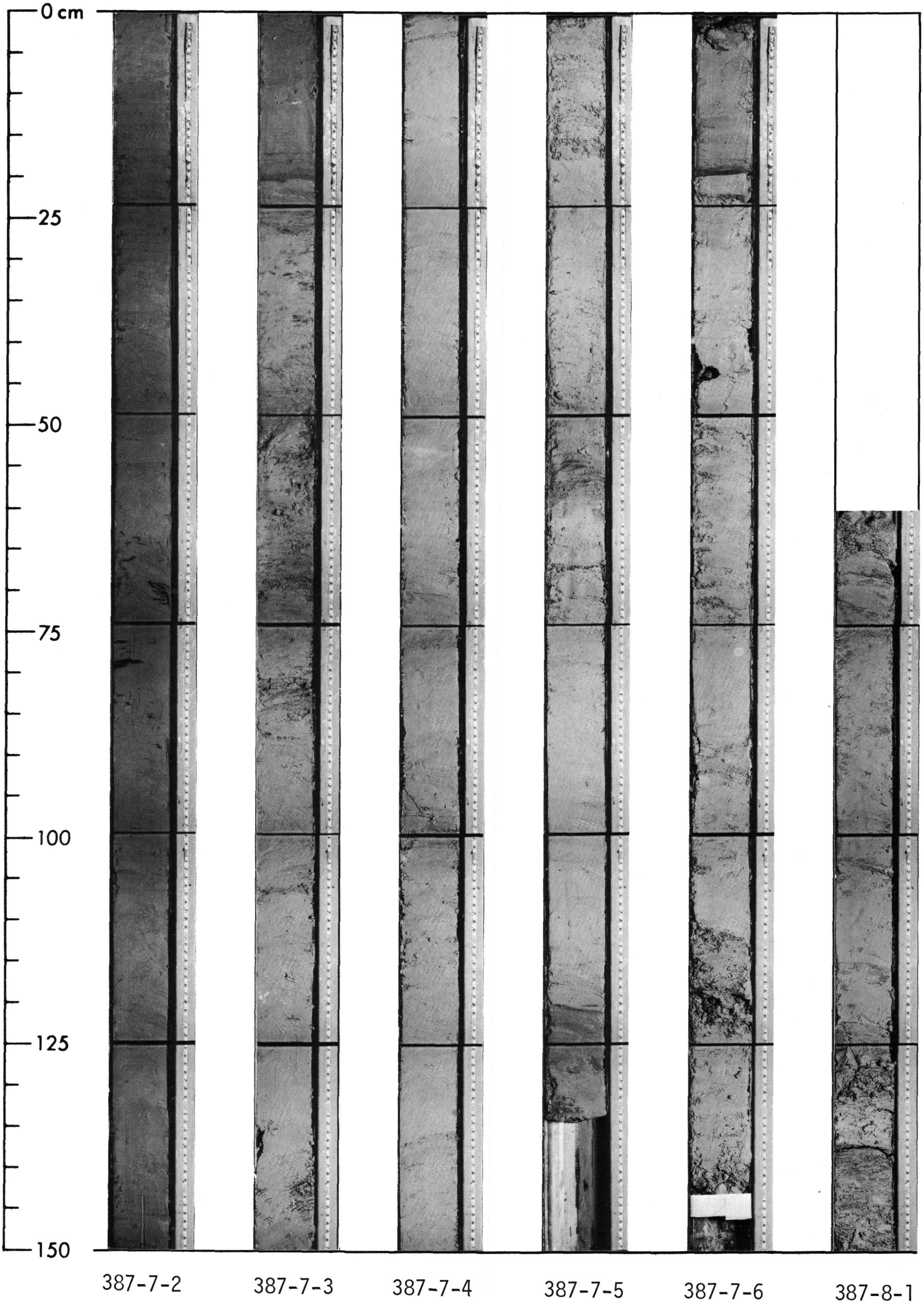
0 cm
25
50
75
100
125
150
387-7-2
387-7-3
387-7-4
387-7-5
387-7-6
387-8-1

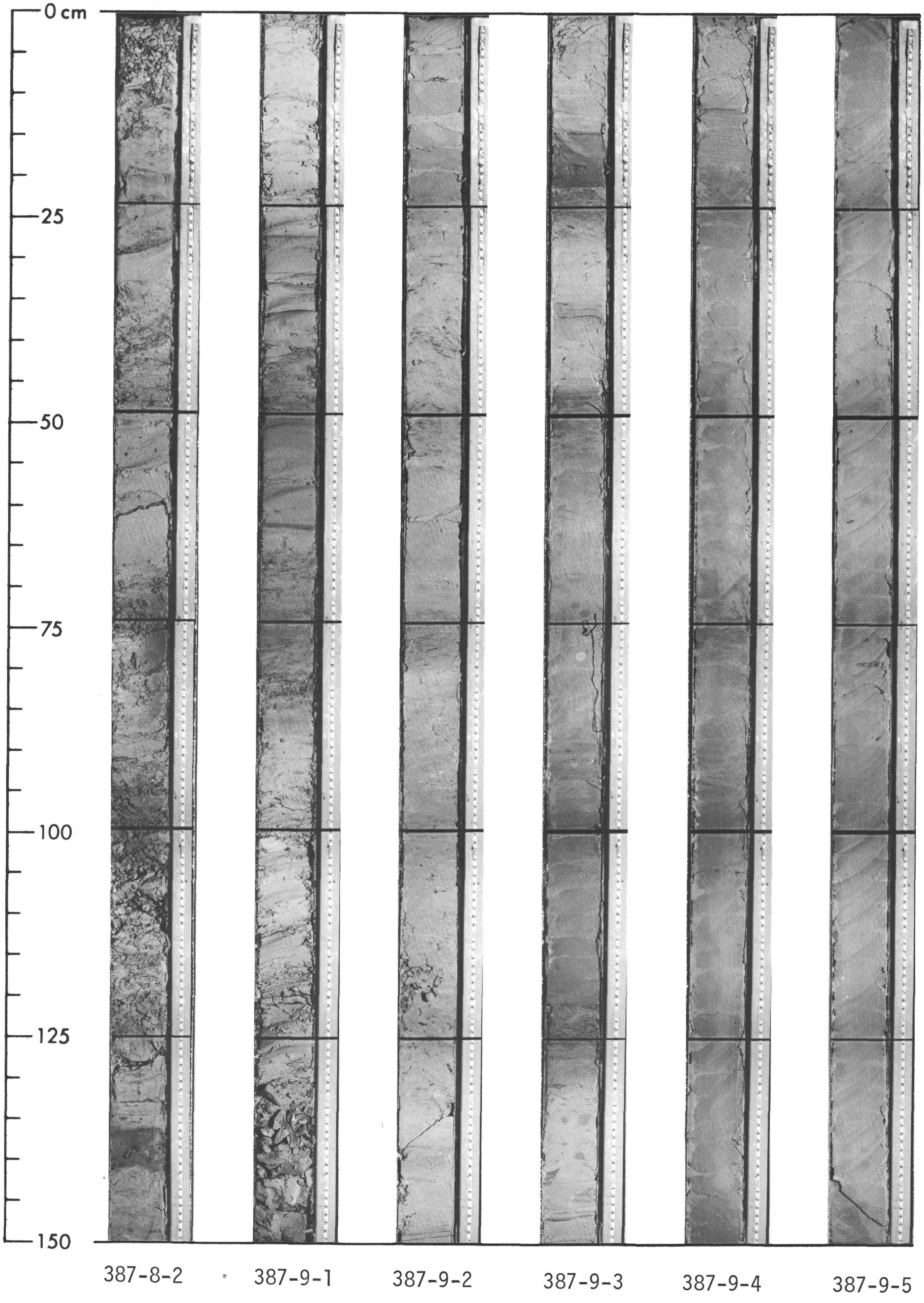
0 cm
25
50
75
100
125
150
387-8-2
387-9-1
387-9-2
387-9-3
387-9-4
387-9-5

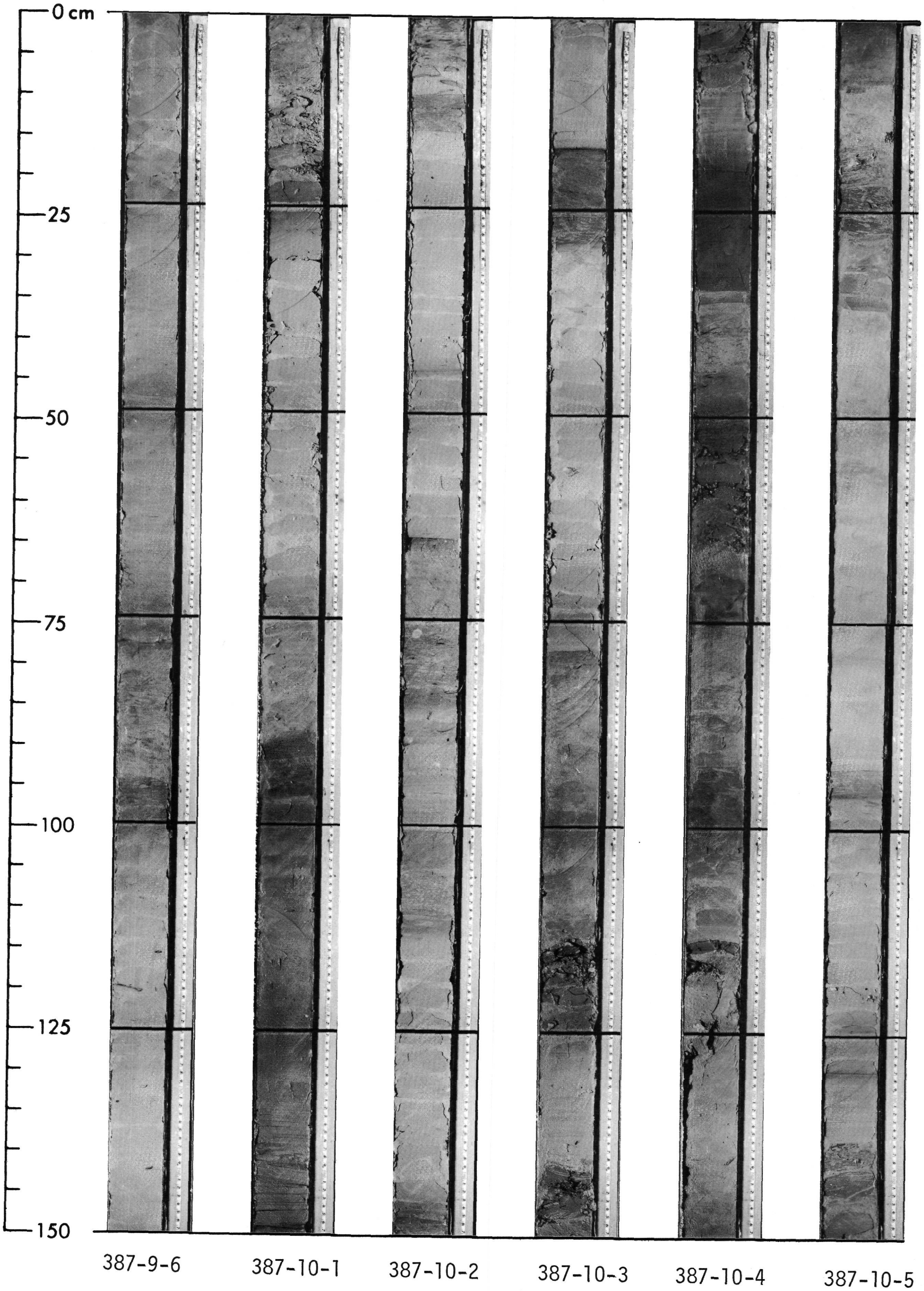
0 cm
25
50
75
100
125
150
387-9-6
387-10-1
387-10-2
387-10-3
387-10-4
387-10-5

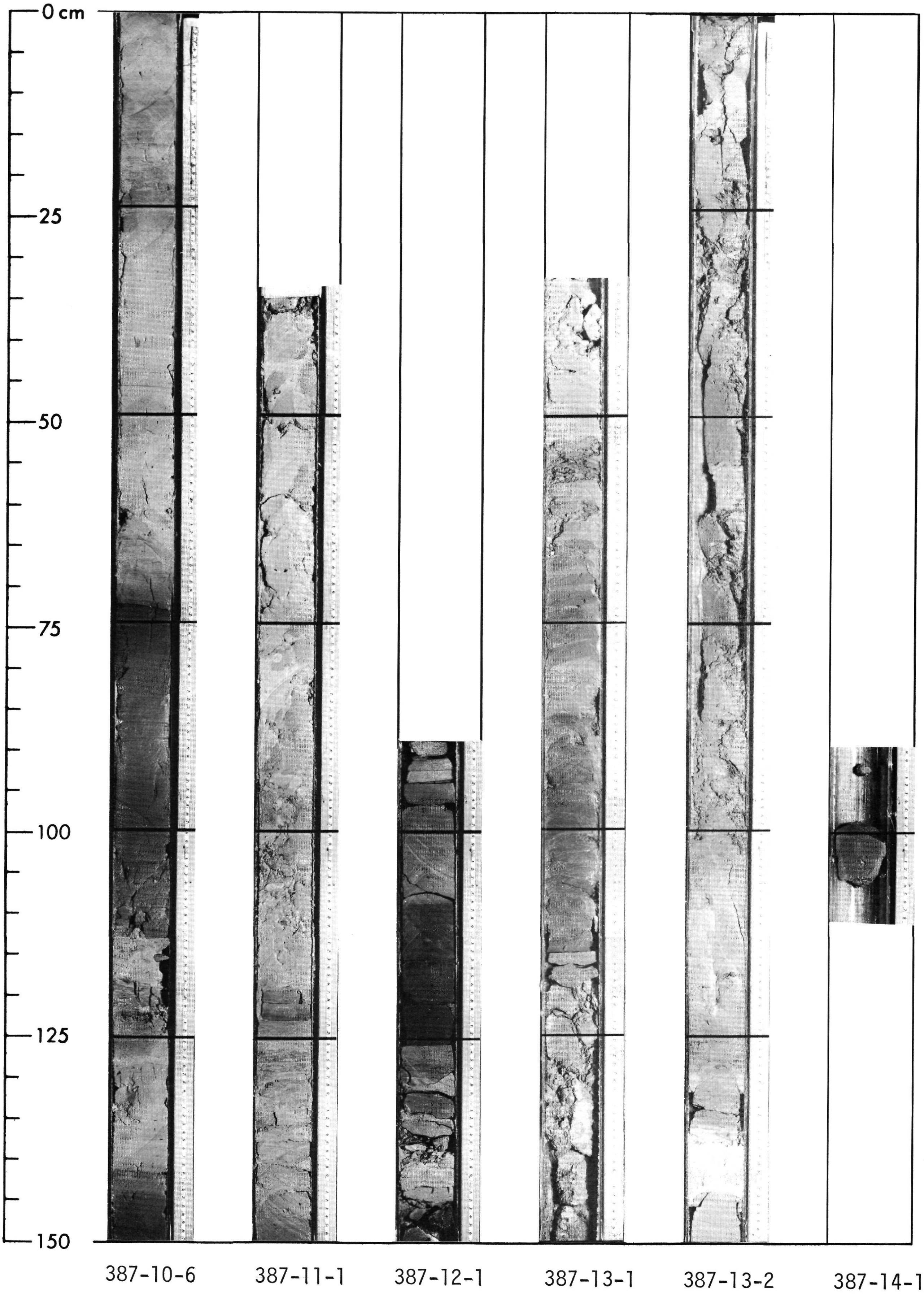
0 cm
25
50
75
100
125
150
387-10-6
387-11-1
387-12-1
387-13-1
387-13-2
387-14-1

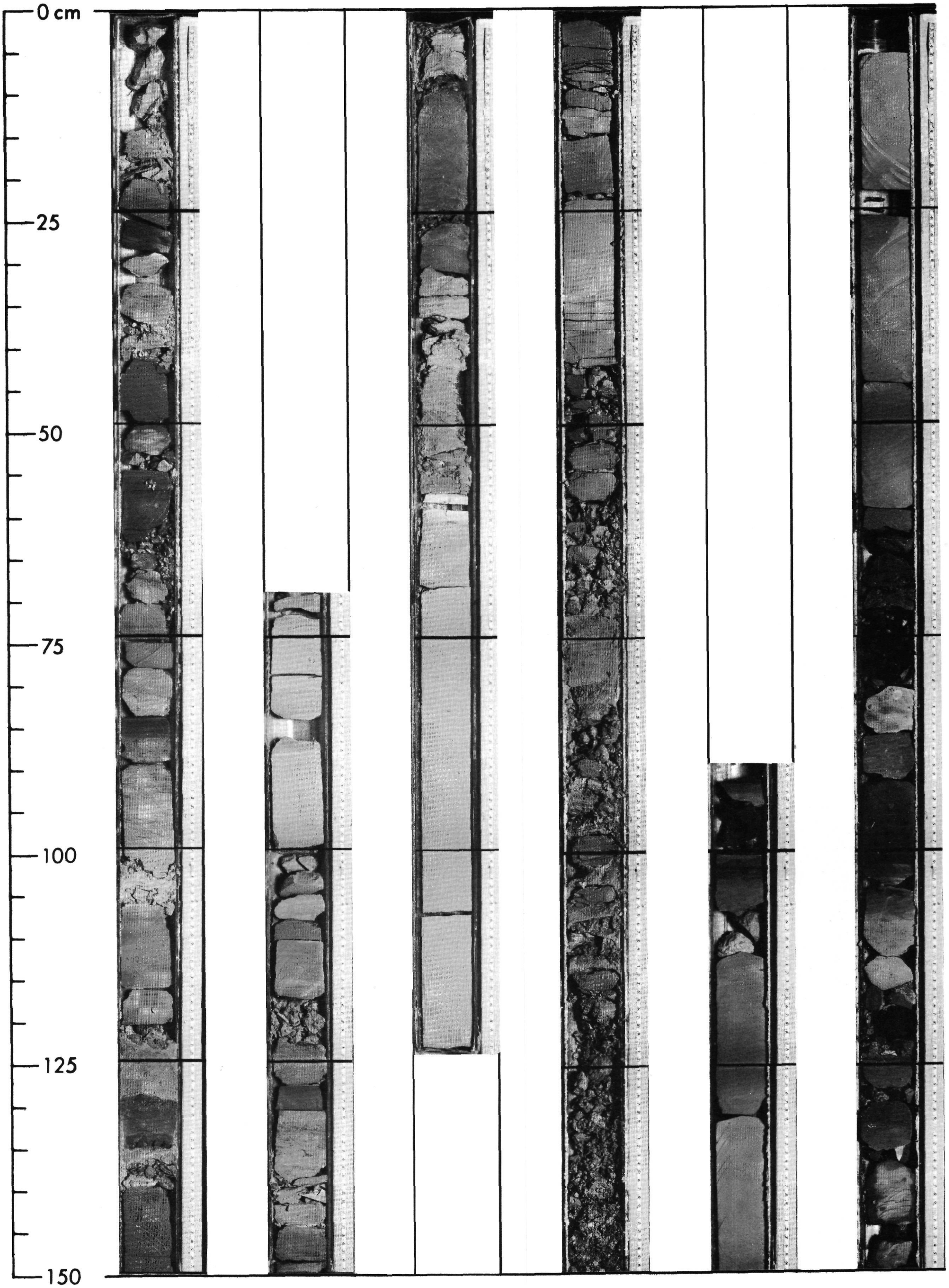

387-14-2 387-16-1 387-16-2 387-16-3 387-17-1 387-17-2

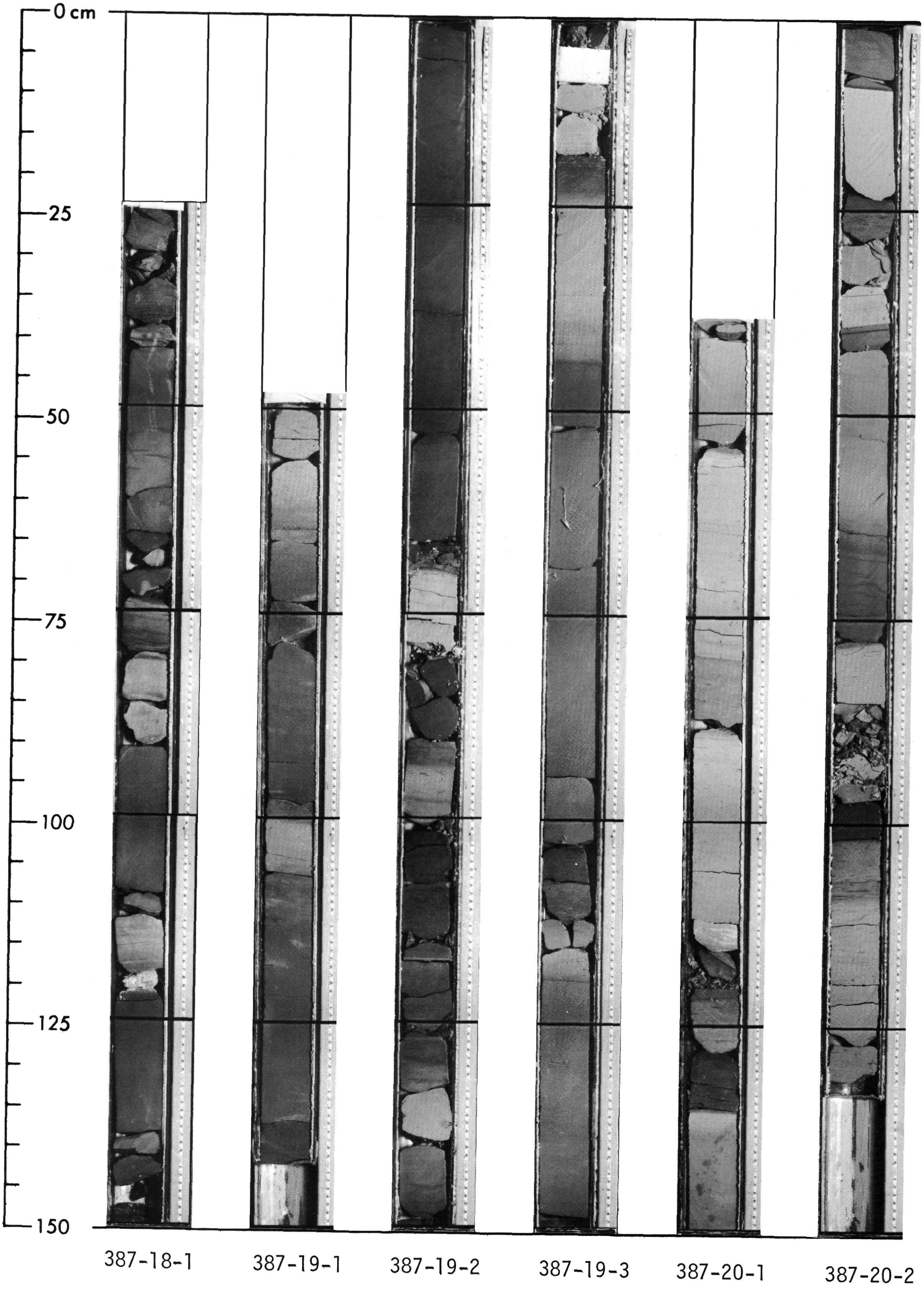
0 cm
25
50
75
100
125
150
387-18-1
387-19-1
387-19-2
387-19-3
387-20-1
387-20-2

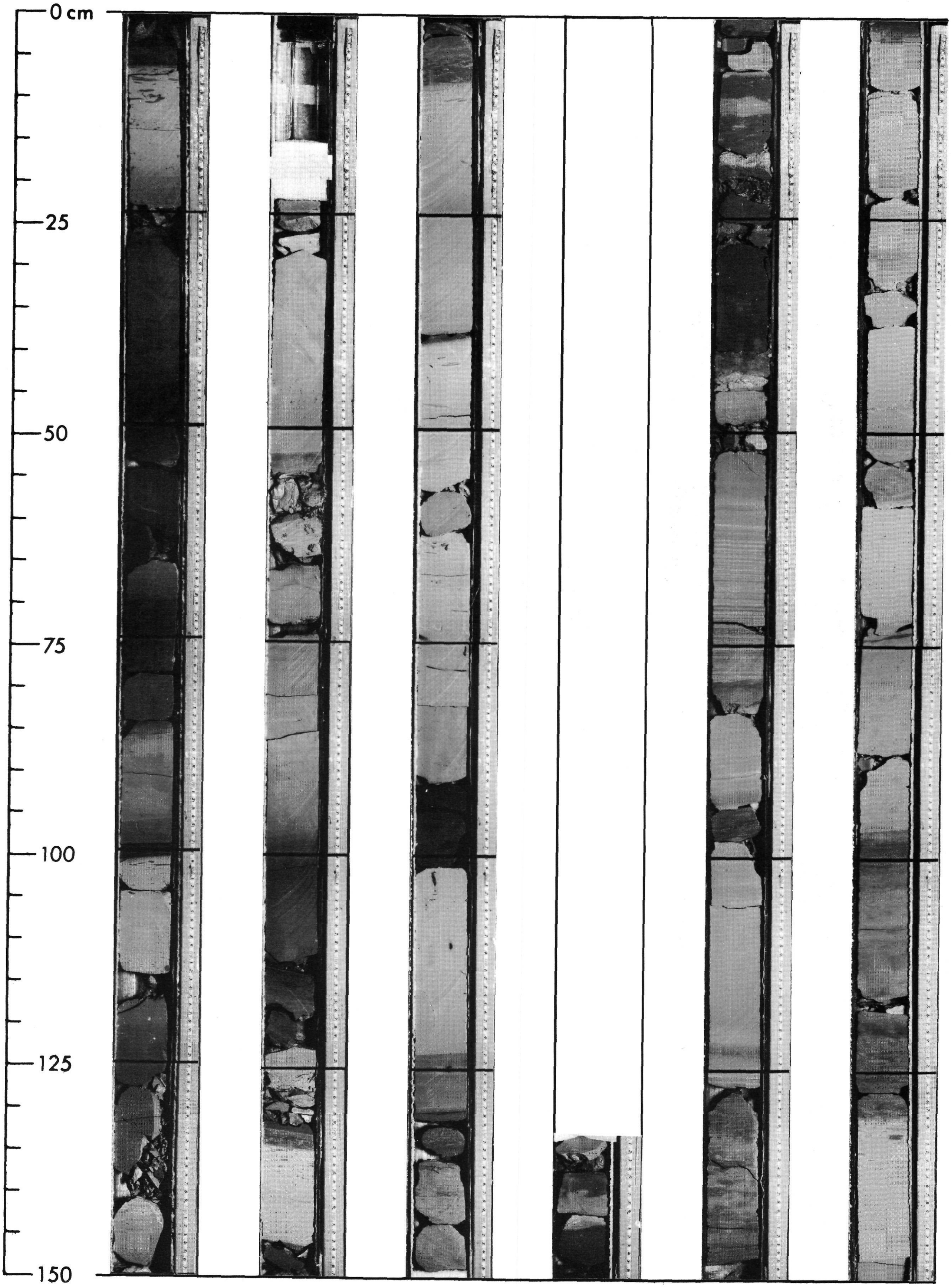

387-20-3 387-21-1 387-21-2 387-22-1 387-22-2 387-22-3

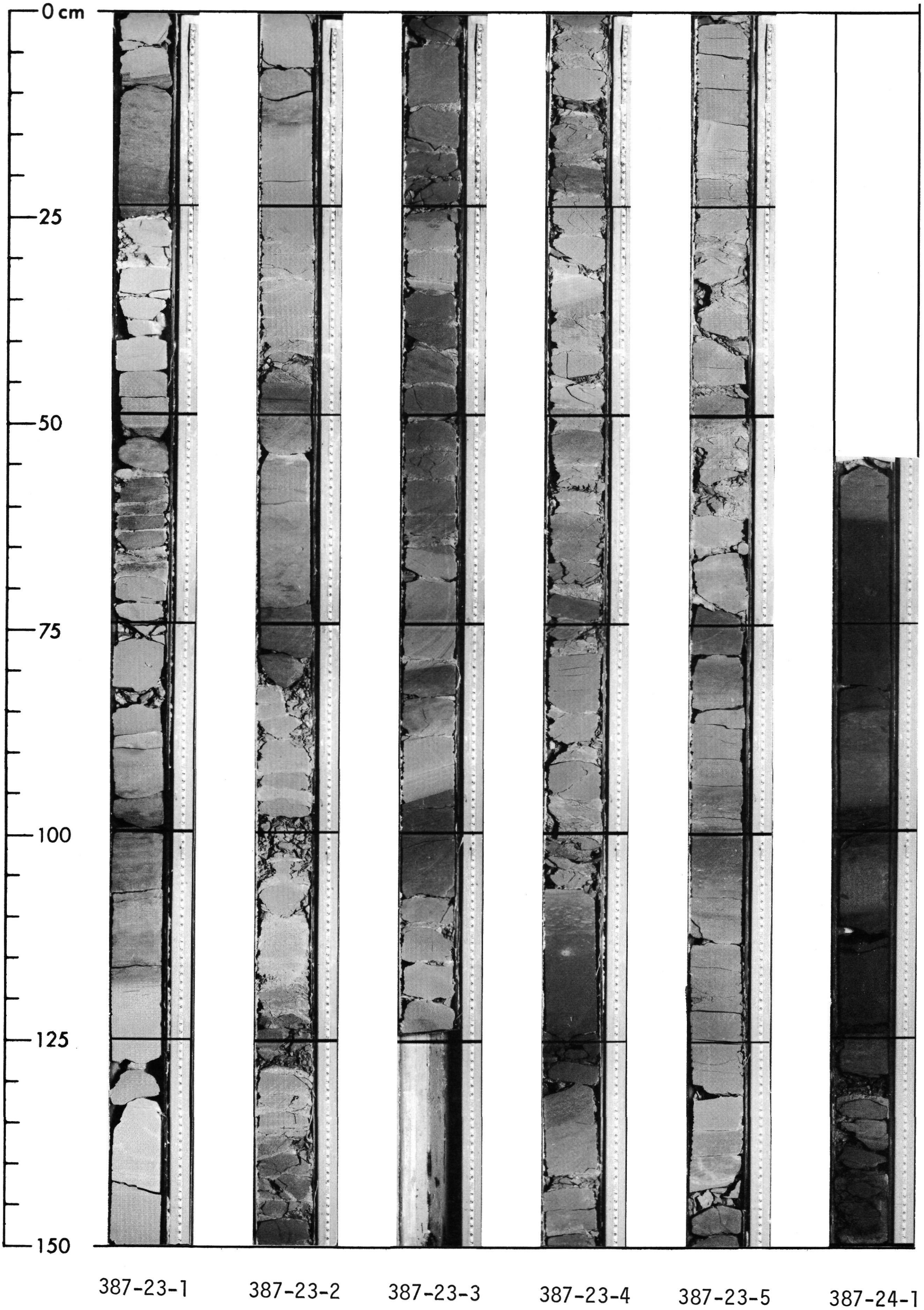
0 cm
25
50
75
100
125
150
387-23-1
387-23-2
387-23-3
387-23-4
387-23-5
387-24-1

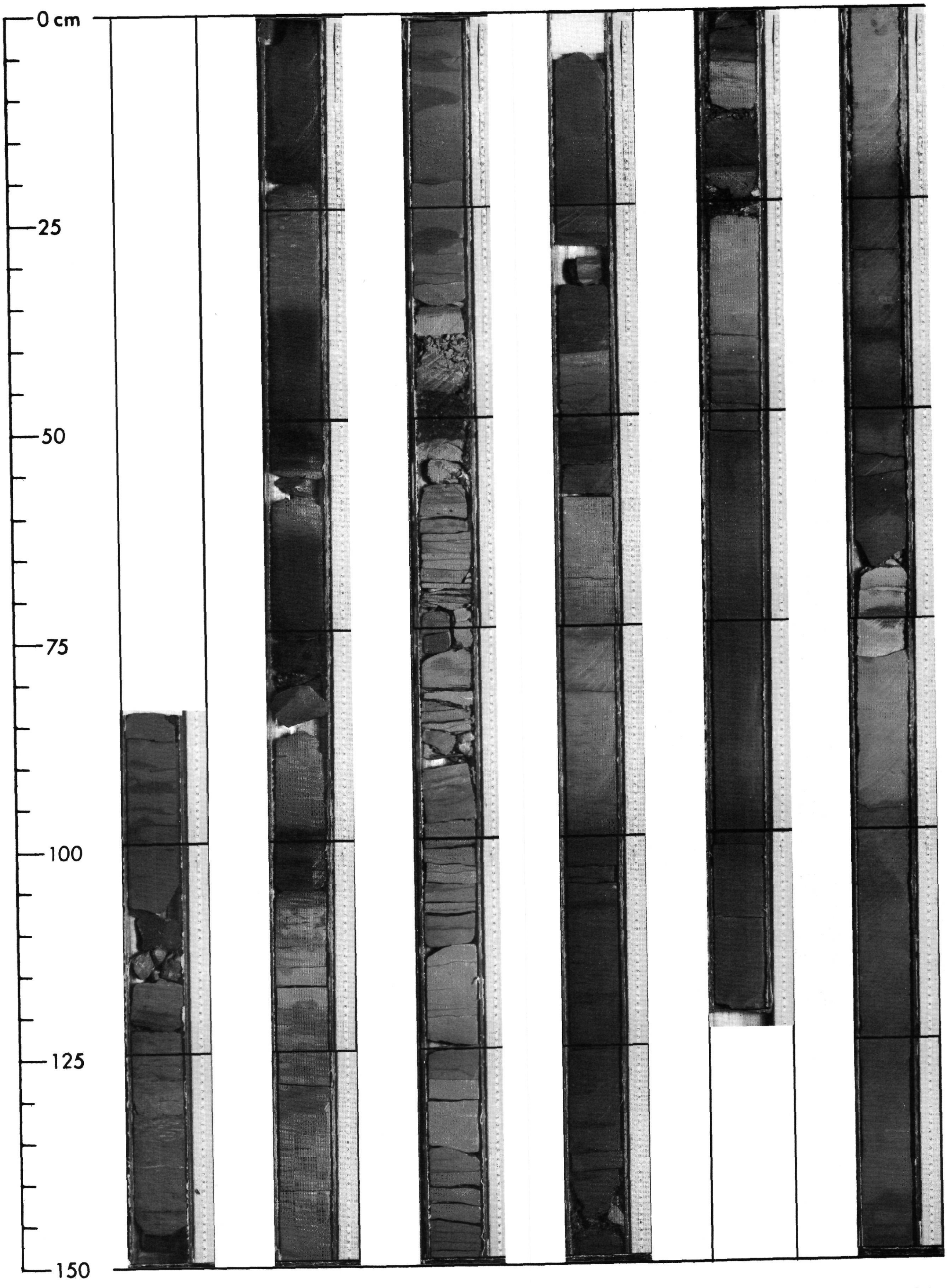
0 cm
25
50
75
100
125
150
387-25-1
387-25-2
387-25-3
387-26-1
387-26-2
387-26-3

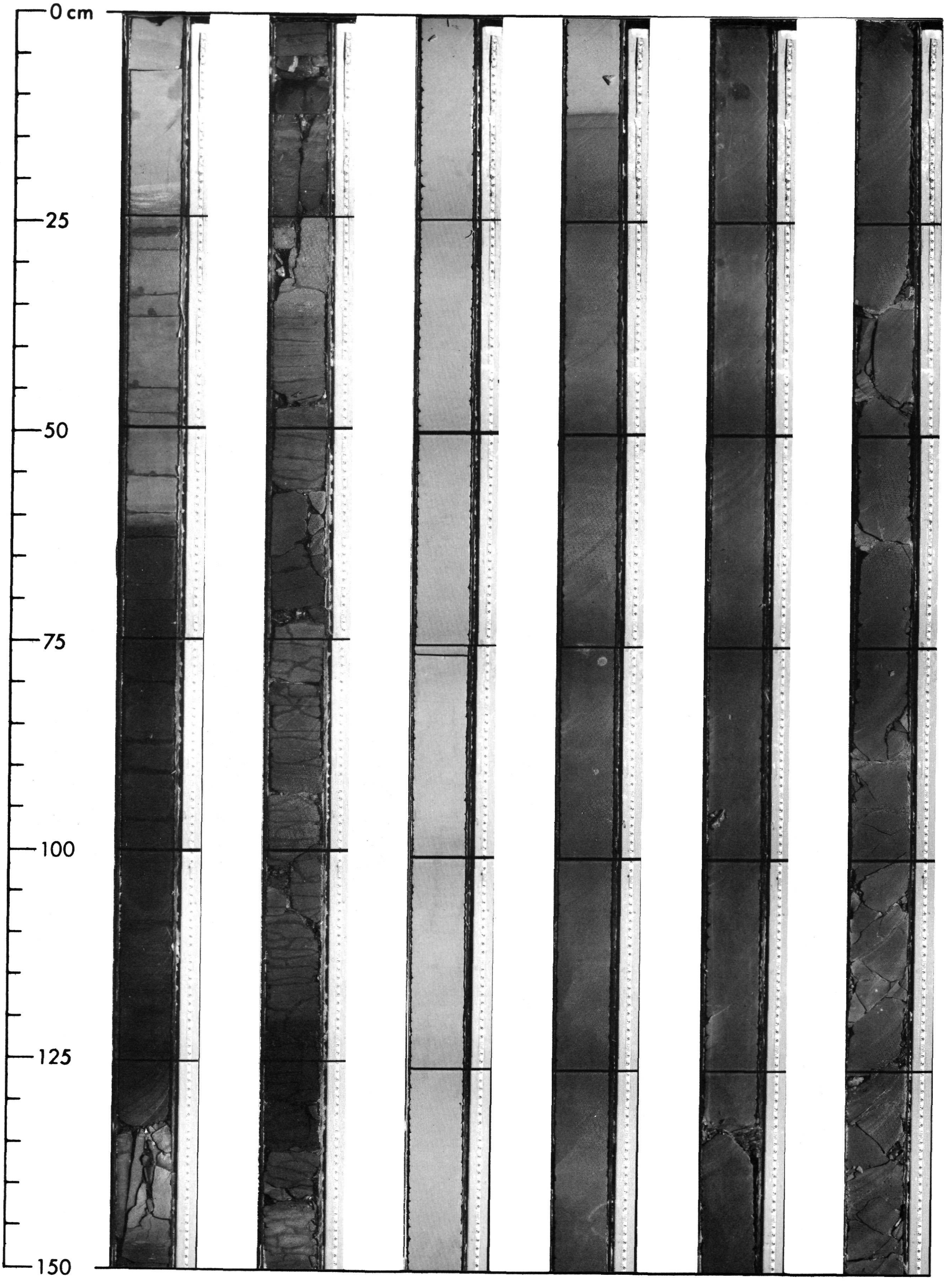
0 cm
25
50
75
100
125
150
387-27-1
387-27-2
387-27-3
387-27-4
387-27-5
387-27-6

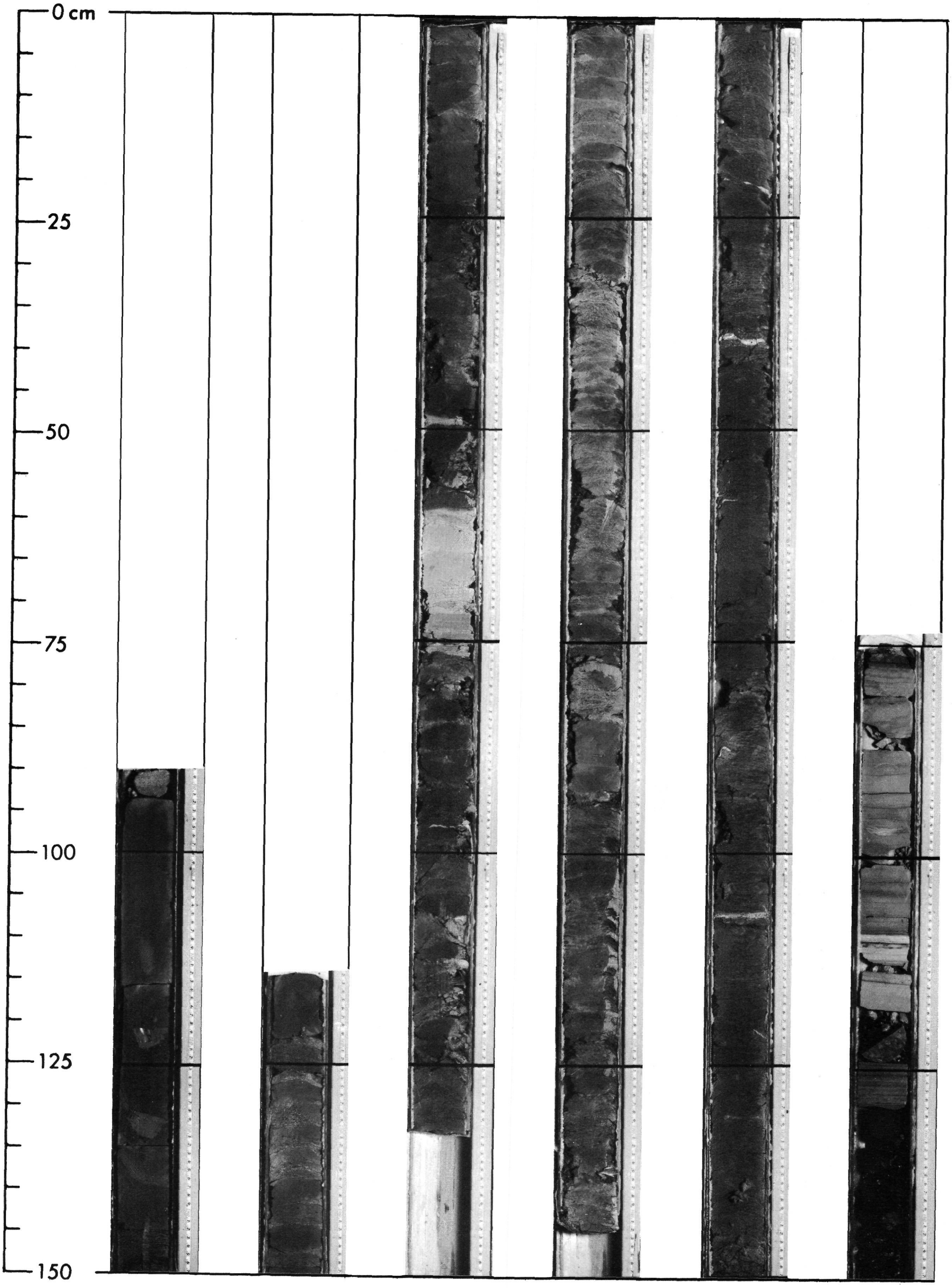
0 cm
25
50
75
100
125
150
387-28-1
387-29-1
387-29-2
387-29-3
387-29-4
387-30-1

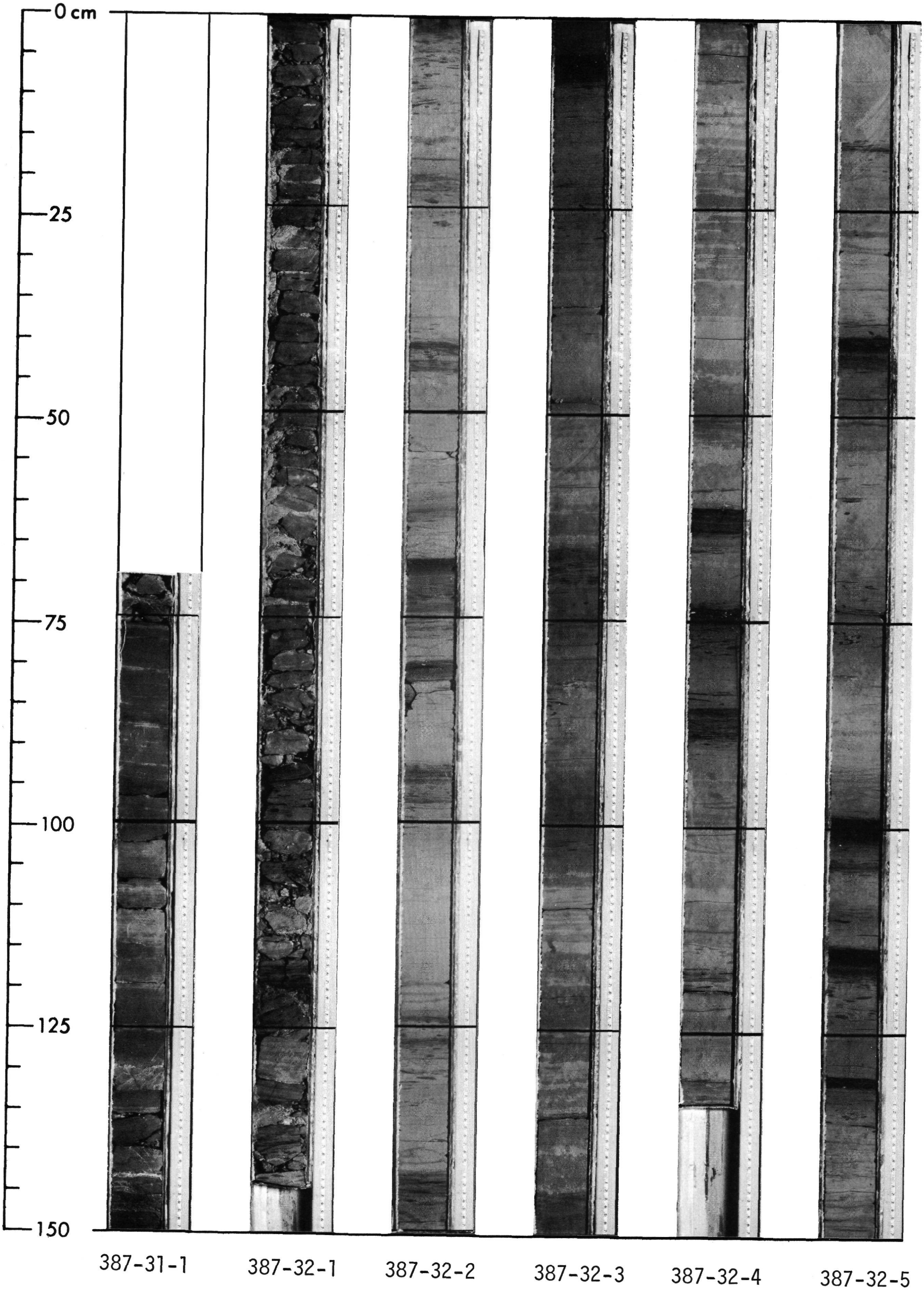
0 cm
25
50
75
100
125
150
387-31-1
387-32-1
387-32-2
387-32-3
387-32-4
387-32-5

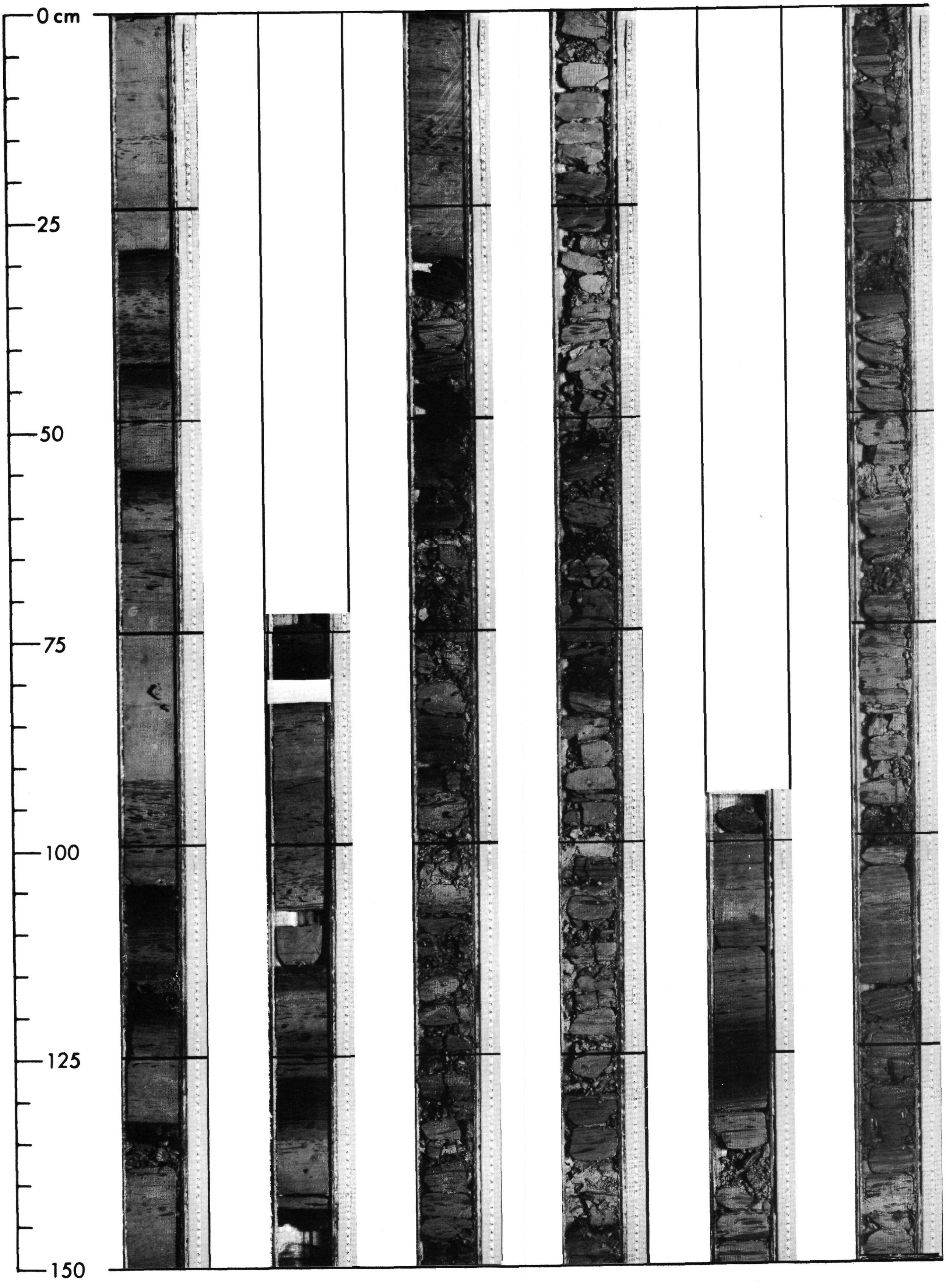
0 cm
25
50
75
100
125
150
387-32-6
387-33-1
387-33-2
387-33-3
387-34-1
387-34-2

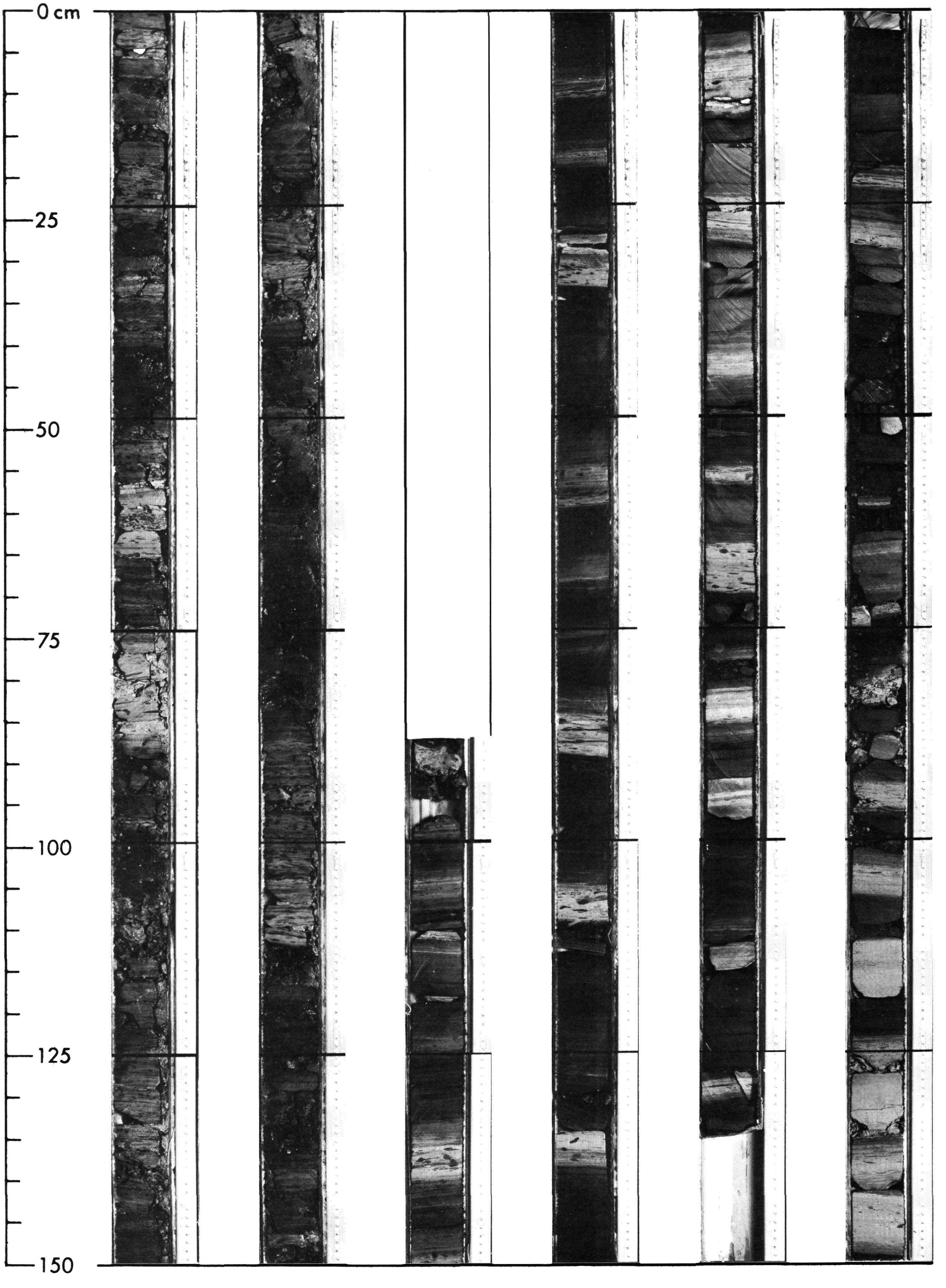
0 cm
25
50
75
100
125
150
387-34-3
387-34-4
387-35-1
387-35-2
387-35-3
387-35-4

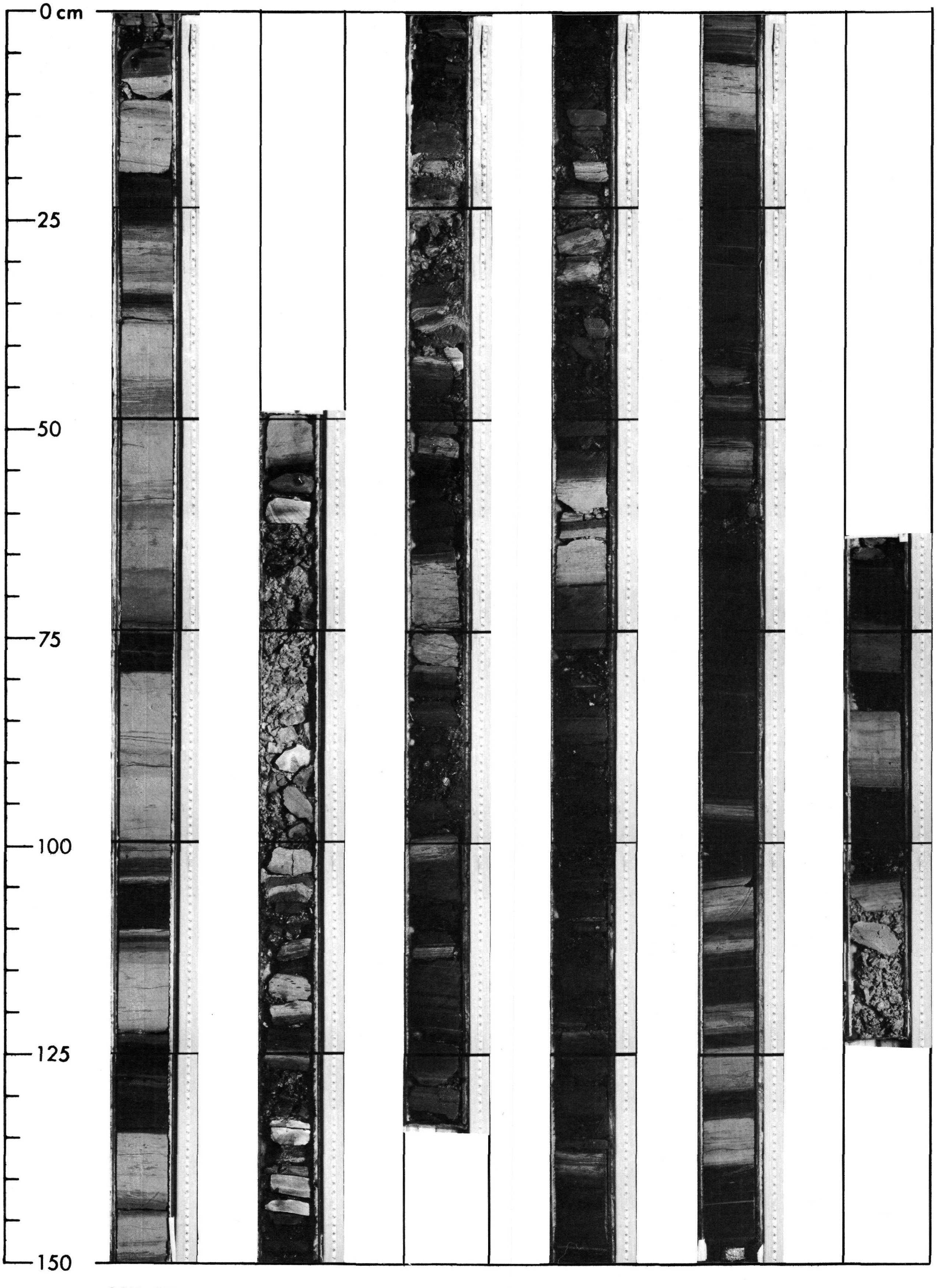
0 cm
25
50
75
100
125
150
387-35-5
387-36-1
387-36-2
387-36-3
387-36-4
387-37-1

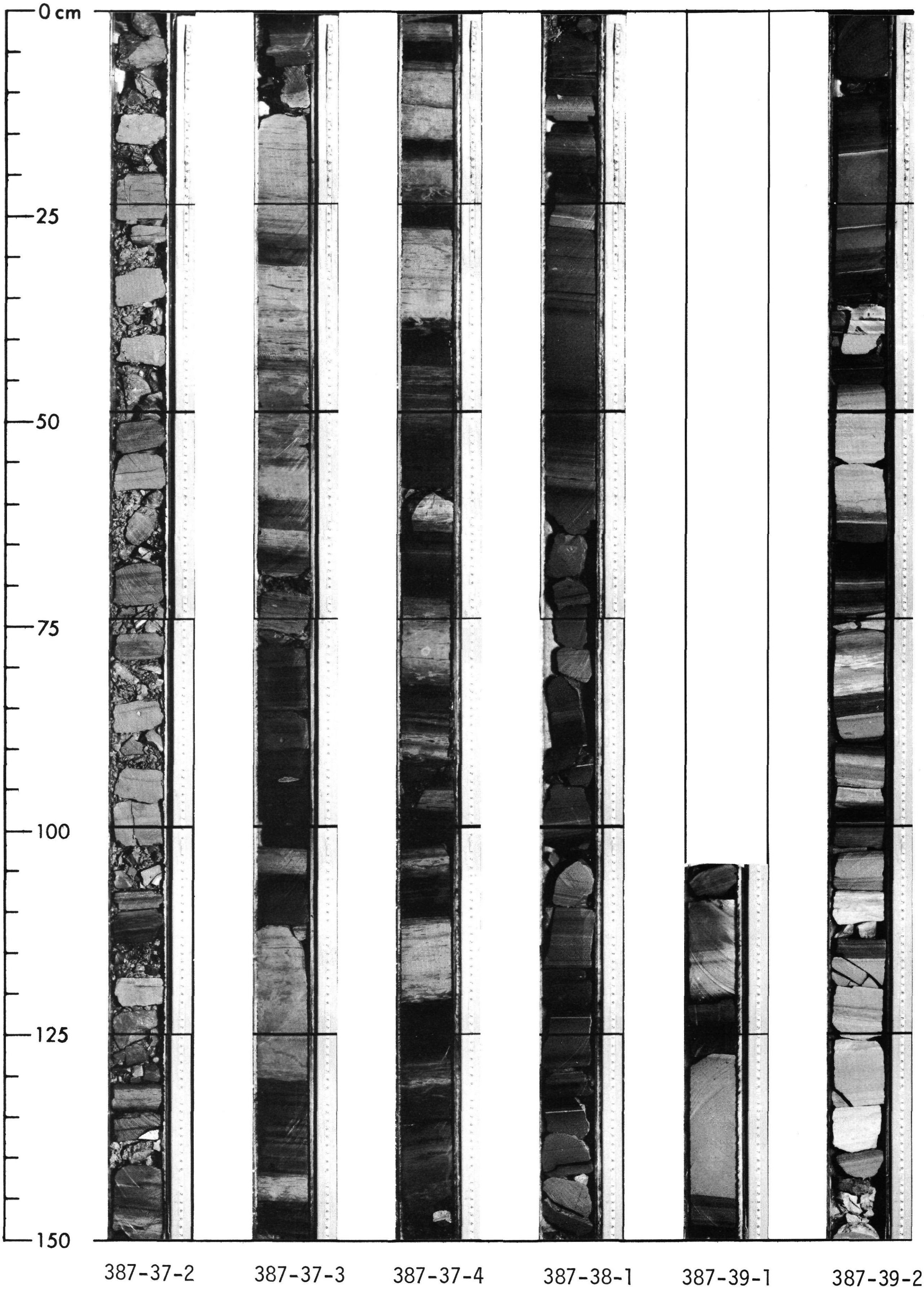
0 cm
25
50
75
100
125
150
387-37-2
387-37-3
387-37-4
387-38-1
387-39-1
387-39-2

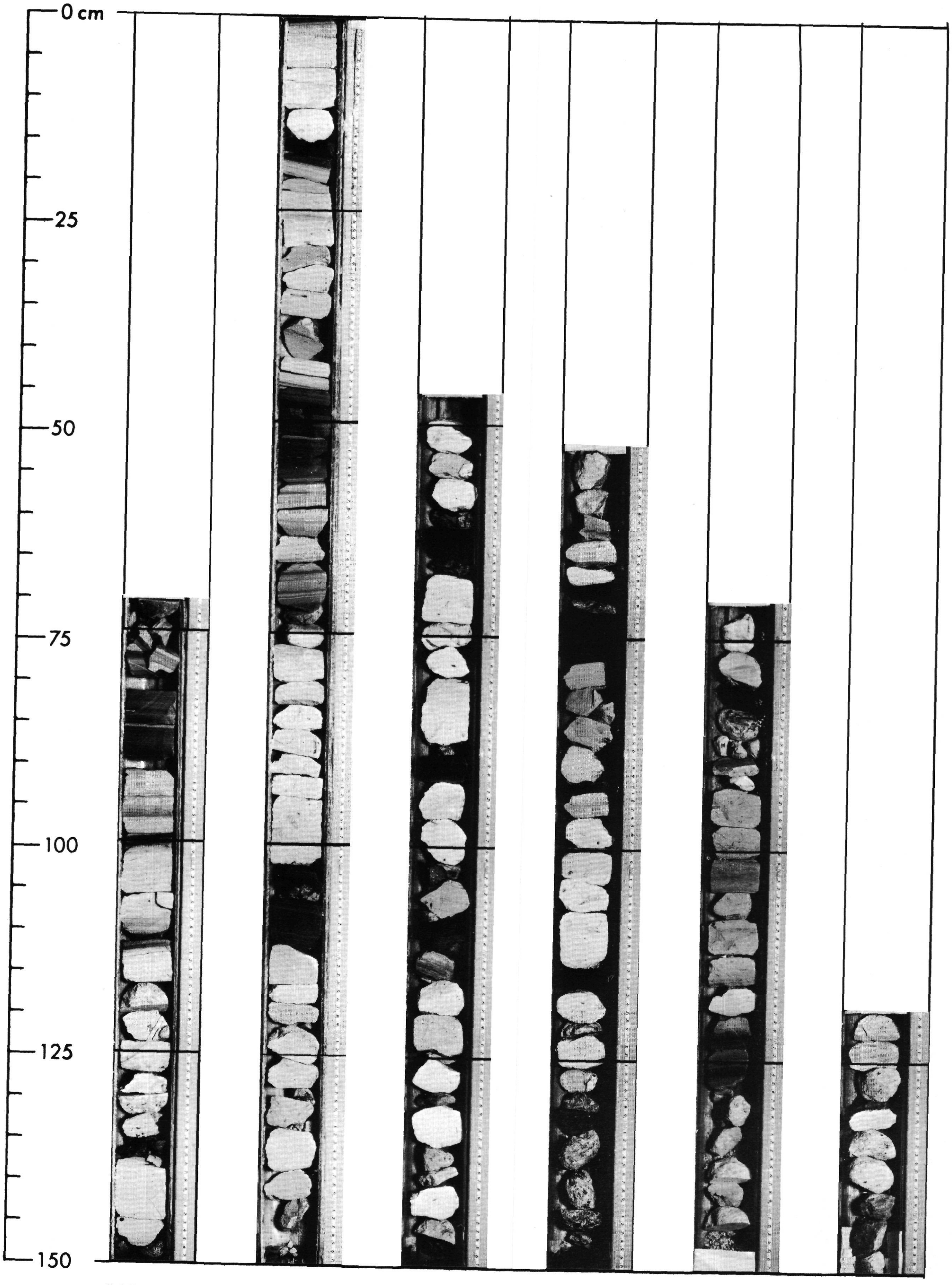
0 cm
25
50
75
100
125
150
387-40-1
387-40-2
387-41-1
387-42-1
387-44-1
387-45-1

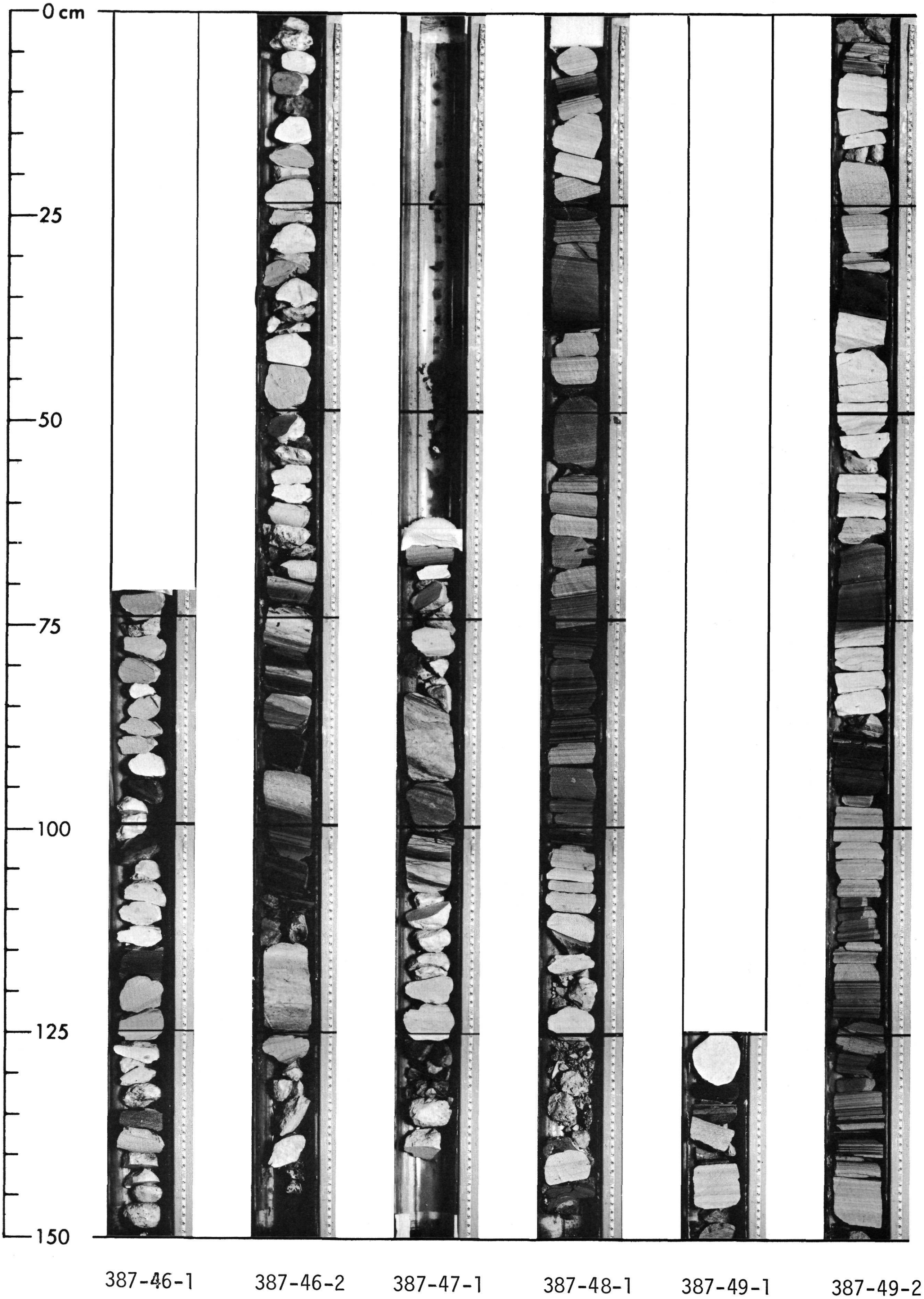
0 cm
25
50
75
100
125
150
387-46-1
387-46-2
387-47-1
387-48-1
387-49-1
387-49-2

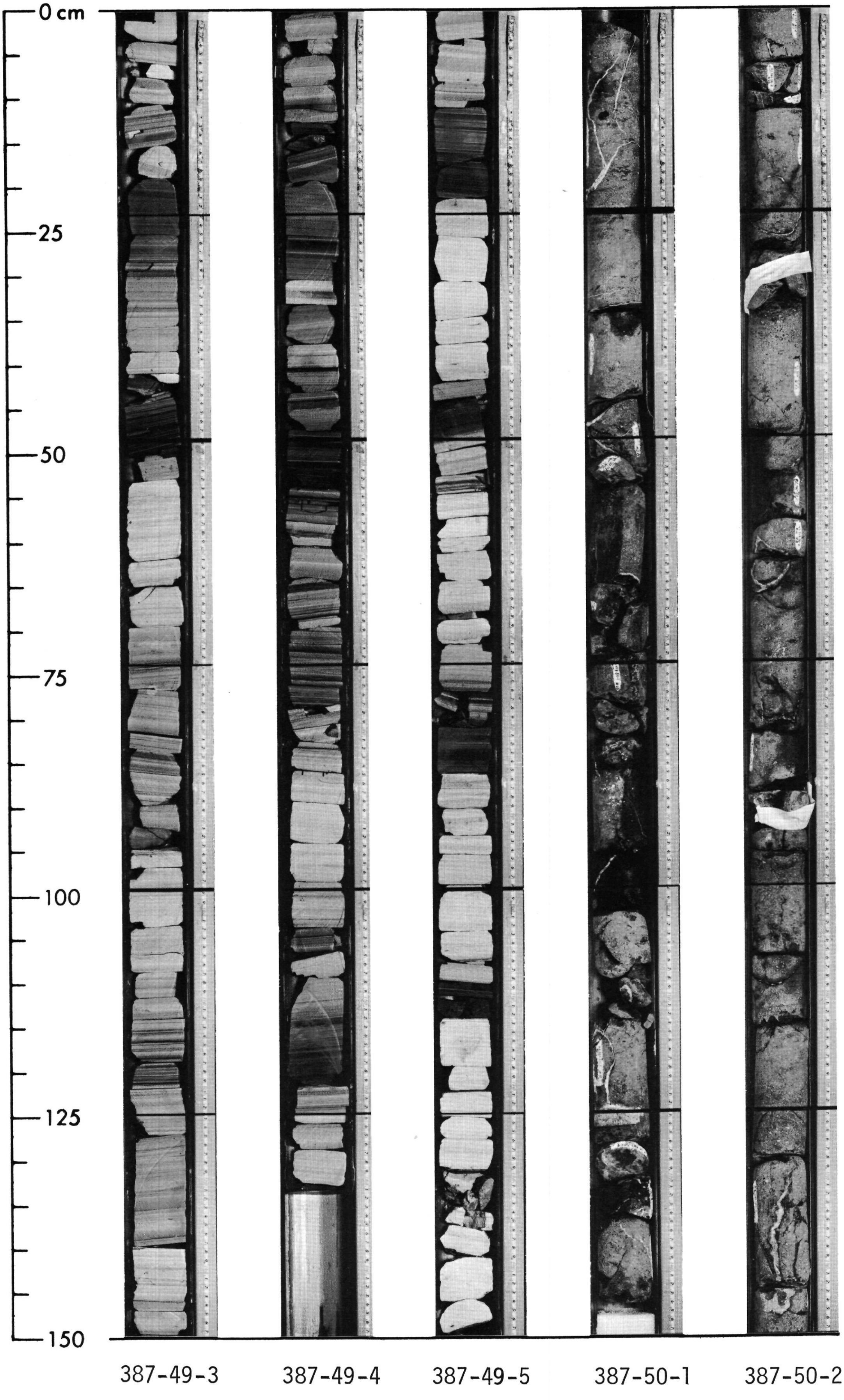
0 cm
25
50
75
100
125
150
387-49-3
387-49-4
387-49-5
387-50-1
387-50-2